DESIGN OF BIO-BASED MATERIALS DERIVED FROM FOOD INDUSTRY WASTES

Jone Uranga Gama
Department of Chemical and Environmental Engineering

eman ta zabal zazu
Universidad del País Vasco
Euskal Herriko Unibertsitatea

Donostia-San Sebastián, 2020

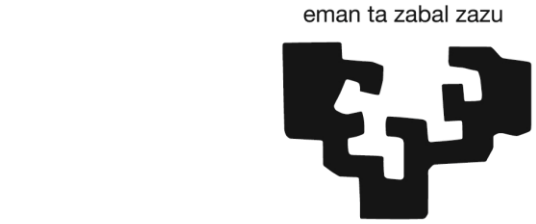

Design of bio-based materials derived from food industry wastes

Jone Uranga Gama

Supervisors: Koro de la Caba & Pedro Guerrero

Department of Chemical and Environmental Engineering

Donostia-San Sebastián, 2020

Nigan sinestu dutenei,

Badira bihotz txikietan handiak diren ametsak, lortuko diren ametsak.

Libre ta zabal dugu aurrean, baina ezin dugu edan.

Zauriak gatzez itxi ditzagun, malkoak urez eraso.

~Benito Lertxundi~

Acknowledgements

Bidaia batetan garrantzitsuena ez da helmuga izaten, ibilbideak dotoretzen du bidaia, izandako esperientziek, ikasitako lezio guztiek eta ondoan edukitako lagun zahar zein berriek. Beraz, tartetxo hau nire ikerkuntza bidaia dotoretzea, osatzea eta nola ez, erraztea, lortu duten guztiei nire eskerrak eskaintzeko erabili nahiko nuke.

En primer lugar quisiera agradecer a mis directores de tesis Koro de la Caba y Pedro Guerrero por haberme ofrecido la oportunidad de poder trabajar con ellos. Desde que comencé con vosotros el trabajo fin de grado, me disteis impulso para poder creer que el trabajo de un investigador, aunque muchas veces no salga como uno quiere, siempre vale para aprender, aportar y evolucionar. Este camino juntos ha sido un aprendizaje constante y esta tesis ha sido posible gracias a vuestra dedicación, constancia, vuestras sugerencias, correcciones…a vuestro trabajo.

I would also like to thank Maria Letizia Focarete, for offering me the mobility opportunity in their group in Bologna and leading me working with electrospinning. There will come a time you will plug yourself into electricity… Moreover, my special thanks to Giacomo Ciamician lab colleagues and Silvia Panzavolta for the unconditional aid supported. Grazie mille per tutto.

No puedo dejar sin agradecer a Maite Dueñas y a Ana Isabel Puertas. La estancia en la facultad de química me enseñó que el mundo de los “bichos” es tan bonito como difícil. Gracias por hacer que lo difícil fuera entretenido en vuestra compañía.

Eusko Jaurlaritzak doktorego-tesia burutzeko (PRE_2015_1_0205) emandako diru-laguntza eta ikerketa egonaldia egiteko luzatutako beka (EP_2018_1_0050) ere eskertu nahiko nituzke. Biomat ikerketa taldeari (GIU18/154) baita, eskerrak emandako babes ekonomikoagatik. UPV/EHU-ko SGIker ikerkuntza zerbitzu orokorrak ere eskertu nahiko nituzke.

Amaitzeko, ibilbide honetan uneoro laguntzen jardun dutenei NIRE ESKERRAK. Laborategiko kide lagunei, edozertarako laguntzeko prest beti egon zareten horiei. Mila esker bidea errazten laguntzeagatik bene-benetan. Beste herrialdeetatik etorri eta kultura eta lan egiteko modu berriez irakatsi didazuen horiei ere bai, nire ezagutzak aberastea lortu duzue. Lagunei, zuen jakinminak eta animuak ezinbestekoak izan dira ibilbide honetan. Nola ez, Ugaitzi, nire ondoan momentu onak ospatzen zein txarrak samurtzen egoteagatik, nigan sinesteagatik. Eskerrak bihotz bihotzez. Eta azkenik, nigan itsuki sinestu duten horiei, familiakoei. Eta bereziki amari, emandako indar guztiari esker nigan sinesten laguntzeagatik.

Summary

Functional properties, such as chemical and mechanical resistance, make plastic materials useful for a huge range of applications in food and pharmaceutical industries, among others. However, plastic stuffs are derived from non-renewable resources and lead to environmental problems associated to their treatment after disposal, especially when they are employed for short-term or single-use applications. Therefore, research on alternative materials is needed to reduce the use of these non-biodegradable and non-renewable materials. In this context, the use of polymers derived from biomass, such as proteins and polysaccharides, has grown in the last years, mainly due to their film forming ability, biocompatibility and biodegradability. Among proteins, gelatin is the most widely used due to its abundance. This biopolymer is obtained by the hydrolytic treatment of collagen, the major structural protein of most connective tissues, and specifically fish gelatin can be extracted from fish bones, skins, scales and tendons, promoting the valorisation of food processing wastes. In this regard, the main objective of this thesis was to develop and characterise novel fish gelatin-based materials employing diverse processing methods and different additives, some of them extracted from biowastes.

This study is made up of nine chapters. Chapter 1 is an overall view of biowaste valorisation and current protein materials' processing methods and applications, with special emphasis on gelatin based materials for food shelf life extension. Afterwards, in chapter 2, the materials and reagents employed, the extraction methods used to promote the valorisation of some food processing wastes, the techniques utilized for the development of gelatin products and the characterization methods carried out in this research work are described.

Different processing methods have been used for fish gelatin materials preparation in this doctoral thesis. Gelatin electrospinning is a big challenge and this is analysed in chapter 3. Hence, in order to overcome gelatin electrospinning difficulties

and select suitable solution compositions to be electrospun, rheological measurements of fish gelatin/citric acid solutions were studied. Since it was observed that the acidic pH hindered the reaction between gelatin and citric acid, basic pH conditions are analysed in chapter 4 for fish gelatin films prepared by solution casting, with the aim of promoting cross-linking and enhancing gelatin films properties. Furthermore, environmental assessment of films is carried out.

In the following chapters, active and/or intelligent packaging materials prepared via solution casting, compression moulding or freeze-drying are described. In that way, the combined effect of citric acid and chitosan on the antibacterial activity and functional properties of fish gelatin films obtained by solution casting is considered in chapter 5. Along with antibacterial agents, a wide series of antioxidant compounds are used in food packaging materials. In this sense, an antioxidant extracted from food production wastes, specifically anthocyanin extracted from red cabbage residues, is studied in chapter 6. Moreover, a deep analysis of anthocyanins containing fish gelatin films obtained by compression moulding is carried out. In chapter 7, fish gelatin samples prepared by lyophilisation, using chitin, extracted from squid pens, as a reinforcing agent, are analysed; furthermore, tetrahydrocurcumin (THC) is incorporated in order to design gelatin products as antioxidant carriers.

Finally, the general conclusions of this doctoral thesis are summarised in chapter 8, and the references cited along this research work are listed in chapter 9.

Objectives

The overall aim of this doctoral thesis was to develop fish gelatin-based materials with enhanced properties that can be tailored as a function of processing methods.

The specific aims of this study were:

- Analyse functional properties of fish gelatin-based materials and study the reaction between gelatin and citric acid.
- Optimise electrospinning parameters to obtain gelatin mats.
- Valorise some biowastes derived from food industry, to obtain anthocyanins and chitin, and analyse their effect on fish gelatin-based materials.
- Asses the environmental aspects involved in the production of fish gelatin-based films as well as in the chitin extraction process.
- Test the behaviour of citric acid, chitosan, anthocyanins and tetrahydrocurcumin bioactives: release, antibacterial or antioxidant activity.

Index

1 Introduction

1.1 Summary

Biowaste is one of the main concerns in most of the industrialised countries. In particular, food waste is not only an economic issue, but also an ethical and environmental one since it implies the waste of natural resources. Therefore, many factors must be considered through the whole food chain in order to prevent and reduce food waste, from producers to retailers and consumers (Guerrero et al., 2015; Mirabella et al., 2014). In this regard, the use of polymers derived from residues has grown in the last years, among others the employment of by-products generated from food processing industries like fish canning, lobster industry and fishery landed biowastes.

Among biopolymers, a lot of attention has been dedicated to proteins and polysaccharides, alone or in combination, for both films and biomaterials production (Chiralt et al., 2018; Costa et al., 2018; Lin et al., 2015). Regarding proteins, these heteropolymers are comprised of more than one type of monomers that present wide variety of functional groups which promote the self-folding due to forces such as disulphide bridges, as well as hydrophobic and hydrophilic interactions, leading to globular or fibrous proteins (Balcão & Vila, 2015; Gudipati, 2013). Proteins offer valuable characteristics for the production of food packaging products due to their abundance, film forming ability, transparency and excellent barrier properties against O_2, CO_2 and lipids (Lacroix & Vu, 2014). Low O_2 permeability, for example, enables the extension of food shelf life without creating anaerobic conditions. Concerning proteins' performance as biomaterials, they are significant components in the extracellular matrix, which is an essential constituent of any tissue with an active role in cell behaviour. Along with biocompatibility, proteins generally exhibit hydrophilic character, low immunogenicity and biodegradability, which could greatly suppress the foreign body reaction for *in vivo* applications. Therefore, protein-based materials have been extensively assessed for tissue engineering, bioactive/drug delivery systems, and wound dressings for the development of biomaterials that can provide a temporary extracellular matrix for cell

adhesion and proliferation while biologically active compounds are released in a controlled manner (Barbosa & Martins, 2018). As abovementioned, proteins are heteropolymers that contain a great variety of functional groups and so, the properties of protein-based materials can be tailored by means of enzymatic, chemical and/or physical modifications to obtain the desirable final properties required for food packaging and biomedical applications (Hammann & Schmid, 2014).

It is worth noting that protein-based products function as excellent vehicles of a wide variety of biologically active compounds (Gudipati, 2013). Taking the benefits of bioactive compounds into account, new opportunities for developing biopolymeric materials with great potential in food packaging and biomedical applications have been opened (Chen et al., 2017; Lau et al., 2017; Yu et al., 2018). Proteins can be used to improve the quality of food products, but also can contribute to a better regeneration of tissues as well as enhance the recovery of patient after surgery by acting as efficient carrier agents of bioactive compounds such as essential oils, phenolic compounds, vitamins, minerals and peptides, which present antimicrobial, antioxidant and anti-inflammatory properties, among others (Etxabide et al., 2017a, 2018; Santoro et al., 2014).

In this context, active packaging materials have been developed to interact with food, with the aim of protecting food against the effect of the external environment but also with the aim of extending the shelf life, maintaining or improving quality and safety of packaged food. Active food packaging materials have been designed to incorporate bioactives and functional additives in order to promote interactions between the food product and its environment and so, to cause a modification of the conditions of the packaged food in order to maintain the product quality for longer (Grumezescu & Holban, 2017). Active packaging involves the use of antioxidants, antimicrobials, and other naturally occurring bioactive molecules to accomplish this goal. Additionally, bioactive compounds have been used for biomedical applications in order to design a sustained

release of these molecules from the implantable/administered biomaterials and provide a faster and more comfortable recovery of the patients (Moaddab et al., 2018; Patel et al., 2018; Raja & Fathima, 2015; Ruiz-Ruiz et al., 2017).

This chapter provides an overview of materials based on biopolymers, specifically biopolymers derived from marine sources. First, the techniques used for their extraction will be described briefly and, hereafter, the preparation methods of animal and vegetal protein materials will be analysed. Among animal proteins, gelatin-based materials will be reviewed, with emphasis on fish gelatin materials employed for extending food shelf life.

1.2 Biowaste valorisation

The valorisation of by-products from seafood industry, rich on proteins and polysaccharides, can be a worthy approach to prepare sustainable and value-added products. The global fish production (fish, crustaceans, molluscs and other aquatic animals, including fisheries and aquaculture) peaked at about 171 million tonnes in 2016 (FAO, 2018), with an estimated loss or wastage between landing and consumption of 27% of landed fish, crustaceans and molluscs (**Figure 1.1**). Additionally, high amounts of solid waste generated in fishery industries must be considered; for instance, in fish canning operations, the amount of waste can be as high as 50% by weight of raw products (Kafle et al., 2013). In all these fish by-products (skins, bones, scales, tendons), there is a considerable amount of collagen, a fibrous protein with a structural function (Ferraro et al., 2017; Venkatesan et al., 2017). Carrying out thermal denaturation or partial hydrolysis of collagen, gelatin is obtained (Huang et al., 2017), whose properties differ from fish species. In general, cold-water fish gelatins have relatively lower gel strength than warm-water fish gelatins due the lower content of imino acid residues (Lin et al., 2017). In this regard, gelatin from salmon skin (cold-water fish) has 166 residues per 1000 total amino acid, whereas gelatin from seabass skin (warm-water fish) contains around 198-202 residues per 1000 total amino acid (Sinthusamran et al., 2014).

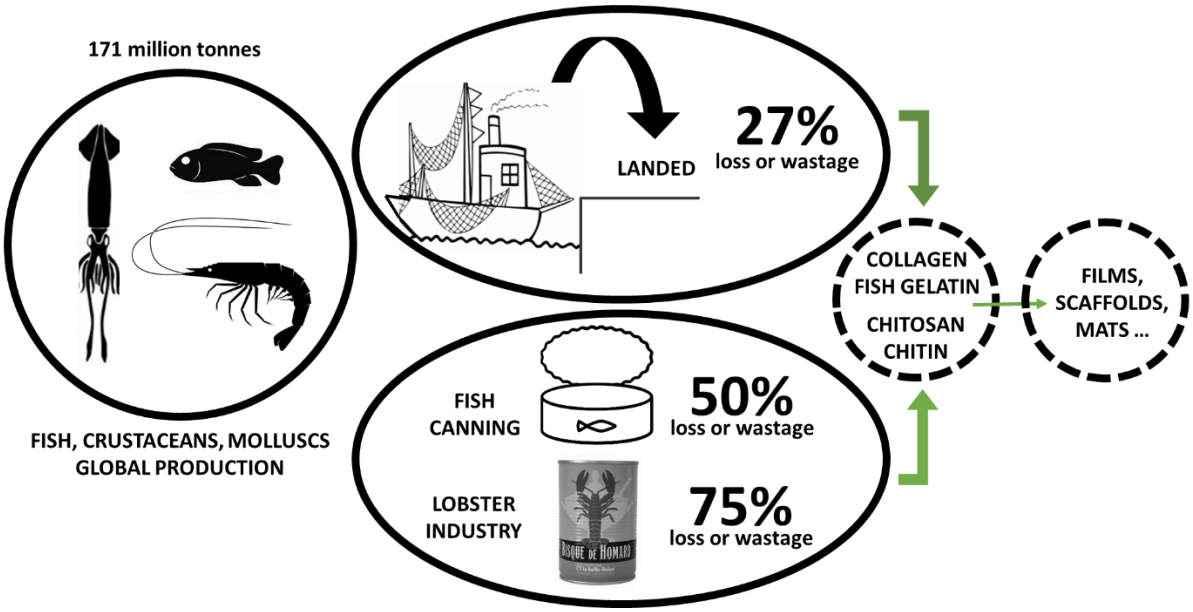

Figure 1.1 Global fishery production (2016), wastage and possible valorisation strategies.

In regards to crustacean and molluscs by-products, shrimp and crab shells can be used to obtain chitin (Arya et al., 2017). As an example, lobster processing industry by-products account for around 75% by weight of the starting material (**Figure 1.1**). Chitin is a polysaccharide that has a similar structural function to that of collagen. Chitin is the second most abundant natural polymer after cellulose, and it is usually transformed into chitosan, a water-soluble polymer, to broaden its application. This transformation process is based on chitin deacetylation under alkaline conditions (Hamed et al., 2016; Sayari et al., 2016; Soares et al., 2016). It must be considered that the functional properties of the chitosan obtained depend on structural features, such as average molecular weight and degree of deacetylation (Rocha et al., 2017).

As previously mentioned, collagen can be obtained from fish skin, scales, tendons and bones, which are cleaned and reduced in size to facilitate the extraction (Chen et al., 2016). The extraction process from fishery wastes consists of two main steps: pretreatment of raw materials and collagen extraction. With regard to fish gelatin extraction, this protein is obtained from the thermal denaturation or chemical degradation of collagen. These processes involve the loss of the collagen triple-helix structure and

the formation of the typical random coil structure of gelatin. However, gelatin macromolecules can rearrange, under certain conditions, thus forming again sequences of triple-helix, even if the fibrillar collagen structure cannot be recovered and the material becomes highly soluble in aqueous environment. Many studies in the literature have reported different protocols for the obtainment of fish gelatin. The extraction protocols typically include the use of acid or alkaline chemicals as pretreatments. In that way, two type of gelatins can be differentiated: type A gelatin, derived from collagen by acid pretreatment, most fish gelatins are within this group; and type B gelatin, as a result of an alkaline pretreatment of collagen (Hattrem et al., 2015).

Regarding chitin and chitosan extraction, chemical and/or biological treatments have been employed for that purpose (Hou et al., 2016). When chitin is extracted from crustacean shells, three steps are required, including deproteinisation, decolouration, and demineralisation (Hou et al., 2016; Muxika et al., 2017). In the case of the extraction from squid pens, decolouration is not needed since pens are colourless; furthermore, demineralisation step can also be avoided due to the low content of inorganic components in pens (Garrido et al., 2017). After extracting chitin, chitosan is obtained by a deacetylation process. Depending on the aggressiveness of the treatment, the deacetylation degree of chitosan may differ, affecting the final properties of the material (Castillo et al., 2017).

1.3 Techniques for the development of protein products

Along with the selection of the appropriate biopolymers and additives, the design and processing methods deeply influence the final properties of products, such as porosity, degradation behaviour, surface and mechanical properties, and biocompatibility, due to the different degrees of thermo-mechanical history involved during the manufacturing processes. Like other biopolymer-based products, proteins can be processed by various methods to produce films, fibre mats and scaffolds for different applications. These technologies include, but are not limited to, solution casting,

compression moulding, freeze-drying, electrospinning and three-dimensional (3D) printing (Ebnesajjad, 2012). Generally, these fabrication techniques can be divided into two categories, including non-designed and designed manufacturing methods. The majority of available manufacturing techniques, such as solution casting, compression moulding, freeze-drying, electrospinning and the combination of these techniques, belong to the non-designed manufacturing techniques, while the 3D printing is classified as a designed manufacturing technique (**Figure 1.2**).

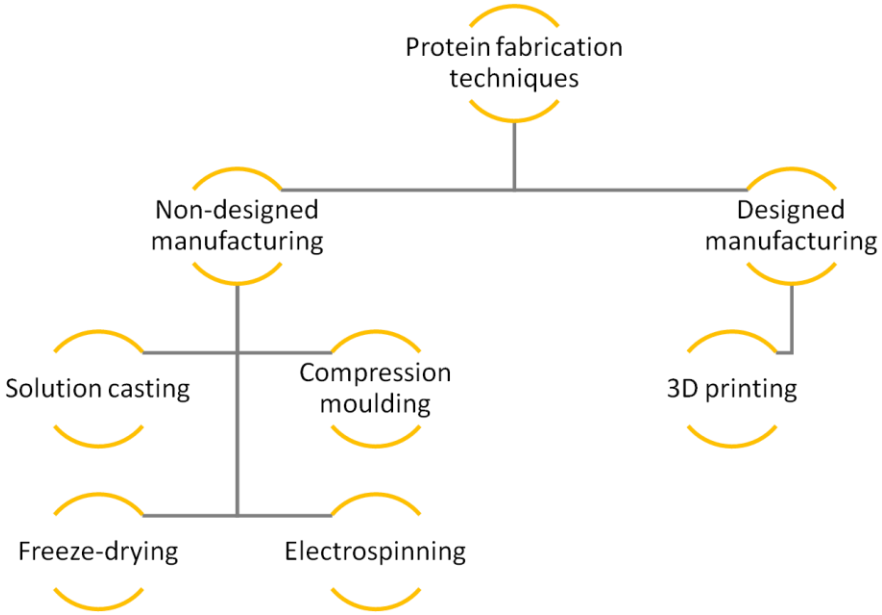

Figure 1.2 Non-designed and designed protein fabrication techniques.

1.3.1 Solution casting

Films are one of the most common types of materials developed from plant and animal proteins and they are used for food packaging and tissue engineering applications. In this context, solution casting is the preferred method used to prepare protein films at laboratory scale. This method involves solubilisation, casting, and drying steps (**Figure 1.3**). The process starts dissolving polymer along with additives, such as plasticizers or bioactive compounds, in a suitable solvent, usually water or water-alcohol solutions. Heating and/or pH changing alter solution conditions, which affect the final properties of the film. Then, the solution is cast onto Petri dishes and, finally, solvent

evaporation takes place when solutions are subjected to drying processes, leading to the film formation. Drying processes can be carried out at room conditions or under controlled temperature and relative humidity, which may affect the film properties (Cerqueira et al., 2016).

Figure 1.3 Schematic illustration of solution casting processes.

A wide variety of protein films have been manufactured by solution casting for food packaging applications (Arrieta et al., 2013; Etxabide et al., 2017b; Hassan et al., 2018). In this regard, some protein films have been used as carriers of different extracts. In order to increase the antioxidant activity of protein films, liquorice residue extract was incorporated into soy protein isolate film forming formulations (Han et al., 2018). Total phenolic content was measured in aqueous (10% ethanol) and fatty (95% ethanol) food simulants, and the results showed that the extract incorporation notably increased the phenolic compound release, giving values of 4.0-5.6 mg gallic acid/g film in the aqueous simulant and 2.2-5.5 mg gallic acid/g film in the fatty food simulant. Additionally, the extract addition decreased water vapour permeability and increased tensile strength.

In another study (Kaewprachu et al., 2018), kradon extract, obtained by using a microwave at 500 W for 62 s, was incorporated into fish myofibrillar protein, together with catechin, to prepare active films. The low DPPH radical scavenging activity and ferric reducing antioxidant power (FRAP) of fish myofibrillar protein films were improved with the incorporation of the extract/catechin mixture; furthermore, these films showed higher elongation at break. These films were used to wrap tuna slices (Kaewprachu et al., 2017). While the tuna colour markedly changed from bright red to brown for the

unwrapped samples after 4 days of storage, the tuna fillets wrapped using active films maintained the red colour after 8 days of storage. In this regard, the TBARS values of the wrapped samples showed lower values (2.16 mg MDA/kg sample) than the unwrapped samples (7.35 mg MDA/kg sample). Additionally, tuna texture was improved with the wrapping; therefore, these results along with the sensory assessment indicated that the wrapped tuna fillets showed a 4-fold shelf life extension compared to unwrapped samples.

Protein films have also been used for biomedical applications (Etxabide et al., 2017c; Posati et al., 2018). Collagen was mixed with fucoidan, a seaweed-derived polysaccharide with a broad spectrum of physiological and biological activities such as anti-cancer, anti-tumour, anti-coagulant, and antioxidant activities, in order to prepare films for tissue engineering application (Perumal et al., 2018). It was found that fucoidan-added films exhibited smaller pore size and a more fibril-like structure when compared to control films, which could improve cell adhesion and infiltration within the membrane. Furthermore, the *in vitro* biodegradation assay carried out by collagenase to assess enzymatic degradation revealed a significant reduction in collagen degradation rate when compared to native collagen (control), indicating that fucoidan protected the active binding sites of collagen from collagenase.

Also for biomedical applications, gelatin films with galactomannan, extracted from *Delonix regia*, were prepared by solution casting (Siqueira et al., 2015). Films were cross-linked by immersion into an aqueous solution of 1-(3-dimethylaminopropyl)-3-ethylcarbodiimide hydrochloride for 2 h. The swelling of cross-linked films showed a 2-fold decrease compared to uncross-linked films due to the formation of a denser structure. Furthermore, the biological test carried out on L929 cells showed no cytotoxicity regardless of the galactomannan concentration, suggesting the potential application of these films for wound dressings.

Film preparation via the classical solution casting technique does not allow for the production of large dimension films and so, in recent years, tape casting has been suggested as a suitable approach to scale-up film manufacturing and provide the possibility of producing larger films in shorter times. Tape casting is an upgrading of the casting method and consists of spreading film forming solutions with an adjustable blade at the bottom of the spreading device (doctor blade), which allows controlling the thickness. After that, the spread solution is dried by heat conduction, convection, infrared radiation, or by a combination of these mechanisms at a controlled temperature (de Moraes et al., 2015). In this regard, soy protein films were prepared by tape casting to analyse the influence of drying methods and temperatures (heat conduction at 40, 50 and 60 ºC, and infrared radiation at 60 ºC) on the film physical properties (Ortiz et al., 2017). Hence, soy protein film forming solutions containing 5.0, 10.0, 10.5, 11.0 and 12.5% w/v soy protein were prepared at pH 10.5 and spread at a speed of 1.8 cm/s onto a 30 cm × 84 cm plate. A doctor blade was used to spread the film forming solution on the plate and get a thickness of 2 mm. It was determined that 10.5% w/v was the minimal protein concentration to produce soy protein films by tape casting technique. Film moisture content, solubility, water vapour permeability and colour parameters showed no change irrespective of drying method and temperature. However, the conduction method at 60 ºC resulted into films with superior mechanical properties and heat seal strength than the films dried at 40 and 50 ºC or dried by infrared radiation at 60 ºC. Additionally, opacity was notably reduced with the increase in drying temperature.

1.3.2 Compression moulding

Protein-based films can also be manufactured by compression moulding (Garrido et al., 2016a; Uranga et al., 2018). This technique involves the pressing of a deformable material placed between the two halves of a heated mould, and its transformation into a solid product under the effect of the mould temperature (**Figure 1.4**). The parameters

(pressure, temperature and time) for each step of the process depend on the protein used.

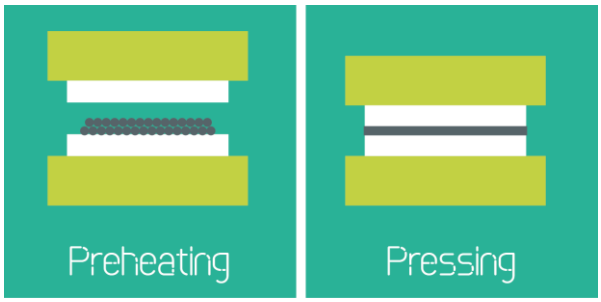

Figure 1.4 Schematic illustration of compression moulding processes.

Unlike synthetic polymer-based thermoplastics, plant proteins are inherently non-thermoplastic biopolymers and, consequently, the modification of proteins is needed to make them flow. In this regard, protein-polysaccharide mixtures have been used for film preparation by compression moulding. In particular, soy protein films were used as carriers of agar (3, 6 and 9 wt %) extracted from red algae *Gelidium sesquipedale* (*Rodophyta*) in order to describe the conformational changes during the film obtaining process and the effect of agar addition on the final structure of protein films (Garrido et al., 2016b). Soy protein/agar films were transparent, homogeneous and showed excellent barrier properties against UV light in the range of 200-280 nm. The addition of agar decreased solubility but increased water uptake capacity of films, mainly in films with 9 wt % agar; therefore, these films could be used for the controlled delivery of active substances for pharmaceutical and food applications. In fact, soy protein films have been used as carriers of bioactives such as red grape extract (Ciannamea et al., 2016). Different amounts of the extract (0-10 wt %) were added and thermo-compressed in a three-step operation: 150 ºC for 5 min at 10 kg/cm^2, 150 ºC for 2 min at 100 kg/cm^2, and cooling up to 30 ºC at 100 kg/cm^2 for about 30 min. The results showed that the incorporation of the extract resulted in lower elongation at break and higher elastic modulus values. Furthermore, the addition of 5% of the extract improved the antioxidant activity of the film since DPPH radical scavenging activity increased from 58 to 81% due

to the presence of polyphenolic compounds, such as catechin, epicatechin and procyanidin, in the red grape extract. Moreover, it was observed that higher concentrations of the extract (10 wt %) did not affect the antioxidant activity of films.

Compression moulding can also be used to prepare active packaging. In this context, a mixture of gelatin, starch, water and glycerol, was pre-heated for 5 min at 160 ºC in the press plate and then thermally compacted at 3000 kPa for 2 min and 13000 kPa pressure for 6 min at 160 ºC (Moreno et al., 2018). Thereafter, a cooling cycle to 6 ºC was applied for 3 min. These thermo-compressed films extended the shelf life of chicken breast fillets and the microbiological limit of acceptability for total viable counts was reached after 12 storage days for the fillets packaged.

1.3.3 Electrospinning

Electrospinning (electrostatic spinning) has gained considerable interest in recent decades for continuous ultrafine solid fibre formation, ranging from micrometres to nanometres, with a large surface area per unit volume, due to its simplicity, cost-effectiveness and versatility (Deng et al., 2018; Moheman et al., 2016). The technique relies on using electrostatic charge to draw viscous or melted polymer solution into fibres, employing a high-voltage power supply, a precisely controlled syringe pump, a syringe with a needle, and a grounded collector (**Figure 1.5**) (Santos et al., 2018). In that way, a polymer solution, held by its surface tension at the end of a capillary tube, is subjected to an electric field, and an electric charge is induced on the liquid surface, increasing electrostatic forces with the increase of electric field strength. When the electrostatic force equals to the surface tension of the polymer solution, the liquid drop becomes a cone (Taylor cone), and electrostatic force, bigger than surface tension, leads to a charged jet ejected from the tip of the Taylor cone. The jet is moved toward grounded collecting metal screen or drum, in which the fibre discharges while the solvent evaporates (Drosou et al., 2018). Electrospun fibres can be assembled into three

dimensional (3D) porous and random nonwoven mats as a result of a bending in the spinning jet.

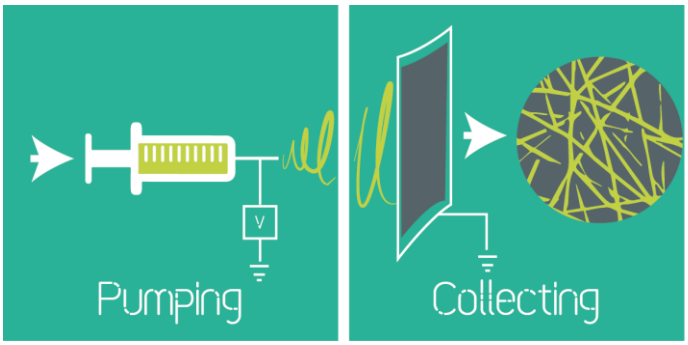

Figure 1.5 Schematic illustration of electrospinning processes.

Using this technique, various biopolymers have been electrospun into fibres or mats (Jiang et al., 2015). In this context, proteins have been widely employed for biomedical and food packaging applications (Aytac et al., 2017; Luo et al., 2018a; Mendes et al., 2017). In the last years, electrospinning has been explored as a method for bioactives encapsulation and controlled-release technologies (Altan et al., 2018; da Silva et al., 2018; Wang et al., 2016, 2017a). In fact, this technique exhibits a number of advantages when compared to traditional encapsulation techniques (spray drying or emulsification). The most interesting characteristics of electrospinning for encapsulation applications are related to the one-step process, the production of dried samples, and the use of conditions (room temperature and atmospheric pressure) suitable for heat-sensitive materials performance (Bhushani & Anandharamakrishnan, 2014). Different proteins can be used via electrospinning in the field of bioactive encapsulation. Active bilayer packaging structures were prepared by encapsulating α-tocopherol antioxidant in different proteins (whey protein, soy protein or zein) and electrospinning the hydrocolloid mats directly as a coating onto a wheat gluten film (Fabra et al., 2016). Zein fibres showed higher encapsulation efficiency of α-tocopherol and a slower release compared to whey or soy protein capsules, indicating that encapsulation efficiency was greater in fibres than in beads. Furthermore, when submitting these structures to a typical industrial

sterilisation process, the α-tocopherol stability was preserved, especially when zein was used as a matrix.

Also blends have been found to be suitable for bioactive encapsulation via electrospinning. In particular, folic acid, a water-soluble B vitamin, was encapsulated using amaranth (*Amaranthus hypochondriacus* L.) protein isolate and pullulan blend (Aceituno-Medina et al., 2015). Amaranth protein isolate is derived from a traditional under-utilized Mexican crop with highly nutritious grains and leafs, whereas pullulan is a water-soluble microbial polysaccharide produced by *Aureobasidium pullulans* in starch and sugar cultures. Encapsulation within the amaranth protein isolate/pullulan structures decreased photodegradation of folic acid, which may be useful for food applications, such as food fortification to increase recommended basal folate intake levels. Also for nutraceutical applications, kafirin, prolamine protein from sorghum grain, and polycaprolactone were blended to obtain hybrid fibre mats (Xiao et al., 2016). To simulate the nutraceutical release in the body fluids, carnosic acid was selected as a model, and release behaviour was found to be diffusion controlled. The amorphous region of kafirin dominated the release rate, while polycaprolactone functioned as a hydrophobic skeleton to maintain the structure of the 3D fibre matrix scaffold.

In terms of the incorporation of hydrophobic bioactives into protein electrospun mats, some difficulties can be found due to their solubilisation inability. In that way, surfactants are dispersed in aqueous solutions, above the critical micelle concentration, to form micelles spontaneously, and solubilise hydrophobic bioactives, favouring electrospinning process (García-Moreno et al., 2016). In this context, non-ionic Tween 80, cationic cetyltrimethyl ammonium bromide, and anionic sodium dodecyl sulfonate surfactants were used in gelatin solutions in order to modulate the morphology of gelatin nanofibres and affect the release, antioxidant and antimicrobial activities of the encapsulated curcumin for nutraceutical carrier applications in food industry (Deng et al.,

2017). Unlike sodium dodecyl sulfonate, Tween 80 and cetyltrimethyl ammonium bromide surfactants greatly improved curcumin release into polar solvents.

Along with surfactants, solvents employed for electrospinning have influence on the final properties of the material. In this respect, the effect of aqueous ethanol and isopropanol solvents on zein mats that contain ω-3-rich fish oil was assessed for nutraceutical applications (Moomand & Lim, 2015). It was observed that the electrospinning process generated beaded fibres when aqueous isopropanol was used as a solvent, while smooth and continuous fibres were obtained when aqueous ethanol solvent was employed, influencing the encapsulation efficiency and release velocity. It is worth noting that a modified inverted setup was used to make possible a continuous fibre spinning, since zein solutions tend to clog the needle tip during electrospinning and the addition of lipids to the zein solution further slows down the electrospinning process. Thus, the solvent reservoir in this setup provided a vapour source to reduce effectively the evaporation rate of solvent and to prevent the solidifying of the polymer solution at the needle tip. In addition to inverted electrospinning, coaxial method can also be used with protein-bioactive electrospun materials. Moreover, comparing the single needle electrospinning with the coaxial electrospinning, the latter provides greater control on encapsulation layering, morphology, bioactive loading capacity and retention. Considering this, the microencapsulation of rose hip seed oil into a zein prolamine fibre matrix using the coaxial technique was studied (Yao et al., 2016), and the oil and zein solution were selected as internal medium and sheath material (enveloping medium), respectively. These fibrous zein/oil films showed a significant effect on prolonging the shelf life of selected fruits through a simple packaging process. On top of that, it was concluded that coaxial electrospinning provides better encapsulation for sensitive bioactive compounds compared to the uniaxial electrospinning (Isik et al., 2018).

Nowadays, a novel electrospinning technique, known as free surface or needleless electrospinning, is also used. This modified electrospinning methodology is

used for commercial production of nanofibres whereby electrospinning occurs from a free surface that is not constrained by the geometry of the system (Moreira et al., 2018). Several geometries have been explored, such as rotating drum, disk, wire, and gaseous bubbles (Bhattacharyya et al., 2016).

1.3.4 Freeze-drying

Freeze-drying or lyophilisation technique is used to manufacture 3D protein porous structures (Teimouri et al., 2015; Varley et al., 2016) and generally is employed in the biomedical sector. The use of this method involves solubilisation, pouring, freezing and drying steps (**Figure 1.6**). A suspension of protein is poured into a mould, such as a well of a multiwell plate, and it is solidified (frozen). The freezing step affects the nucleation and growth of ice crystals and so, it determines the morphology and pore sizes of the ice and protein phases. Then, the ice is removed by a freeze-dryer in which the sublimation process of the frozen water leads to the formation of highly porous sponges. It is certain that using this method to produce protein scaffolds, factors such as protein solution concentration and freeze-drying parameters, among others, play very important roles in forming the scaffolds with the desired porous structures (pore geometry, pore size and size distribution, pore interconnectivity, and thickness of pore walls) and therefore, mechanical properties (Deng & Kuiper, 2017; Horn et al., 2018).

Figure 1.6 Schematic illustration of freeze-drying processes.

Collagen scaffolds were prepared by freeze-drying to understand the effect of initial protein concentration on the biophysical properties of the scaffolds (Offeddu et al., 2016). Hence, collagen was suspended in acetic acid at a fixed concentration between

0.5% w/v and 1.5% w/v in increments of 0.25% w/v. The freezing step was carried out at -20 ºC at a rate of 0.5 ºC/min from room temperature, while the drying step took place at 0 ºC under a vacuum of 10.7 Pa. The collagen scaffolds were then cross-linked with 1-ethyl-3-(3-dimethylaminopropyl)carbodiimide hydrochloride and N-hydroxysuccinimide in ethanol-water (95% v/v) at 5:2:1 molar ratio. SEM micrographs showed qualitatively similar pore architecture for all concentrations; however, an increase in both pore wall and strut thickness was observed with increasing collagen concentration. These factors determined the swelling volume on hydrated samples, which increased with collagen concentration. Furthermore, it was observed that the presence of pore walls affected the fluid mobility within the scaffolds. This result could have implications for the diffusion of nutrients and waste, the infiltration of cells, and also the time-dependent mechanical response of scaffolds for tissue engineering applications.

Along with the effect of initial gelatin concentration, lactose-induced cross-linking reaction and bioactive addition on the physicochemical, mechanical and biological properties of porous gelatin scaffolds prepared by freeze-drying were analysed (Etxabide et al., 2018). Gelatin scaffolds were used as carriers of tetrahydrocurcumin, a water-soluble, colourless and tasteless antioxidant, anti-diabetic, anti-cancer and anti-inflammatory plant-derived bioactive compound, for tissue engineering applications, specifically for cartilage regeneration. Tetrahydrocurcumin is a major metabolite of curcumin and it can be extracted from *Curcuma longa* L. (turmeric) by Soxhlet, ultrasonic and microwave extractions methods (Li et al., 2014). The cross-linking reaction between gelatin and lactose notably improved the physical integrity of scaffolds in phosphate buffer solutions (PBS) at 37 ºC, irrespective of the initial gelatin concentration (2.5 and 4.0% w/v). Furthermore, along with the chemical reaction, the increase in the initial gelatin concentration reinforced the scaffold and modified the scaffold morphology, showing less porous structure with larger pores in 4.0% w/v gelatin scaffolds. The water uptake of scaffolds was also affected by the initial gelatin concentration, which affected

the release of tetrahydrocurcumin into PBS media since 82 ± 4% tetrahydrocurcumin was released from 2.5% w/v scaffolds while 64 ± 9% was released from 4.0% w/v scaffolds in the first 8 h. Finally, the biological characterization of scaffolds demonstrated that both gelatin concentrations with tetrahydrocurcumin showed healthy and proliferating cells in the scaffolds.

Protein-polysaccharide mixtures have also been used for scaffolds preparation by freeze-drying (Horn et al., 2018). Nanocomposite scaffolds of zein/chitosan/nanohydroxyapatite at different weight ratios were fabricated by freeze-drying and characterized in order to analyse the scaffold mechanical and *in vitro* properties (Shahbazarab et al., 2017). The increase in nanohydroxyapatite content caused the reduction in porosity and water-uptake capacity of scaffolds, related to the intermolecular hydrogen bonding between the components. With the addition of nanohydroxyapatite into the composite, the degradation rate of scaffolds decreased. By the end of 28 days, the rate of weight reduction for each composite was about 15-20%. This degradation control by changing nanohydroxyapatite, chitosan, and zein amounts could be desirable for tissue engineering applications. During the *in vitro* evaluation of cytotoxicity, an enhancement of cell adhesion, growth, and proliferation was seen with the increase of chitosan and zein.

Several processing technologies and engineering strategies have been combined to create scaffolds with a superior performance for efficient tissue regeneration. In this context, a combination of salt-leaching and freeze-drying technologies was carried out to produce enzymatically cross-linked robust and interconnected porous silk fibroin scaffolds for cartilage tissue engineering (Ribeiro et al., 2018). The salt-leaching method is a simple process to fabricate scaffolds with high porosity and larger interconnected pores and involves the addition of salt particles, such as NaCl or KCl, into polymer solution, the removal of the solvent from the polymer solution, and particle leaching by sample immersion. Granular NaCl particles

(500-1000 µm) were added to the silk fibroin solution and a horseradish peroxidase solution was used to enzymatically cross-link scaffolds. After NaCl particle removal in distilled water, the scaffolds were freeze-dried. The samples presented similar macro- and micro-porous structure at both surface and interior of scaffolds with macro-pores (> 500 µm) and micro-pores (< 50 µm). The enzymatic degradation of the cross-linked scaffolds was also analysed by using protease XIV. It was observed that the scaffold degradation rate was faster in the presence of protease XIV as compared to the control in which the original weight after soaking in PBS solution for 30 days was maintained. Finally, the *in vivo* compatibility of the cross-linked scaffolds was assessed by subcutaneous implantation in a mice model. Staining images showed that a thick layer of connective tissue was adhered on the entire surface of the scaffolds and deeply infiltrated into the porous structures, as well as the presence of connective tissue filling the inner pores of the scaffolds. The absence of edema or signs of neutrophils after the implantation periods revealed that no acute inflammation was induced by the cross-linked scaffolds. Protein-polysaccharide mixtures such as gelatin and chitosan biopolymers have also been used for the fabrication of cell-loaded scaffolds by the combination of salt-leaching/freeze-drying methods for skin tissue engineering applications (Pezeshki-Modaress et al., 2014).

1.3.5 3D printing

3D printing technologies were primarily developed for industrial applications (automotive, aerospace, construction, and cosmetic industry). However, due to their flexibility in creating complex 3D shapes, they have become attractive candidates for biomedical applications, specifically in the field of tissue engineering. In fact, the abovementioned traditional methods of scaffold fabrication generally offer limited control over the macro-architecture since 3D shapes and geometries are determined by moulds and manual processes. With the development of new and more accurate technologies, such as 3D printers, there has been an improvement in the ability to control spatially the

scaffold architecture on the macro and micro level, which resulted in greater reproducibility, higher-level details, and even patient-specific constructs (Bracaglia et al., 2017).

In general, in any 3D printing process, scaffold digital external and internal structures are first designed using a computer aided design (CAD) software or patient specific medical imaging data such as CT scans or X-rays. Then, surface features of the 3D digital files are exported to a file typically with a .STL extension. The .STL file is sliced in a virtual environment into many two-dimensional (2D) layers, used by the 3D printer to create the physical structure. Finally, each layer is processed sequentially one on top of the other to form a designed 3D structure (**Figure 1.7**). Since each part is fabricated layer-by-layer, this type of manufacturing approach is also called "additive manufacturing" (Balakrishnan et al., 2018). Surface modifications can be completed in post-processing in order to modify the nanoarchitecture of printed scaffolds.

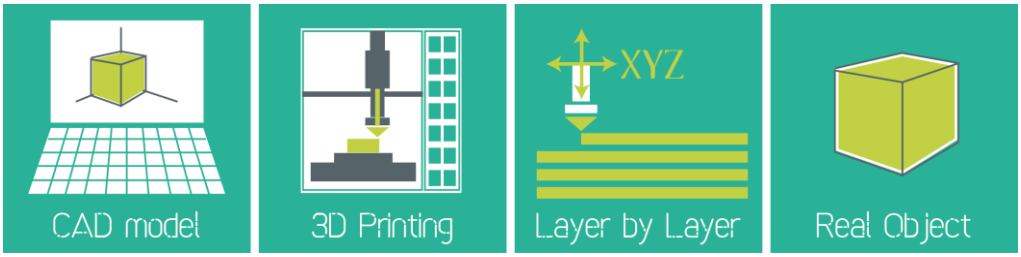

Figure 1.7 Schematic illustration of 3D printing processes.

Currently, there are more than thirty commercial 3D printing systems, such as direct 3D printing, 3D bioprinting, fused deposition modelling, selective laser sintering, stereolithography and indirect 3D printing (Deng & Kuiper, 2017). These systems can be classified based on the form of the model material used in each system, namely liquid (hydrogels/inks), solid (filaments) and powder. With regard to protein printing processes, water soluble biopolymers forming hydrogels (inks) are the major material group used for printing due to their chemical tunability and favourable conditions for cell growth in 3D (Włodarczyk-Biegun & del Campo, 2017).

The 3D printing technology has generally been used in non-food sectors, for instance, to print temporary cell-free scaffolds for use in surgery and/or to print cell-laden inks (bioprinting) (Duan et al., 2013; Luo et al., 2018b; Mandrycky et al., 2016; Na et al., 2018; Pourchet et al., 2017; Rodriguez et al., 2017). However, applying 3D printing in food manufacturing has recently been accelerated (Sun et al., 2015). The purpose of applying 3D printing technology to print food materials is to simplify the production process and combine the design of food with new textures and enhance its nutritional value (Pallottino et al., 2016). For example, various protein food ingredients have been 3D printed in order to design healthy low in fat structures or sugars (Lille et al., 2018; Wang et al., 2018).

1.4 Applications of gelatin-based materials

Among proteins, gelatins are materials with swelling and gelling capacity, as well as with thermal stability (Hashim et al., 2015; Patel et al., 2018). Porcine skin was the first raw material used for the manufacture of gelatin in the 1930s (Gómez-Guillén et al., 2011). Nowadays, commercial gelatin is mainly produced from bovine and porcine skin and bones (Roy et al., 2017), although an increased interest in other sources of gelatin, such as fish gelatin, has been shown. In this context, active gelatin films and coatings can be highlighted (**Table 1.1**).

Regarding porcine gelatin, some antioxidants, such as ascorbic acid (Kowalczyk, 2016) or ethanolic hop extract (Kowalczyk & Biendl, 2016), were incorporated into films and a controlled antioxidant release from gelatin films was observed. Also the ethanolic extract of curcuma was added to porcine gelatin films (Bitencourt et al., 2014). Curcuma contains phenolic compounds responsible for its antioxidant and anti-inflammatory activities. The incorporation of this additive into porcine gelatin films resulted in interactions between the phenolic compounds and gelatin, improving the ultraviolet-visible light barrier properties of gelatin films, besides the improvement of their antioxidant capacity.

Table 1.1 Porcine-, bovine- and fish gelatin-based active films and coatings.

Gelatin	Bioactives	Bioactivity	Reference
Porcine	Ascorbic acid	AO	Kowalczyk 2016
	Ethanol hop extract	AO	Kowalczyk & Biendl 2016
	Curcuma ethanol extract	AO	Bitencourt et al. 2014
Bovine	α-tocopherol, cinnamaldehyde and garlic essential oils	AO	Córdoba & Sobral 2017
	Carrot residue fibre	AO	Iahnke et al. 2015
	Brown seaweed extract	AO	Kadam et al. 2015
	Oregano and lavender essential oils	AM AO	Martucci et al. 2015
Fish	Curcumin/β-cyclodextrin	AO AM	Sun et al. 2019
	Mango peel extracts	AO	Adilah et al. 2018
	Tyrosol, ferulic and caffeic acids, and chitosan	AO	Benbettaïeb et al. 2018
	Aqueous extracts of henna	AM AO	Jridi et al. 2018
	Cinnamon-bark essential oil	AO AM	Kim et al. 2018
	Epigallocatechin gallate	AO	Nilsuwan et al. 2018
	Curcumin/β-cyclodextrin	AO	Wu et al. 2018
	Olive phenols	AM	Bermúdez-Oria et al. 2017
	Aloe vera	AO	Chin et al. 2017
	Tea polyphenol	AM AO	Feng et al. 2017
	Esculine	AO	Liang et al. 2017
	Boldine	AO AM	López et al. 2017
	Coumarin and chitosan	AO	Benbettaïeb et al. 2016
	Chitosan	AM	Feng et al. 2016
	Chitosan nanoparticles	AM	Hosseini et al. 2016
	Thyme essential oil	AM	Lee et al. 2016
	Peppermint and citronella essential oils	AM	Yanwong & Threepopnatkul 2015

AO = antioxidant; AM = antimicrobial

Concerning bovine gelatin, essential oils have been incorporated to inhibit the growth of microorganisms; specifically, oregano and lavender essential oils were found to be effective against food spoilage bacteria, especially gram-positive bacteria, being oregano the essential oil that exhibited the most effective antimicrobial and antioxidant effect (Martucci et al., 2015). Furthermore, α-tocopherol, cinnamaldehyde and garlic

essential oils were nanoemulsified in water and applied to bovine gelatin films in order to manufacture films with a high antioxidant activity (Córdoba & Sobral, 2017). The effect of other natural additives, such as brown seaweed extract, on bovine gelatin films was also analysed and results showed that higher contents of seaweed extract led to an increased antioxidant activity (Kadam et al., 2015). Even waste from minimally processed carrots was used to prepare bovine gelatin films that retard sunflower oil oxidation (Iahnke et al., 2015).

Fish gelatin films and coatings can also be employed to improve food quality and extend food shelf life. Different strategies have been used for this purpose. Cross-linking usually enhances film barrier properties, increasing water, light, and chemical resistance (Azeredo & Waldron, 2016). In this regard, Etxabide et al. (2016a) employed a commercial cod fish gelatin, using lactose as a cross-linker, and Taghizadeh et al. (2018) incorporated riboflavin into fish gelatin film forming solutions to carry out a photosensitizer-induced cross-linking. Both studies showed improved light barrier properties, which highlight the potential of these films to prevent food oxidation caused by light, contributing to extend food shelf life. In recent years, gelatin derived from diverse aquatic fish species has also been employed to prepare active films with antioxidant and/or antimicrobial properties. In this regard, essential oils have been used to produce fish gelatin-based active packaging; in particular, thyme (Lee et al. 2016), oregano (Hosseini et al., 2016), and peppermint and citronella essential oils (Yanwong & Threepopnatkul, 2015), which showed antimicrobial properties against some food spoilage bacteria such as *Staphylococcus aureus* and *Escherichia coli*. Moreover, the incorporation of polyphenols extracted from olives into fish gelatins was found to extend the shelf life of strawberries owing to their antimicrobial activity (Bermúdez-Oria et al., 2017). Also extracts have been incorporated into fish gelatin film forming solutions. Adilah et al. (2018) incorporated mango peels extract, obtaining a material with excellent free radical scavenging activity due to the high presence of polyphenols, carotenoids,

phytochemicals, enzymes, vitamin C and vitamin E on mango peels. It is worth mentioning that mango skins contribute about 7-24% from the whole fruit weight and so, using this by-product will help in reducing waste. *Aloe vera* was also used as an antioxidant agent with fish gelatin, obtaining films that exhibited antioxidant properties dependent on *Aloe vera* concentration (Chin et al., 2017). Thereby, control and 9% *Aloe vera* films showed 66% and 75% DPPH as well as 33% and 65% ABTS radical scavenging activity values, respectively. Similarly, epigallocatechin gallate, one of the major flavanols obtained from tea extract, was added into tilapia skin gelatin film forming solutions in order to prepare active films (Nilsuwan et al., 2018). Apart from providing antioxidant activity, epigallocatechin gallate enhanced the UV light barrier properties of films, contributing significantly to food shelf life extension. In another work, Liang et al. (2017) employed a commonly used traditional Chinese medicine for the extraction of esculine, a natural antioxidant agent, which was then incorporated into sturgeon skin gelatin film forming solutions to prepare films intended to be used as food packaging materials for long-term preservation. Moreover, films containing this antioxidant formed non-covalent cross-linkages between the hydroxyl group of esculine and the amino acid residues of gelatin, which enhanced chemical, physical and mechanical properties. However, some antioxidants show limitations, such as poor solubility; this is the case of curcumin, the major bioactive compound of curcuma rhizome (*Curcuma zedoaria*), which has been regarded as a spice, food preservative, flavouring and colouring agent, approved for use in food industry. Wu et al. (2018) and Sun et al. (2019) encapsulated curcumin in β-cyclodextrin to overcome this problem, and combined the complex with silver carp skin to prepare active films and coatings, respectively. Furthermore, it was observed that curcumin could inhibit microbial propagation. This combination of antioxidant and antimicrobial activities can be observed in several additives used with fish gelatin, for instance, in cinnamon-bark essential oil (Kim et al., 2018), in aqueous extracts of henna (Jridi et al., 2018), and in tea polyphenol (Feng et al., 2017). Furthermore, some fish gelatin species have inherent antimicrobial or antioxidant

activity, as it is the case of Atlantic salmon (López et al., 2017) or cuttlefish (Kchaou et al., 2017), respectively.

Beside cross-linkers and antimicrobial and antioxidant agents' incorporation into fish gelatin films and coatings, blending with other biopolymers, such as polysaccharides, could be another approach to extend food shelf life. For instance, fish gelatin and chitosan, a polymer that has intrinsic antimicrobial properties, have been shown to be compatible. When chitosan is positively charged and gelatin is negatively charged, under proper pH conditions, both biopolymers can be associated through electrostatic and hydrogen bonding. Thus, tilapia fish gelatin-chitosan coatings were analysed and it was found that these coatings significantly prevented deterioration of golden pomfret fillets at 4 ºC, inhibiting the degradation of myosin light chain and myoglobin (Feng et al., 2016). Furthermore, the addition of natural antioxidants (ferulic acid, caffeic acid) showed that gelatin-chitosan films containing caffeic acid or a caffeic-ferulic acid mixture exhibited a high radical scavenging activity (Benbettaïeb et al., 2018).

1.5 Future perspectives and concluding remarks

Massive biowaste is generated by food processing industries. This biowaste can be valorised to obtain raw materials for both food packaging and biomaterials production, reducing the use of non-renewable and non-biodegradable materials in line with the sustainability principles. Actually, biopolymers like collagen and chitin have raised attention because of their natural abundance and the possibility of being obtained from fishery waste and by-products. The chemical and/or biological modification of these biopolymers has been employed for the removal of non-desired substances and the subsequent extraction of gelatin and chitosan. Nowadays, the production of these polymers has been scaled up and these materials are commercially available. In addition to biopolymers extraction, some bioactive compounds can be extracted from food processing wastes or by-products, useful additives for active packaging and biomedical applications.

Vegetal and animal proteins have been considered promising alternatives to develop new sustainable materials. Edible, renewable and environmental friendly are just a few characteristics that turn proteins into excellent raw materials to develop films, mats or scaffolds, among others. In this context, non-designed and designed manufacturing methods have been recently used for the production of protein materials. In this way, films prepared by solution casting or compression moulding are used for food packaging applications in order to extend food shelf life as well as for biomedical applications such as wound healing. Fibre mats obtained by electrospinning can be employed for bioactives' encapsulation for both food and biomedical applications. Scaffolds produced by freeze-drying or 3D printing are mainly used for biomedical applications, such as tissue engineering. Although the addition of bioactives by solution casting, compression moulding and electrospinning has been widely studied, other recent techniques such as 3D printing need in-depth research works to maximize the benefits of bioactives addition into protein-based biomaterials. A technological innovation has been carried out in terms of protein products development, but more research is needed to overcome some engineering limitations of the manufacturing techniques in order to scale-up the production of protein products from proto-type to volume manufacturing processes.

In terms of animal proteins, gelatin has been reported as a potential source for the development of food packaging materials, and it can be an alternative to plastic materials, which use non-renewable resources and lead to environmental problems associated to their treatment after disposal, especially when they are employed for short-term or single-use applications. Thereby, gelatin films, and specially fish gelatin materials, could become more sustainable food packaging.

2 Materials and methods

2.1 Materials and reagents

Commercial fish gelatin (type A, 240 bloom, 125-150 kDa), supplied by Healan Ingredients (East Yorkshire, UK), was used as the main component of the formulations. The amino acid composition of gelatin is showed in **Table 2.1**. Anhydrous citric acid provided by Panreac (Barcelona, Spain), high molecular weight chitosan (deacetylation degree > 75%) gained from Sigma-Aldrich (Madrid, Spain), anthocyanins extracted from red cabbage (*Brassica oleracea* var. *capitata* f. *rubra*) purchased from a local market, and tetrahydrocurcumin (THC) obtained from Sabinsa Europe GmbH (Langen, Germany) were used as bioactive compounds. Glycerol with a purity of 99.01% provided by Panreac (Barcelona, Spain) was used as a plasticizer and β-chitin extracted from fresh squid pens (*Loligo* sp.), fished in the Cantabrian Sea (Spain) during the fishing season (March-August) and kindly supplied by a local fish market, was employed as a reinforcing agent. Gelatin from porcine skin (type A, 280 bloom) utilized as a reference in chapter 3, was obtained from Italgelatine SpA (Cuneo, Italy). Distilled water was used in all formulations.

50% ethanol solution, purchased from Panreac (Barcelona, Spain), was employed as food simulant. Sodium bicarbonate, sodium hydroxide, hydrochloric acid, 2,4,6-trinitrobenzenesulfonic acid (TNBS) and diethyl ether, provided by Sigma-Aldrich (Milano, Italy), were used for the cross-linking extent study. Acetonitrile, formic acid and water, gained from Fisher Scientific (Fair Lawn, NJ, USA), were employed for ultrahigh performance liquid chromatography (UHPLC). Enkephalin hydrated leucine acetate (95% purity) and 0.1 M sodium hydroxide solution obtained from Sigma-Aldrich Chemie (Steinheim, Germany), and trifluoroacetic acid purchased from Merck (Darmstadt, Germany) were also used. 2,2-diphenyl-1-picryl hydrazyl (DPPH) and α-tocopherol supplied by Sigma-Aldrich (Saint-Louis, USA), ethanol purchased from Scharlab (Barcelona, Spain), and pure methanol gained from VWR international (Fontenay-sous-Bois, France) were utilized for assessing parameters related with the antioxidant activity.

Table 2.1 Fish gelatin amino acid composition obtained by ion exchange chromatography.

Fish gelatin amino acids	Composition (%)
Aspartic acid	4.3
Threonine	2.1
Serine	2.8
Glutamic acid	7.2
Proline[a]	19.7
Glycine	33.7
Alanine	13.8
Cysteine	-
Valine	1.7
Methionine	1.5
Isoleucine	0.6
Leucine	2.4
Tyrosine	0.4
Phenylalanine	1.5
Histidine	0.5
Lysine[b]	3.0
Arginine	4.7
Tryptophan	-

[a]Value for proline and hydroxyproline
[b]Value for lysine and hydroxylisine

2.2 Anthocyanins extraction

Anthocyanins were extracted by a conventional solid-liquid extraction, Soxhlet extraction, employing water as solvent. Red cabbage was cut, frozen and lyophilised to obtain the powder and, thus, the filters could be filled more easily and a more efficient process could be carried out. The extraction was repeated twice and the obtained liquid, containing mostly water and anthocyanins, was frozen and then, lyophilised. The extracted anthocyanin powder was kept packaged in a desiccator protected from light.

2.3 Chitin extraction

Before the chitin isolation procedure, squid pens were collected and washed with abundant tap water to remove soluble organics and impurities. Subsequently, pens were

frozen and preserved at -20 ºC until processing. Prior to use, pens were defrosted, cut into 1 × 2 cm^2 pieces, and allowed to dry at room temperature. Squid pens were treated with NaOH (1 M) in a ratio of 1:20 (w/v) at room temperature for 24 h under continuous stirring to avoid possible degradation and deacetylation of native chitin. Then, the mixture was filtered and the solid fraction (β-chitin) was washed several times with distilled water until neutral pH was obtained. Finally, β-chitin was freeze-dried and milled to obtain the powder.

2.4 Mats, films and freeze-dried samples preparation

Three type of samples can be found in this research work: electrospun mats, films obtained by solution casting or compression, and freeze-dried samples. The preparation of these samples are explained in this section.

2.4.1 Electrospinning

Fish gelatin solution (FG solution) was prepared by dissolving citric acid and gelatin in 3 mL of distilled water with citric acid/gelatin/water weight ratio of 0.9:1.0:3.0. The components were mixed together and kept at 50 ºC under constant stirring at 200 rpm for 40 min. In order to modify the pH of this solution, another fish gelatin solution was prepared with NaOH (FG+NaOH solution) at the same conditions (50 ºC under constant stirring at 200 rpm for 40 min). Hence, citric acid and gelatin were dissolved in 2.3 mL of distilled water with a citric acid/gelatin/water weight ratio of 0.9:1.0:2.3 and then 0.7 mL of NaOH (5 M) were added. The pH of the solutions was measured by a calibrated pH meter (XS Instrument pH7). Indeed, the pH of FG was 1.8, while the pH of FG+NaOH was 3.7. The compositions of these fish gelatin solutions were selected on the basis of rheological measurements, taking as a reference a porcine gelatin solution (PG solution). This porcine gelatin solution was prepared as previously described by Panzavolta et al. (2011). In particular, porcine gelatin was dissolved in a solution of acetic acid and distilled water (60/40% v/v acetic acid/distilled water) at a concentration of 30% w/v. The obtained solution was stirred at 50 ºC and 200 rpm for 60 min.

Fish gelatin mats were prepared by the electrospinning technique. The electrospinning apparatus consisted of a high voltage power supply (Spellman SL 50 P 10/CE/230), a syringe pump (KD Scientific 200 series), and a glass syringe containing the polymer solution connected to a stainless-steel blunt-ended needle (inner diameter = 0.51 mm) through a PTFE tube. Electrospinning was performed at room temperature and relative humidity of 40-50%. FG was electrospun by using the following processing conditions: applied voltage = 20 kV, feed rate = 0.3 mL/h, and needle-to-collector distance = 15 cm. The electrospinning of FG+NaOH was carried out using the same parameters employed for FG, except for the voltage and flow rate which were increased up to 23 kV and decreased up to 0.1 mL/h, respectively, due to the higher solution viscosity conferred by NaOH. After fabrication, some mats were subjected to a thermal treatment carried out at 80 ºC for 30 min under vacuum. The obtained mats were stored in a desiccator at 4 ºC until further analysis.

2.4.2 Solution casting

Fish gelatin films were prepared by mixing gelatin and citric acid in distilled water. The acid contents employed in this work were 10, 20, 30 and 40 wt % on gelatin dry basis. Solutions were heated at 80 ºC for 30 min and stirred at 200 rpm. Then, 20 wt % glycerol (on gelatin dry basis) was added as plasticizer and solution pH was adjusted to pH 10 with NaOH (1 M). The heating procedure was repeated and finally, solutions were poured into Petri dishes and allowed to dry for 48 h at room temperature. Films were designated as 0CA, 10CA, 20CA, 30CA and 40CA, as a function of the citric acid content. The films prepared without citric acid (0CA) were used as control films.

Additionally, **fish gelatin/chitosan composite films** were prepared by solution casting. Firstly, 10 and 20 wt % (on gelatin dry basis) citric acid solutions were prepared. These citric acid concentrations were selected based on the previous study of fish gelatin films (Uranga et al. 2016). Then, chitosan was dissolved in 100 mL of citric acid solution and it was maintained under continuous stirring for 30 min. After that, 5 g gelatin were

added and the resultant solution was heated at 80 ºC for 30 min and stirred at 200 rpm. Finally, 20 wt % glycerol (on gelatin dry basis), used as plasticizer, was added, pH was adjusted to 4.5 using NaOH (1 M), and the solution was stirred for other 30 min at 80 ºC and 200 rpm. Film forming solutions were poured into Petri dishes and allowed to dry for 48 h at room temperature as described above. The amount of chitosan in films was 0, 3, 6 and 9 wt % (on gelatin dry basis) and films were designated as 10CAXCHI or 20CAXCHI for the films prepared with 10 and 20 wt % citric acid, respectively, as a function of the chitosan content (X). Furthermore, control films without citric acid and chitosan (0CA0CHI) were prepared.

All films were conditioned in a controlled environment chamber (ACS SU700V) at 25 ºC and 50% relative humidity before testing. The film thickness was measured to the nearest 0.001 mm with a hand-held QuantuMike digimatic micrometer (Mitutoyo Spain, Elgoibar, Spain) and the obtained values were 116 ± 29 μm in fish gelatin films and 50 ± 2 μm in fish gelatin/chitosan films.

2.4.3 Compression moulding

Anthocyanin containing fish gelatin films were prepared by compression moulding. Firstly, all components were mixed: 5 g of gelatin, 40 wt % water, 20 wt % glycerol, 10 wt % citric acid, and 10 wt % anthocyanins (on gelatin dry basis). Secondly, mixtures were thermally compacted using a caver laboratory press, previously heated up to 60 ºC, by applying a pressure of 0.8 MPa for 2 min, conditions determined after some preliminary tests. All films were conditioned in a controlled environment chamber (ACS SU700V) at 25 ºC and 50% relative humidity before testing. The film thickness was measured to the nearest 0.001 mm with a hand-held QuantuMike digimatic micrometer (Mitutoyo Spain, Elgoibar, Spain) and the average value obtained was 86 ± 7 μm.

2.4.4 Freeze-drying

Chitin and THC containing fish gelatin samples (**Table 2.2**) were prepared by freeze-drying. Fish gelatin solutions (3.5 g gelatin in 50 mL distilled water) with citric acid, chitin and THC were heated at 80 ºC for 30 min and stirred at 200 rpm. Then, glycerol was added and solution pH was adjusted to 10 with NaOH (1 M). Solutions were heated at 80 ºC for other 30 min stirring at 200 rpm and finally poured into a 24 multiwell plate, which was kept in the fridge at 4 ºC to cool down. Once the solutions were gelled, the plate was kept in a freezer at -23 ºC and then, freeze-dried for 48 h (Alpha 1-4 LDplus, CHRIST, Germany). Finally, freeze-dried gelatin samples (1.5 cm diameter and 1 cm height) were taken out from the wells.

Table 2.2 Composition of the freeze-dried samples.

Sample	Fish gelatin (% w/v)	Citric acid (% w/w)	Glycerol (% w/w)	Chitin (% w/w)	THC (% w/w)
Control	7	20	20	0	0
CHI15	7	20	20	15	0
CHI30	7	20	20	30	0
CHI15-THC	7	20	20	15	5
CHI30-THC	7	20	20	30	5

Fish gelatin percentage is expressed on water basis, while additives percentages are expressed on gelatin dry basis.

2.5 Rheological assessment

The rheological measurements of electrospinning solutions were performed using a rotational rheometer (Anton Paar MCR 102) operating in a plate-plate configuration. Experiments were performed keeping the temperature constant at 25 ºC, through the integrated Peltier system and a Julabo AWC100 cooling system. The sample was kept hydrated during the measurements through the use of a solvent trap (H-PTD200). Time-sweep oscillatory tests were carried out at a fixed strain amplitude of 0.3% and an angular frequency of 1 rad/s.

2.6 Surface and structure characterization

2.6.1 Optical microscopy (OM)

A polarized optical microscope (Zeiss Axioscop) was used to detect electrospun fibres directly collected on glass slides during electrospinning.

2.6.2 Scanning electron microscopy (SEM)

The morphology of electrospun materials was observed employing a 515 scanning electron microscope (Philips) at an acceleration voltage of 15 kV. Samples were mounted on a metal stub with a double-side adhesive tape and sputter-coated with gold before SEM observation. This analysis was carried out 24 h after mat fabrication. The distribution of fibre diameters (average and standard deviation) was measured on the SEM images of about 50 fibres by means of ImageJ software.

On the other hand, the morphology of the fracture surfaces of anthocyanin containing films as well as the morphology of chitin containing samples were visualized using an S-4800 field emission scanning electron microscope (Hitachi High-Technologies Corporation). Samples were mounted on a metal stub with a double-side adhesive tape and coated under vacuum with gold (JFC-1100) in an argon atmosphere prior to observation. Anthocyanin containing films were examined using an accelerating voltage of 5 kV, whilst chitin containing samples were analysed employing an accelerating voltage of 10 kV. Moreover, SEM images were analysed by ImageJ software for pore size evaluation.

2.6.3 Wide angle X-ray diffraction (WXRD)

WXRD analysis for electrospun mats was carried out using a powder diffractometer (PANalytical) endowed with a fast X'Celerator detector. The radiation was generated from a CuK_{α} (λ = 0.15418 nm) source (40 mA, 40 kV). WXRD data were obtained from 2θ values from 5º to 60º, where θ is the incidence angle of the X-ray beam on the sample.

2.7 Physicochemical characterization

2.7.1 Fourier transform infrared (FTIR) spectroscopy

FTIR spectra were carried out on a Nicolet Nexus FTIR spectrometer using ATR Golden Gate (Specac). A total of 32 scans were performed at a resolution of 4 cm^{-1} in the wavenumber range from 800 to 4000 cm^{-1}. Savitzky-Golay function was used for the spectra smoothing. Second-derivative spectra of the amide region were used at peak position guides for the curve fitting, according to the procedure described by Byler & Susi (1986), using OriginPro 9.1 software.

2.7.2 Cross-linking extent

The cross-linking extent of mats was measured according to the method of Panzavolta et al. (2011). Three specimens were tested for each composition. Briefly, an UV assay of uncross-linked ε-amino groups was performed on differently treated mats and on fish gelatin as reference. After the reaction with 0.5% TNBS, gelatin was hydrolysed with HCl (6 M) and extracted with diethyl ether. The solution's absorbance was measured against a blank at 346 nm. The moles of free ε-amino groups per gram of gelatin were calculated by the following equation:

$$[\mathrm{NH_2}] = \frac{2 \cdot \mathrm{A} \cdot \mathrm{V}}{\varepsilon \cdot \mathrm{b} \cdot \mathrm{x}}$$

where A is the sample absorbance, V is the final sample volume (L), ε is the molar absorptivity of TNP-lys, precisely 1.46 x 10^4 L/(mol·cm), b is the cell path length (cm) and x is the sample weight (g).

The cross-linking extent was determined from the ratio between the moles of cross-linked ε-amino groups of treated gelatin mats (obtained as a difference between uncross-linked groups before and after cross-linking) with respect to ε-amino groups measured in fish gelatin.

2.7.3 Moisture content (MC) and total soluble matter (TSM)

To determine the MC of films, three specimens of each film were weighed (w_0) and then dried in an oven at 105 ºC for 24 h. After this time, samples were reweighed (w_1) to determine their MC:

$$\mathrm{MC}\ (\%) = \frac{w_0 - w_1}{w_0} \cdot 100$$

To obtain TSM values, the dried specimens were immersed in 200 mL of distilled water for 24 h. Afterwards, the films were dried in the oven at 105 ºC for 24 h and weighed (w_2). TSM values were calculated by the following equation:

$$\mathrm{TSM}\ (\%) = \frac{w_1 - w_2}{w_1} \cdot 100$$

2.7.4 Swelling measurement

In order to study the swelling of fish gelatin/chitosan composite films, first, three film disks (Ø = 52 mm) of each composition were weighed (w_H) and then, immersed into distilled water. Samples were weighed after immersion into water for specific times (w_T), until getting constant values. The swelling (S) was calculated according to the following equation:

$$S\ (\%) = \frac{w_T - w_H}{w_H} \cdot 100$$

Swelling of chitin containing samples was calculated by immersing three specimens of each composition into 50% ethanol solution and repeating the procedure above explained.

2.8 Thermal characterization

2.8.1 Thermo-gravimetric analysis (TGA)

Thermal stability was analysed by TGA and measurements were performed in a Mettler Toledo TGA SDTA 851 equipment (Mettler Toledo S.A.E.). The samples were

heated from 25 to 800 ºC at a heating rate of 10 ºC/min under inert atmosphere conditions (10 mL N_2/min) to avoid thermo-oxidative reactions.

2.8.2 Differential scanning calorimetry (DSC)

DSC was carried out in a Mettler Toledo DSC 822 (Mettler Toledo S.A.E.). Samples (3.0 ± 0.2 mg) were sealed in aluminium pans to avoid mass loss during the experiment. Filled pans were heated from 25 to 250 ºC at a rate of 10 ºC/min under inert atmosphere conditions (10 mL N_2/min) to avoid thermo-oxidative reactions.

2.9 Optical properties

2.9.1 Colour measurement

Colour parameters (L*, a*, b*) were determined using a CR-400 Minolta Chroma-Meter colourimeter (Konica Minolta). Films were placed on the surface of a white standard plate (calibration plate values: L* = 97.39, a* = 0.03 and b* = 1.77) and colour parameters were measured using the CIELAB colour scale: L* = 0 (black) to L* = 100 (white), -a* (greenness) to +a* (redness), and -b* (blueness) to +b* (yellowness). Measurements were taken five times for each sample. Colour difference (ΔE*) was calculated referred to the control specimen:

$$\Delta E^* = \sqrt{(\Delta L^*)^2 + (\Delta a^*)^2 + (\Delta b^*)^2}$$

2.9.2 Gloss measurement

Film gloss was determined using a Multi Gloss 268 Plus gloss meter (Konica Minolta). Gloss values were measured at 60º incidence angle, according to ASTM D523-14 (ASTM, 2014). Measurements were taken ten times for each sample.

2.9.3 Ultraviolet-visible (UV-vis) spectroscopy

Light absorption was measured in the UV-vis range (200-800 nm) using a V-630 UV-vis spectrophotometer (Jasco). Transparency (T) values were calculated by the following equation:

$$T = \frac{A_{600}}{x}$$

where A_{600} is the absorbance at 600 nm and x is the film thickness (mm).

2.10 Barrier properties and moisture scavenging

2.10.1 Water contact angle (WCA)

OCA20 Contact Angle System (DataPhysics Instruments) was used to measure WCA values. For each measurement, a 3 µL droplet of distilled water was placed on the film surface. The image of the drop was taken using SCA20 software. Measurements were taken five times for each sample.

2.10.2 Water vapour permeability (WVP)

WVP values were measured in a controlled humidity environment chamber PERME™ W3/0120 (Labthink Instruments Co. Ltd.). Film disks (Ø = 7.4 cm) were sealed to cups containing distilled water, three specimens for each composition. Then, cups were placed into the chamber at 38 ºC and 90% relative humidity, according to ASTM E96-00 (ASTM, 2000). WVP was determined gravimetrically as follows:

$$WVP\left(\frac{g}{s \cdot cm \cdot Pa}\right) = \frac{w \cdot x}{A \cdot t \cdot \Delta P}$$

where w is the weight change (g), x is the film thickness (cm), A is the film area (cm^2), t is time (s) and ΔP is the partial pressure difference of water vapour across the film (Pa).

2.10.3 Moisture absorption kinetics

The moisture absorption of chitin containing samples was measured according to the method of Bovi et al. (2018) with some modifications. Three specimens of each composition were measured. First, samples were dried in a desiccator and then, stored in a controlled chamber at room temperature and 100% relative humidity in order to simulate extreme humidity conditions. Moisture absorption was gravimetrically

determined by measuring the weight increase at regular intervals for 31 days. The moisture absorbed (MA) was calculated as follows:

$$\mathrm{MA}\left(\frac{\mathrm{g\ water}}{\mathrm{g\ sample}}\right) = \frac{\mathrm{w_{tm}} - \mathrm{w_i}}{\mathrm{w_i}}$$

where w_i and w_{tm} are the weight of the samples (g) at the beginning of the test and at specific times, respectively.

After calculating MA values, the probabilistic Weibull model was used to define the moisture scavenging and describe the curves of moisture absorbed versus time:

$$\mathrm{MA} = \mathrm{M_0} + (\mathrm{M_\infty} - \mathrm{M_0}) \cdot \left[1 - e^{\left(\frac{-\mathrm{t}}{\beta_1}\right)}\right]$$

where M_0 is the initial moisture content of the sample (g water/g sample), which is zero as specimens were previously dried; M_∞ is the moisture holding capacity (g water/g sample) at equilibrium; and β_1 is the kinetic parameter that defines the rate of moisture uptake process and represents the time needed to accomplish approximately 63% of the moisture uptake process. Thus, this Weibull model offers the possibility of estimating the M_∞ with the experimental MA data.

2.11 Mechanical properties

2.11.1 Tensile test

Tensile strength (TS) and elongation at break (EB) were determined using Insight 10 Electromechanical Testing System (MTS Systems), equipped with a tensile load cell of 250 N. According to ASTM D638-03 (ASTM, 2003), the crosshead speed was set at 1 mm/min and samples with 22.25 mm length and 4.75 mm width were used. Five samples were analysed for each composition.

2.11.2 Compression test

Compression tests of chitin containing samples were performed using a TA XT plus Texture Analyser (Stable Micro Systems) equipped with a 30 kg load cell. The analysis was carried out with a 36 mm Dia Aluminium Radiused AACC probe, which has a contact area of 1017.88 mm^2. The crosshead speed was set at 1 mm/s, the activation force was 0.01 N and the software utilized was Exponent. The chitin containing samples were previously dried in a desiccator for 24 h and then, stored in a controlled chamber (100% relative humidity and room temperature) for 6 days, in order to get approximately 63% of the moisture absorbed. Compression resistance of three humid samples for each composition was evaluated at room temperature and load was applied until the specimen was compressed to around 80% of its original height. At the end of this first test, samples recovered their initial size, thus, specimens were stored again in a controlled chamber (100% relative humidity and room temperature) for 11 days, in order to get absorbed nearly 100% of the moisture uptake and make a second compression test. A graph representing stress (MPa) against strain (%) was plotted with the obtained values in both tests.

2.12 Antibacterial assessment

The antibacterial activity of fish gelatin/chitosan composite films was tested against the growth of a Gram-negative bacteria, *Escherichia coli* DH5α, to analyse the influence of citric acid and chitosan. *E. coli* was grown overnight in Luria Bertani (LB) broth (Sambrook et al., 1989) at 37 ºC with shaking (160 rpm). Then, it was inoculated into fresh LB medium and grown up to the mid-exponential phase at 37 ºC and it was used to inoculate 10 mL media containing 0.04 g of film and incubated for 24 h at 37 ºC and 160 rpm. The experiments were repeated twice for the evaluation of each composition. Samples from cultures were taken at 5 h since *E. coli* had grown up actively after this time. The plate dilution method was used to monitor cell viability on LB agar plates incubated at 37 ºC and results were reported as CFU/mL.

2.13 Anthocyanins characterization by UHPLC-Q-TOF-MS/MS analysis

Ultrahigh performance liquid chromatography (UHPLC) was carried out by using an ACQUITY UPLC™ system (Waters, Milford, MA, USA), equipped with a binary solvent delivery pump, an autosampler, a column compartment and a PDA detector. UHPLC analysis was carried out immediately after the dilution of samples in 0.1% trifluoroacetic acid solutions in water. A reverse phase column (Acquity UPLC BEH C18 1.7 µm, 2.1 mm × 100 mm) and a precolumn (Acquity UPLC BEH C18 1.7 µm VanGuard™) from Waters (Milford, USA) were used at 40 ºC for the separation of individual anthocyanins. The flow rate was 0.25 mL/min and the injection volume was 7.5 µL. Mobile phases consisted of 0.1% trifluoroacetic acid in water (A) and 0.1% trifluoroacetic acid in acetonitrile (B). Separation was carried out in 17 min under the following conditions: 0.00-3.17 min, linear gradient from 5 to 15% B; 3.17-5.43 min, 15% B; 5.43-6.00 min, linear gradient from 15 to 20% B; 6.00-12.00 min, linear gradient from 20 to 21% B; 12.00-13.00 min, linear gradient from 21 to 100% B; and finally, washing and re-equilibration of the column prior to the next injection. All samples were kept at 4 ºC during the analysis. The wavelength range of the PDA detector was 210-500 nm (20 Hz, 1.2 nm resolution). Anthocyanins were monitored at 500 nm.

All mass spectrometry (MS) data acquisitions were performed on a SYNAPT™ G2 HDMS with a quadrupole time of flight (Q-TOF) configuration (Waters, Milford, MA, USA), equipped with an electro-spray ionisation (ESI) source operating in positive mode. The capillary voltage was set to 1.0 kV. Nitrogen was used as the desolvation and cone gas at flow rates of 1000 L/h and 10 L/h, respectively. The source temperature was 120 ºC, and the desolvation temperature was 400 ºC. A leucine-enkephalin solution (2 ng/µL) in acetonitrile:water (50:50 (v/v) + 0.1% formic acid) was utilized for the lock mass correction and the ions at mass-to-charge ratio (m/z) 556.2771 and 278.1141 in the positive ionisation mode from this solution were monitored (0.3 s scan time, 10 s interval, 3 average scans, ± 0.5 Da mass window, 30 V cone voltage, 10 µL/min flow

rate). Data acquisition took place over the 50-2000 u mass range in resolution mode (FWHM ≈ 20,000) with a scan time of 0.1 s and an interscan delay of 0.024 s. All the acquired spectra were automatically corrected during acquisition based on the lock mass. Before analysis, the mass spectrometer was calibrated with a sodium iodide solution.

To perform MS^E mode analysis, the cone voltage was set to 20 V (ESI+) and the first quadrupole (Q1) operated in a wide band RF mode only. Two discrete and independent interleaved acquisition functions were automatically created. The first function, typically set at 6 eV in trap cell of the T-Wave, collected low energy or unfragmented data, while the second function collected high energy or fragmented data, using 6 eV in trap cell and a collision ramp of 10-40 eV in transfer cell. In both cases, argon gas was used for collision-induced dissociation (CID) and data were recorded in centroid mode.

MS^2 product ion spectra was performed using the protonated molecule $[M]^+$ as precursor ion at a cone voltage of 20 V. A collision energy ramp from 10 to 40 eV in trap cell and of 6 eV in transfer cell was used with the aim of acquiring spectra with different fragmentation degrees from the precursor ion and, thus, obtaining as much structural information as possible. MS/MS data were collected at a range of 50-2000 m/z in centroid mode in the same conditions as described above.

The identification of the anthocyanin compounds was carried out using the UV-vis spectrum to assign the phenolic class (Abad-García et al., 2009), the low collision energy MS^E spectrum in positive mode to determine the molecular weight, the high collision energy MS^E and MS^2 product ion spectra to assign the protonated aglycone $[Y_0]^+$ and observed fragmentations in order to elucidate other structural details. The nomenclature proposed by Domon & Costello (1988) for glycoconjugates was adopted to denote the fragment ions.

2.14 Bioactive release

The anthocyanin release was determined by immersion of films (1.5 cm × 2.0 cm) into a 50% ethanol solution (5 mL) at 4 ºC for 2 days, whilst THC release was assessed by immersion of freeze-dried samples into a 50% ethanol solution (20 mL) at room temperature for 3 days. Samples were immersed into dark glass vessels to protect the bioactive compounds from light. V-630 UV-vis spectrophotometer (Jasco) was employed to measure light absorption from 200 to 800 nm. The absorption spectra of the solutions were recorded every 15 min up to 2 h and then, every 24 h up to 2 or 3 days for films and freeze-dried samples, respectively. The experiments were repeated in triplicate for the evaluation of each composition.

2.15 Antioxidant activity by DPPH radical scavenging activity

Anthocyanin aqueous solutions (2 mM) were prepared at three different pHs: acid (2.5), basic (10.0) and non-modified (6.0) pHs to analyse the effect of pH on the antioxidant activity. DPPH radical scavenging activity was measured for each solution as well as for anthocyanin containing films, according to the method of Etxabide et al. (2017b). Briefly, 2 mL of anthocyanin solution or anthocyanin released solution were mixed with 2 mL of DPPH solution (75 μM). The mixture was vigorously shaken and then, allowed to stand at room temperature in the dark for 30 min. The inhibition values (I) were determined by the absorbance decrease at 517 nm as follows:

$$\mathrm{I}\,(\%) = \frac{\mathrm{A_c} - \mathrm{A_{sample}}}{\mathrm{A_c}} \times 100$$

where A_c is the absorbance of the DPPH solution and A_{sample} is the absorbance of the DPPH solution with the antioxidant. All tests were carried out in triplicate.

2.16 Environmental assessment

Life cycle assessment was performed according to ISO 14040 guidelines (ISO 14040, 2006) and recommendations. The analysis was carried out with the SimaPro

software (PRé Consultants, The Netherlands) and data were obtained from Ecoinvent database. On the one hand, the IPCC 2007 method was employed to perform the carbon footprint of gelatin films and it was expressed as global warming potential (GWP). Three stages were taken into account in this study, specifically, raw material extraction, film manufacture, and the end of life, and the functional unit considered was 1 m^2 of film. On the other hand, the environmental assessment of chitin extraction procedure was studied. The inventory analysis of chitin was carried out considering the materials used in the laboratory, the energy consumption regarding the extraction step, as well as the transportation of the squid pens (Hondarribia-San Sebastian) and the residues of the extraction process (San Sebastian-Legutio). The functional unit considered in this study was 1 g of chitin. Environmental impacts were evaluated according to the Hierarchist version of ReCiPe 2016, midpoint. The following impact categories were analysed: global warming, stratospheric ozone depletion, ionizing radiation, ozone formation (human health), fine particulate matter formation, ozone formation (terrestrial ecosystems), terrestrial acidification, freshwater eutrophication, marine eutrophication, terrestrial ecotoxicity, freshwater ecotoxicity, marine ecotoxicity, human carcinogenic toxicity, human non-carcinogenic toxicity, land use, mineral resource scarcity, fossil resource scarcity, and water consumption.

2.17 Statistical analysis

Analysis of variance (ANOVA) was used to determine the significance of differences among samples. The analysis was performed with a SPSS computer program (SPSS Statistic 23.0) and Tukey's test was used for multiple comparisons. All the assays were done at least in triplicate. Differences were statistically significant at the $P < 0.05$ level. In the case of fish gelatin/chitosan composite films, this analysis was carried out separately for the systems with 10 and 20 wt % citric acid, in order to estimate the significant differences as a function of chitosan content.

3 Electrospun fish gelatin mats

3.1 Summary

Due to gelatin biocompatibility, biodegradability and low cost, it is employed in different fields, such as food industry, pharmaceutical and medical applications (Dolci et al., 2018; Gómez-Estaca et al., 2015; Khor, 1997; Su & Wang, 2015). Moreover, gelatin shows binding sites for cell adhesion, signalling and differentiation, which make this polymer suitable in tissue engineering, wound dressing and drug delivery field (Aduba et al., 2013; Angarano et al., 2013; Li et al., 2005; Mano & Reis, 2007; Panzavolta et al., 2011). In these sectors, electrospun fibrous mats are highly demanded, since they mimic the extracellular matrix and promote cell adhesion and proliferation due to their high porosity and surface area.

However, due to water solubility, gelatin mats do not maintain their morphology when they come in contact with water. In order to improve water resistance, physical (Liguori et al., 2016) and chemical (Gualandi et al., 2016; Ratanavaraporn et al., 2010; Zhang et al., 2006) cross-linking methods have been proposed. In this chapter, a natural cross-linker (citric acid) was used. Citric acid is an aliphatic bio-based polycarboxylic acid that contains two reactive primary carboxylic groups, one less reactive tertiary carboxylic group, and one sterically hindered hydroxyl group (Hazarika & Karak, 2015). It is commercially available at low cost and it has non-toxic nature since it is produced as a metabolic product of the body (Krebs or citric acid cycle) in all living cells that use oxygen as part of the cellular respiration (Rocha-García et al., 2017). This acid has been already demonstrated to be suitable for the cross-linking of proteins (Cumming et al., 2018; Jiang et al., 2010, 2013; Reddy et al., 2011). The carboxylic groups of citric acid can undergo nucleophilic acyl substitution with the ε-amines of lysine, leading to the formation of stable amide bonds (Cumming et al., 2018). Saito et al. (2004) reported the use of a citric acid derivative, obtained through the modification of citric acid carboxyl groups with N-hydroxysuccinimide in presence of 1-ethyl-3-(3-dimethylaminopropyl)carbodiimide hydrochloride, for the preparation of cross-linked type A porcine skin gelatin gels. More

recently, Shafagh et al. (2018) reported the use of citric acid to cross-link porcine skin gelatin in presence of Ag nanoparticles to produce, through a green approach in which water was used as solvent, gelatin/Ag nanocomposite hydrogels with swelling and a drug release behaviour both depending on pH. Moreover, Jiang et al. (2014) employed citric acid to produce cross-linked electrospun gelatin fibres using acetic acid as solvent and sodium hypophosphite as a catalyst of the citric acid, followed by a thermal treatment at 150 ºC for 4 h to induce cross-linking.

No works have dealt so far with the production of cross-linked fish gelatin electrospun fibres by using an aqueous solution of citric acid, avoiding acetic acid or other chemicals. Therefore, the aim of the present work was to develop a protocol to make feasible, for the first time, the electrospinning process of fish gelatin by using only a natural and non-toxic cross-linker, such as citric acid, in aqueous solution to obtain cross-linked fibres. The effect of the solution's pH on electrospinnability and morphological and chemical properties of the resulting mats was investigated. Furthermore, the effect of a subsequent thermal treatment of the mat on its morphological and chemical properties was also assessed.

3.2 Results and discussion

3.2.1 Electrospinning of fish gelatin

It has been widely reported that the addition of an acid to water solutions, or the use of solvents such as 1,1,3,3,3-hexafluoro-2-propanol, is required for gelatin electrospinning to prevent gelation that hinders and even blocks the solution flow through the syringe needle and capillary during the spinning process (Djabourov et al., 1988; Erencia et al., 2015). Due to the possible toxicity of the most employed acids or organic solvents, efforts have been devoted to the fabrication of gelatin electrospun fibres using solutions of benign acids in water. Acetic acid, malic acid and citric acid water solutions, as binary, ternary and quaternary solvents, were recently used to manufacture fish

gelatin-based electrospun mats (Erencia et al., 2015; Mahmood et al., 2019). Although positive results on the feasibility of the process were achieved for water/acetic acid solvents, citric acid based binary solvent was reported to be non-suitable for developing fibres (Mahmood et al., 2019).

Considering both the absence of toxicity of citric acid and its potential cross-linking action, in this work efforts have been carried out to identify a procedure for the production of cross-linked fish gelatin electrospun mats using a spinning solution containing only citric acid in an aqueous solution (FG). In particular, the effect of solution's pH on the electrospinning process, mat properties and cross-linking degree was investigated by adding NaOH to the fish gelatin/citric acid/water solution (FG+NaOH) in order to increase the pH of fish gelatin solution from 1.8 to 3.7, on the basis of a previous study on collagen electrospun fibres cross-linked with citric acid (Cumming et al., 2018). In the mentioned work, the highest cross-linking extent was achieved from a solution containing collagen and citric acid with pH 3.5, a result that was attributed to a more effective formation of citric anhydride at this pH (Cumming et al., 2018; Higuchi et al., 1963).

Given the importance of flow properties and viscoelastic behaviour of the solution in the electrospinning process, FG composition was optimised on the basis of rheological measurements, taking as a reference a porcine gelatin solution (PG) whose electrospinnability was previously demonstrated by some authors (Panzavolta et al., 2011). The storage modulus (G') and the loss modulus (G'') for the analysed solutions over 1 h 40 min period are shown in **Figure 3.1**. Fish gelatin showed a rheological behaviour similar to that of porcine gelatin. Indeed, although FG moduli were slightly lower than those of PG, both solutions behaved as viscoelastic liquids (G'<G'') at initial times (up to 12 min for PG and up to 23 min for FG), then they switched to a solid-phase dominated behaviour (G'>G'') as demonstrated by the achievement of the cross-over, referred to as the "gel point" attributed to the increased molecular association. Finally,

the moduli reached a fairly constant value. The presence of NaOH affected the viscoelastic properties of the solutions. Indeed, FG+NaOH presented higher values of G' and G'' than FG, even higher than PG, and it showed no cross-over and a solid-phase dominated behaviour since the beginning of the measurement. This result might indicate that cross-linking reactions due to citric acid were more likely to happen in the solution at pH 3.7 rather than in that at pH 1.8.

For all the solutions, even if a gel point was observed and the solid-like behaviour dominated over time, the small differences between G' and G'' indicated the formation of a weak gel that did not hinder electrospinnability of the solutions.

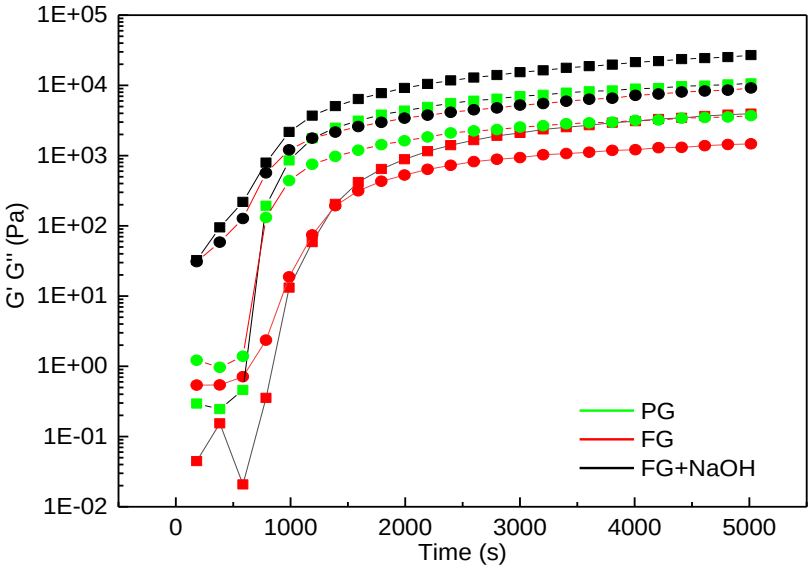

Figure 3.1 Time dependence of storage modulus (G') (square) and loss modulus (G") (circle) of PG (green curves), FG (red curves), and FG+NaOH (black curves).

3.2.2 Characterization of fish gelatin electrospun mats

The OM and SEM images of the electrospun mats obtained from FG and FG+NaOH are reported in **Figure 3.2**. Interestingly, the OM images (**Figures 3.2a**,**d**) showed that bead-free and regular microfibres were obtained for both FG and FG+NaOH. In contrast to previous findings (Mahmood et al., 2019), our results

demonstrated that electrospinning of fish gelatin to form microfibres from a citric acid/water solution without the addition of acetic acid was possible. However, although both the solutions turned out to be electrospinnable, the fibrous morphology of mats obtained from FG was not preserved over time, since the mats turned into films with a barely recognizable fibrous structure in few hours, as demonstrated by the SEM micrographs (**Figure 3.2b**). However, addition of NaOH to fish gelatin solutions increased the pH values from 1.8 to 3.7 and improved the fibre stability over time. The obtained fibrous mat was able to preserve its morphology better than fibres obtained from FG (compare **Figures 3.2b**,**e**), although fibre fusion at their contact points could be noticed. Moreover, in agreement with previous literature findings (Cumming et al., 2018; Jiang et al. 2014), the thermal treatment performed on these mats immediately after their fabrication came out to get a beneficial effect on the resulting morphology, since the fibrous morphology of the mats was better maintained with respect to the as spun mats (**Figures 3.2c**,**f**). It is pointed out that, even if the fibre diameter was hardly measurable due to the many fusion points among fibres, after the thermal treatment a fibre diameter of 2.19 ± 0.07 μm and 4.42 ± 0.05 μm was evaluated for FG and FG+NaOH mats, respectively.

To assess the extent of the cross-linking reaction between gelatin and citric acid, the amount of ε-amino groups of gelatin reacted with citric acid was calculated. In line with the morphological results, only a small amount of ε-amino groups was cross-linked with citric acid in the mats obtained from FG, leading to a cross-linking extent of 12%. On increasing the pH up to 3.7 in FG+NaOH, cross-linking extents of 25% and 38% were achieved for FG+NaOH mat as spun and thermally treated, respectively. These results were in agreement with previous findings (Xu et al., 2015) and highlight that in the water solution of fish gelatin with citric acid the cross-linking reactions can take place also at room temperature, even if an increase of temperature up to 80 ºC is needed to speed up such cross-linking reaction.

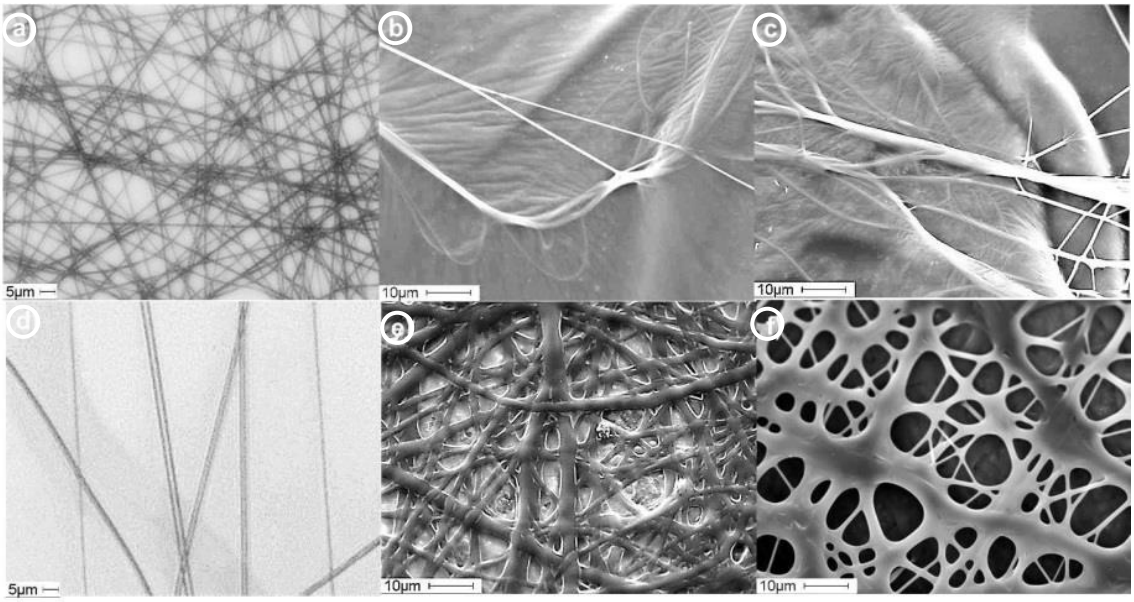

Figure 3.2 OM (a, d) and SEM images (b, c, e, f) of electrospun mats from FG (a, b, c) and FG+NaOH (d, e, f): mats as spun (a, b, d, e) and after the thermal treatment (c, f).

On the basis of the above described results, the following considerations could be drawn. For the mat obtained from FG, the barely recognizable fibrous morphology was well explained by the low cross-linking extent of the fibres and it was mainly ascribed to the low pH of the solution, since at pH 1.8 the cross-linking reactions could difficultly take place. Moreover, the widely reported mechanism driving the cross-linking of proteins or molecules containing amino groups in the presence of citric acid lies in the formation of reactive citric anhydride from citric acid and in the nucleophilic substitution occurring between the carboxyl groups of the anhydride and the amino groups of the considered protein or molecule (Cumming et al., 2018; Higuchi et al., 1963; Xu et al., 2015). Since type A fish gelatin was employed in this work and its isoelectric point is in the pH range of 6.0-9.5 (Alfaro et al., 2015), the protonation of the amine groups took place in the strong acidic conditions of FG (pH 1.8), thus limiting the cross-linking reaction. An increase of pH up to 3.7, even if lower than fish gelatin isoelectric point, would favour the deprotonation of $-NH_3^+$ groups into $-NH_2$, and the above described nucleophilic substitution was more likely to occur with the formation of amide groups. The pH value of 3.7 was thus selected in order to achieve the best compromise between the number

of amine groups available for cross-linking and the known cross-linking mechanism of citric acid, which has been reported to occur at the highest extent at pH 3.5 (Cumming et al., 2018).

The influence of the electrospinning process on structural properties of gelatin was investigated on fish gelatin powder and on the obtained mats through wide angle X-ray diffraction (WXRD) analysis. In that way, the relative triple-helix content of fish gelatin materials was analysed in detail (**Figure 3.3**). It is well known that the collagen WXRD pattern includes two broad diffraction bands. The first one, centered at about 8º, related to the triple-helix diameter, while the second one at around 21º is related to the distance between amino acidic residues in the helix. These reflections are typically observed also in the pattern of partially renaturated gelatin powder and gelatin films (Gioffrè et al., 2012).

In agreement with these data, fish gelatin powder exhibited the two reflections centered at about 8º and 21º (**Figure 3.3**), as previously reported (Etxabide et al., 2016b; Sha et al., 2014). However, reflection at 8º disappeared after the electrospinning process of both FG and FG+NaOH as a consequence of acidic pH. This result could be explained considering that, as previously observed for gelatin solubilised in acetic acid solutions (Panzavolta et al., 2011), citric acid prevented the gelatin's partial renaturation, which takes place during gelling from aqueous solution, and a random coil conformation was favoured, decreasing the number of single left-hand helix chains and residual triple-helix conformations. Furthermore, citric acid also influenced the diffraction reflection located at about 21º, whose intensity decreased as a consequence of the decrease of the single left-hand helix chain content. Addition of NaOH to fish gelatin solution, with a consequent increase of pH from 1.8 to 3.7, did not change the diffraction pattern significantly, whereas the thermal treatment performed on FG+NaOH mat further decreased the broad band at about 21º.

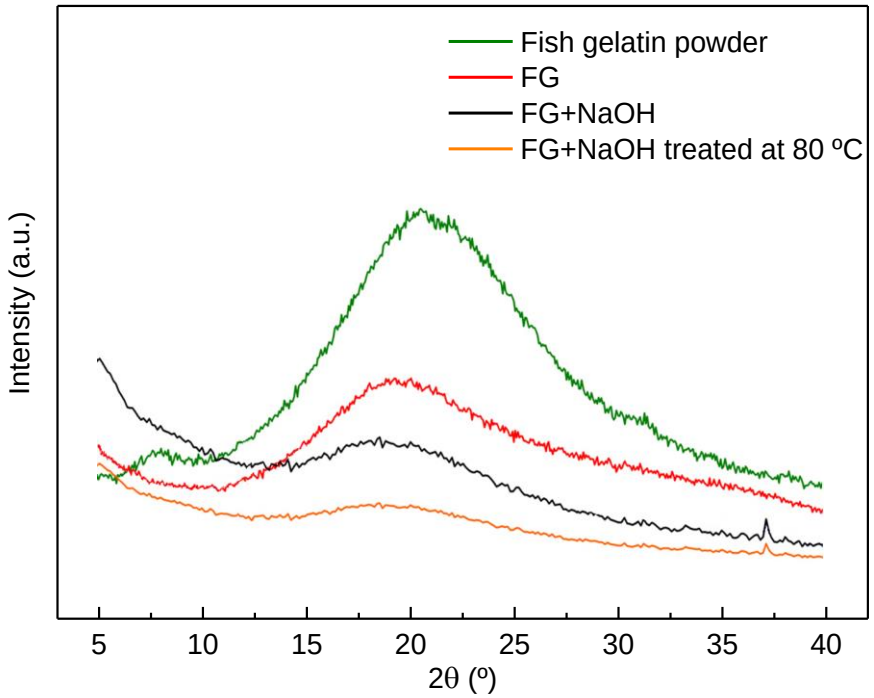

Figure 3.3 WXRD patterns of fish gelatin powder, FG, FG+NaOH and thermal treated FG+NaOH electrospun mats.

FTIR spectra of the electrospun mats obtained from FG and FG+NaOH, before and after the thermal treatment, were collected (**Figure 3.4**); fish gelatin powder was also collected for the sake of comparison. The broad band above 3000 cm^{-1}, observed in all spectra shown in **Figure 3.4a**, corresponded to the hydroxyl and amino groups (Baniasadi et al., 2015). Some changes could be observed in FTIR spectra, in particular, in those bands associated to the peptide bonds in gelatin: amide I (C=O stretching), amide II (N-H bending), and amide III (C-N stretching). As can be seen in **Figure 3.4b**, there was a shift of these bands to higher wavenumbers from FG mat to FG+NaOH mats, indicating that the citric acid incorporated into the formulation caused new interactions between the amino groups of gelatin and the carboxyl groups of citric acid (Cui et al., 2011), in accordance with the shift of the characteristic band related to the carboxyl group in citric acid from 1748 cm^{-1} to 1715 cm^{-1} (Francisco et al., 2018).

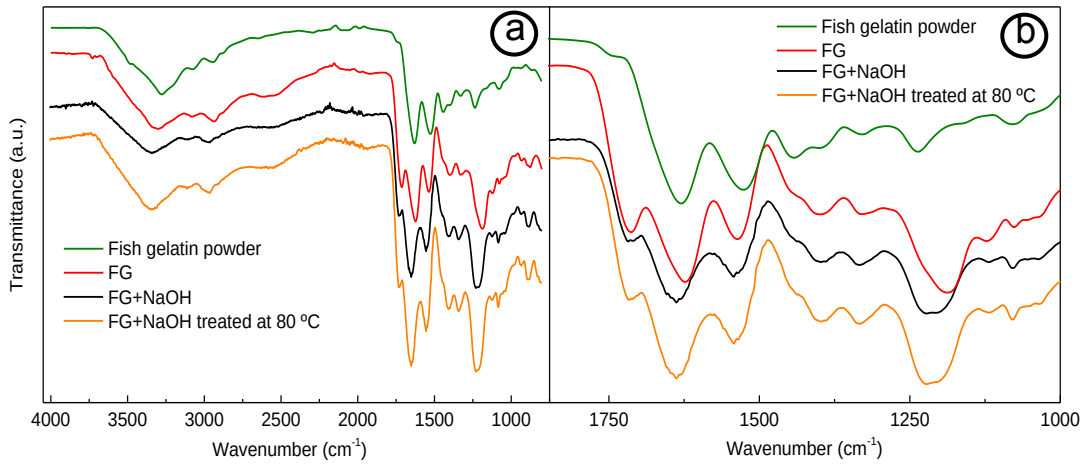

Figure 3.4 FTIR spectra of fish gelatin powder, FG, FG+NaOH and thermal treated FG+NaOH electrospun mats a) from 4000 to 800 cm^{-1} and b) from 1850 to 1000 cm^{-1}.

The band corresponding to amide I is related to the secondary structure of the protein backbone and it is generally used for the quantitative analysis of secondary structures. Hydrogen bonding plays a significant role in stabilisation of protein secondary structure. Indeed, inter-peptide hydrogen bonding stabilizes secondary structures (i.e. α-helix and β-sheet conformations), while peptide-water hydrogen bonding competes against peptide bond-peptide bond hydrogen bonding. Due to the central role of hydrogen bonding in protein folding, the analysis of this band is of great importance (**Figure 3.5**).

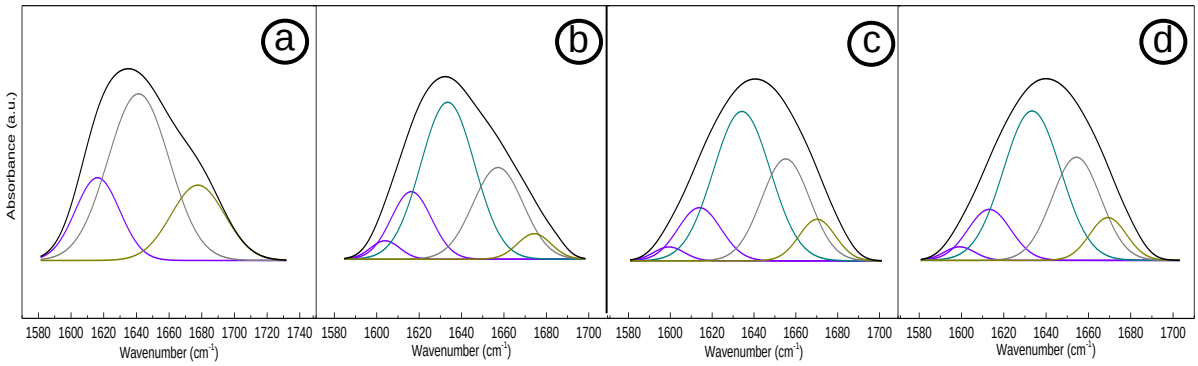

Figure 3.5 Curve fitting spectra of amide I band (black curve) for a) fish gelatin powder, b) FG, c) FG+NaOH and d) thermal treated FG+NaOH electrospun mats.

The assignment of peaks in amide I band is as follows: two peaks from 1603 to 1616 cm^{-1} support β-sheet conformation, the peak at 1634 cm^{-1} corresponds to random coil conformation, the peak from 1641 to 1650 cm^{-1} is associated to α-helix conformation, and the peak centered at 1670-1678 cm^{-1} is assigned to the β-turn conformation of the hairpin-folded antiparallel β-sheet structure (**Table 3.1**).

Table 3.1 Resulting percentage of the curve fitting of amide I for fish gelatin powder, FG, FG+NaOH and thermal treated FG+NaOH electrospun mats.

Amide I area	1603-1616 cm^{-1} (%)	1634 cm^{-1} (%)	1641-1650 cm^{-1} (%)	1670-1678 cm^{-1} (%)
Fish gelatin powder	20.37	-	57.00	22.63
FG	18.75	48.73	26.54	5.98
FG+NaOH	16.94	44.70	29.79	8.57
FG+NaOH treated at 80 ºC	16.16	44.29	30.84	8.71

As shown in **Figure 3.5** and **Table 3.1**, electrospinning caused changes in the secondary structure of gelatin. While fish gelatin powder showed α-helix conformation, random coil was the predominant conformation for electrospun mats, in accordance with the results found by WXRD, which showed amorphous structure with no remaining triple-helix structure.

3.3 Conclusions

An environmentally friendly chemical strategy to successfully electrospun fish gelatin from a solution containing only citric acid in an aqueous solution was demonstrated. Citric acid was used as a benign acid to solubilise gelatin and allow the electrospinning process and, at the same time, as a cross-linking agent. The pH of the spinning solutions turned out to have a strong influence on the viscoelastic behaviour of the solutions, as well as on the cross-linking extent that, in turn, influenced the fibre morphology stability. Rheological measurements provided evidence that in all solutions the solid-like behaviour dominated over time, but the weak gel formed did not hinder electrospinnability of the solution. The solution at pH 3.7, showing higher values of G'

and G'' moduli, was characterized by a higher extent of cross-linking with respect to the solution at pH 1.8. Although microfibres were obtained for both FG and FG+NaOH, the increase of solution pH from 1.8 to 3.7 was necessary to maintain the fibrous morphology in the mat. A subsequent thermal treatment at 80 ºC of the electrospun mat turned out to significantly increase the morphological stability of the mat. The cross-linking degrees of the mats were in line with the morphological results (FG mat = 12%, FG+NaOH mat = 25%, thermally treated FG+NaOH mat = 38%). Gelatin denaturation after the electrospinning process was demonstrated by the absence of the diffraction band related to the triple-helix diameter, as expected since gelatin solubilisation in acidic solvents is known to prevent the partial renaturation of gelatin. FTIR characterization confirmed this result and demonstrated that gelatin structure changed from α-helix to random coil conformation as a consequence of the electrospinning process. Although further studies are necessary to find the best solution composition to further optimise the final morphology as well as the cross-linking extent of the produced mats, this work is the first successful attempt to produce cross-linked electrospun fish gelatin fibres through the use of a citric acid/water solution.

4 Citric acid cross-linked fish gelatin films

4.1 Summary

Pure fish gelatin films are brittle and hydrophilic and so, their properties need to be enhanced to produce competitive products (Zhuang et al., 2015). Different approaches, such as blending of biopolymers, manufacture of multilayers, and chemical cross-linking, have been used to improve the functional properties of bio-based films. With regard to chemical cross-linking, aldehydes have been widely used to react with biopolymers. However, due to their toxicity (Farjami et al., 2015; Reddy et al., 2015; Xu et al., 2015), natural cross-linkers are preferred. In this work, in line with the previous chapter, citric acid was selected to cross-link fish gelatin.

In chapter 3, even if the increase of solution pH up to 3.7 led to a cross-linking extent increase, low cross-linking degrees were achieved since this reaction is hindered at acidic pH. Thereby, in order to favour citric acid and gelatin cross-linking, in this chapter basic pH was employed to prepare gelatin films by solution casting. In this context, the aim of this chapter was to analyse the effect of citric acid content on optical, mechanical and barrier properties of fish gelatin films and relate the final properties achieved to the changes observed by the physicochemical analysis performed. Furthermore, the environmental aspects involved in the manufacture of films were assessed by the carbon footprint analysis.

4.2 Results and discussion

4.2.1 Physicochemical properties

In order to assess the physical properties of fish gelatin films, MC and TSM values were determined. As can be seen in **Table 4.1**, MC values were in the range of 12-16%, lower values than the ones found for other proteins, such as whey protein isolate (Azevedo et al., 2015a), which may be an advantage when intending to use these films as packaging films. Regarding TSM values, film solubility increased ($P < 0.05$) as citric acid content increased. Similar results have been reported for other natural polymers

such as xylan (Wang et al., 2014) or starch (Yoon et al., 2006). This increase in solubility could become an advantage when these materials are intended to be used as oral films for biomedical applications (Yoon et al., 2007). The increase of solubility could be due to the citric acid that did not react with gelatin and dissolved in water. In contrast to other chemical cross-linkers, such as formaldehyde and glutaraldehyde, the two most used cross-linkers for proteins but proved carcinogens and environmental polluters, citric acid is used as a food additive and thus, unreacted citric acid is accepted as a safe component in films (Azevedo et al., 2015b).

Table 4.1 Moisture content (MC) and total soluble matter (TSM) values of fish gelatin films as a function of citric acid content.

Film	MC (%)	TSM (%)
0CA	12.5 ± 0.3^{a}	36.8 ± 0.5^{a}
10CA	14.2 ± 0.2^{b}	45.4 ± 0.8^{a}
20CA	16.2 ± 0.2^{c}	50.6 ± 3.2^{b}
30CA	12.5 ± 0.1^{a}	58.9 ± 1.9^{bc}
40CA	12.0 ± 0.2^{a}	67.5 ± 7.9^{c}

$^{a\text{-}c}$Two means followed by the same letter in the same column are not significantly ($P > 0.05$) different through the Tukey's multiple range test.

In order to explain the results shown above, FTIR analysis was carried out. FTIR spectra of the pure components used in the preparation of fish gelatin films are shown in **Figure 4.1**. The most characteristic bands of gelatin are related to C=O stretching (amide I) at 1632 cm^{-1}, N-H bending (amide II) at 1527 cm^{-1}, and C-N stretching (amide III) at 1238 cm^{-1}, the broad band above 3000 cm^{-1} corresponding to the free and bounded hydroxyl and amino groups, and the absorption band at 1330 cm^{-1} attributable to CH_2 wagging of proline (Guerrero et al., 2011). The main absorption bands of glycerol appear at the 800-1150 cm^{-1} region and are related to the vibrations of C-C and C-O bonds (Gómez-Siurana et al., 2013; Guerrero & de la Caba, 2010). In relation to citric acid, the typical absorption bands are located at 1690 cm^{-1} and 1743 cm^{-1} and are associated to free and hydrogen-bounded carboxylic groups, respectively (Cui et al., 2011).

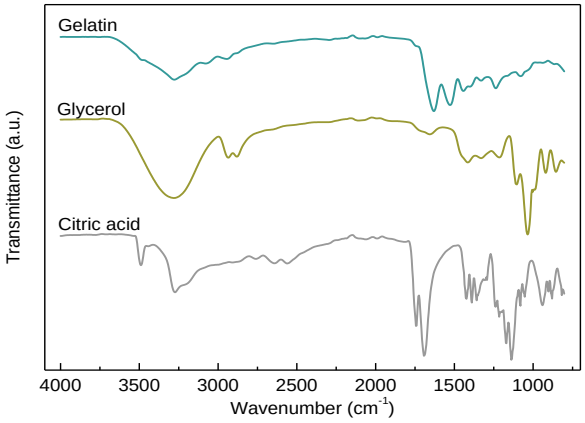

Figure 4.1 FTIR spectra of the pure components used in the preparation of fish gelatin films.

Regarding citric acid-modified films, FTIR spectra are shown in **Figure 4.2**. As can be seen, 0CA and 10CA films exhibited similar spectra (**Figure 4.2a**), although it is worth noting that the relative intensity between the amide I and amide II bands changed. In particular, the relative intensity of the band corresponding to the amide I was lower for the 10CA film, as can be observed in **Figure 4.2b**. The effect of citric acid was more noticeable when higher contents were added into the formulations. Specifically, the amide I and amide II bands joined and became one band, the intensity of the band at 1390 cm^{-1} remarkably increased, and the broad band above 3000 cm^{-1} split into two bands.

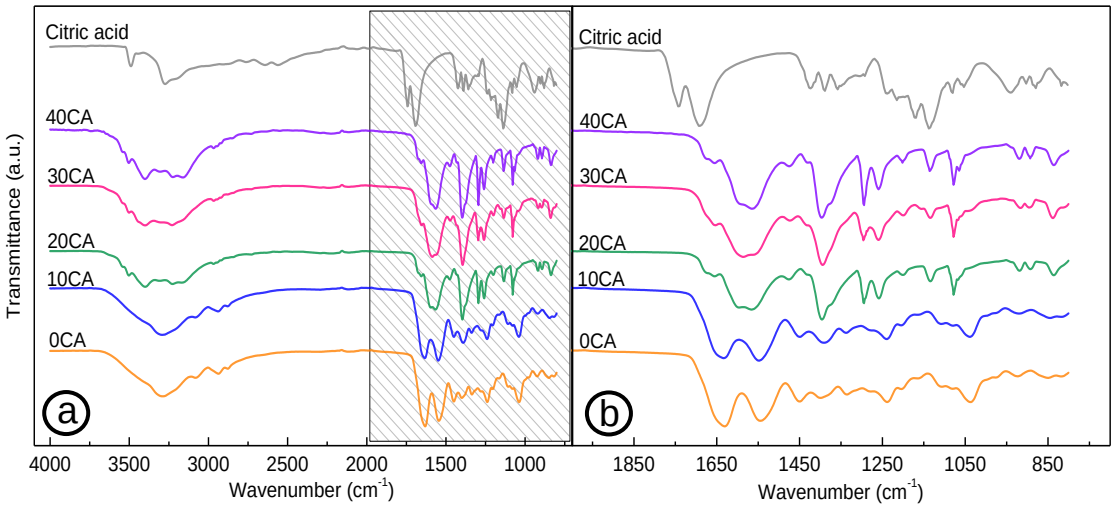

Figure 4.2 FTIR spectra of pure citric acid and fish gelatin films as a function of citric acid content a) in the 4000-800 cm^{-1} range and b) in the 2000-800 cm^{-1} range.

When citric acid was incorporated into the film forming solutions, the peak at 1743 cm^{-1} disappeared, as can be seen in **Figure 4.2b**, indicating the reaction between the carboxylic groups of citric acid and the amino groups of gelatin. When reacting these two groups, both imide and amide formation are theoretically possible (Cui et al., 2011), as shown in **Figure 4.3**.

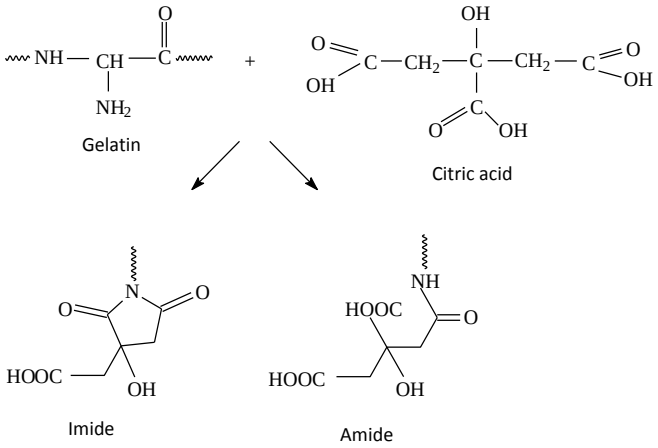

Figure 4.3 Chemical reaction between gelatin and citric acid.

When the imide is formed, a peak at 1770 cm^{-1}, corresponding to the carbonyl group, appears. In contrast, the peak related to the carbonyl group in the amide appears at 1625 cm^{-1}. Considering that no peak was observed at 1770 cm^{-1} in the spectra obtained for the citric acid-modified films, results suggest that no imide but amide was formed as a consequence of the chemical reaction between gelatin and citric acid, as reported by other authors (Xu et al., 2015). Indeed, nucleophilic substitution was the proposed mechanism for the reaction between gliadin (used as a protein model to study the reaction) and citric acid. In our work, gelatin films were prepared at basic conditions (pH = 10) and thus, carboxylic groups in citric acid were in the form of carboxylates. According to Xu et al. (2015), the amine group of protein attacks one of the carboxyl groups of citric acid and forms an amide linkage. If more than one of the carboxylic groups of citric acid reacts, gelatin cross-links, as shown in **Figure 4.4**.

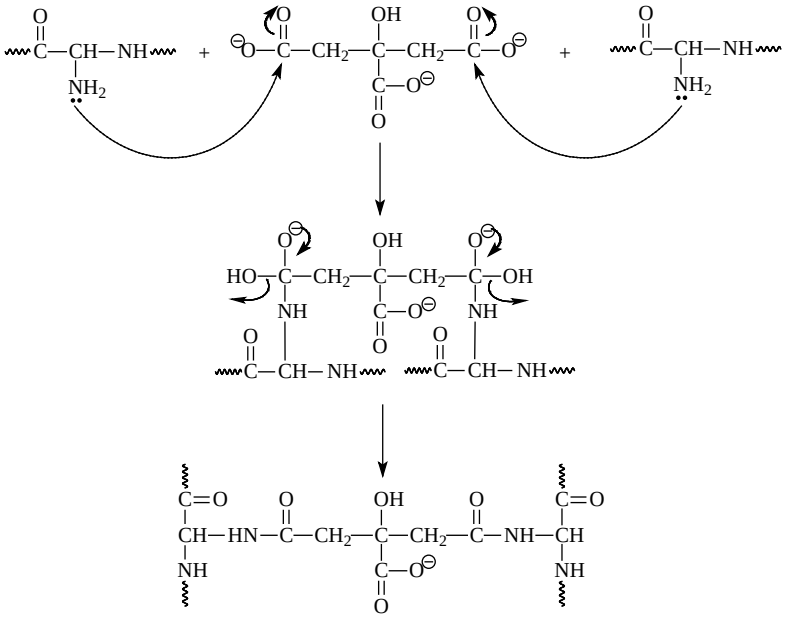

Figure 4.4 Mechanism for the reaction between gelatin and citric acid at basic pHs.

4.2.2 Optical properties

Optical properties, such as gloss, colour and transparency, were determined and are shown in **Table 4.2**. As can be seen, gloss values significantly ($P < 0.05$) decreased by the addition of citric acid. Since gloss is related to surface roughness (Acosta et al., 2015; Etxabide et al., 2015), these results indicate that the incorporation of acid into film forming solutions caused the formation of rougher surfaces as a consequence of the reaction between gelatin and citric acid, which involves the rearrangement of protein chains.

Table 4.2 Gloss, colour and transparency values of fish gelatin films as a function of citric acid content.

Film	Gloss (GU)	L*	a*	b*	ΔE*	Transparency
0CA	143 ± 19^{a}	96.0 ± 0.5^{a}	-0.11 ± 0.03^{a}	2.68 ± 0.09^{a}		0.50 ± 0.01^{a}
10CA	49 ± 2^{b}	96.0 ± 0.1^{a}	-0.14 ± 0.03^{a}	2.71 ± 0.08^{a}	0.17 ± 0.12^{a}	0.65 ± 0.01^{a}
20CA	45 ± 1^{b}	96.0 ± 0.1^{a}	-0.17 ± 0.02^{ab}	2.87 ± 0.08^{a}	0.22 ± 0.12^{a}	1.56 ± 0.04^{b}
30CA	41 ± 1^{b}	96.2 ± 0.1^{a}	-0.22 ± 0.05^{b}	2.67 ± 0.10^{a}	0.14 ± 0.01^{a}	6.13 ± 0.07^{c}
40CA	17 ± 1^{c}	96.3 ± 0.3^{a}	-0.20 ± 0.03^{b}	2.69 ± 0.08^{a}	0.30 ± 0.16^{a}	6.38 ± 0.41^{c}

$^{a\text{-}c}$Two means followed by the same letter in the same column are not significantly ($P > 0.05$) different through the Tukey's multiple range test.

Besides gloss, colour and transparency were analysed. Concerning colour, L*, a* and b* values were determined. As can be seen, there was no significant change ($P > 0.05$) in L* and b* parameters and only a* values slightly changed ($P < 0.05$) at high citric acid contents (30CA and 40CA). However, no significant change ($P > 0.05$) was observed in ΔE* values, indicating that the cross-linking reaction between gelatin and citric acid aforementioned did not change colour, in contrast to other natural cross-linkers, such as sucrose or lactose, that cause a yellowing or even browning of gelatin films (Guerrero et al., 2012). Moreover, all films were transparent, although transparency decreased ($P < 0.05$) as citric acid content increased, especially for 30CA and 40CA films, suggesting a citric acid content in excess, as also mentioned when analysing TSM values. While gloss is related to surface roughness and it is not affected by citric acid content, transparency is related to internal microstructure (Acosta et al., 2015). Therefore, results suggest that non cross-linked citric acid affected the film structure and thus, transparency values.

4.2.3 Barrier properties

In addition to transparency, UV-vis spectroscopy was used to determine light resistance of fish gelatin films. As can be seen in **Figure 4.5**, gelatin films provided excellent UV barrier from 200 to 250 nm, irrespective of citric acid content. This is due to the chromophore groups presented in gelatin, in particular, tyrosine and phenylalanine amino acids (Gómez-Guillén et al., 2009). Furthermore, as citric acid content increased, UV absorbance from 250 to 280 nm increased due to the carboxyl and hydroxyl groups of citric acid that act as auxochrome groups (Jadhav & Phugare, 2012).

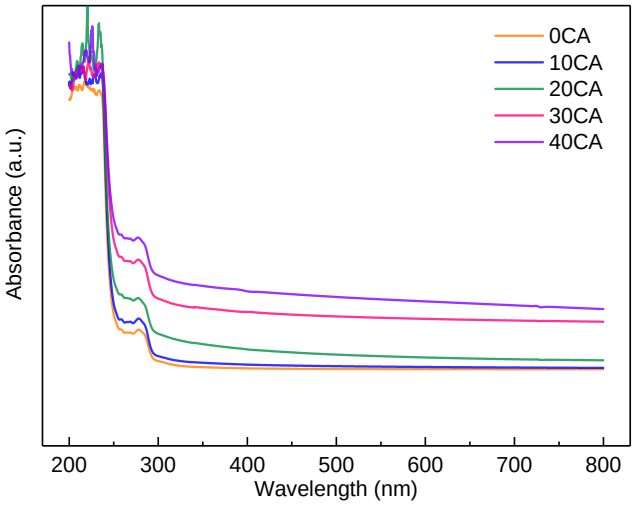

Figure 4.5 UV-vis spectra of fish gelatin films as a function of citric acid content.

Regarding water resistance, WCA values were lower than 90º, as can be seen in **Table 4.3**, so films showed a hydrophilic character (Bharathidasan et al., 2015). However, increasing citric acid content did not significantly ($P > 0.05$) affect WCA values up to 30 wt % citric acid. These results support the fact that acid contents higher than 20 wt % result in citric acid in excess that remains non-reacted, providing films with higher hydrophilicity ($P < 0.05$) and solubility, as previously shown by TSM values. In particular, water droplet was fully absorbed in 40CA films. In a similar manner to WCA values, WVP values were not significantly ($P > 0.05$) affected by citric acid up to the highest acid content.

Table 4.3 Water contact angle (WCA) and water vapour permeability (WVP) values of fish gelatin films as a function of citric acid content.

Film	WCA (º)	WVP 10^{12} (g cm^{-1} s^{-1} Pa^{-1})
0CA	79 ± 10^{a}	2.22 ± 0.22^{a}
10CA	77 ± 3^{a}	2.53 ± 0.45^{ab}
20CA	75 ± 10^{a}	2.53 ± 0.03^{ab}
30CA	55 ± 4^{b}	2.56 ± 0.14^{ab}
40CA	0	3.21 ± 0.33^{b}

$^{a-b}$Two means followed by the same letter in the same column are not significantly ($P > 0.05$) different through the Tukey's multiple range test.

4.2.4 Mechanical properties

The addition of citric acid improved mechanical properties of fish gelatin films. As can be seen in **Figure 4.6**, TS significantly ($P < 0.05$) increased when citric acid was added, regardless of acid content. The increase of TS indicated that the new interactions induced by the reaction occurred between citric acid and gelatin were stronger than the interactions between gelatin chains. EB values also increased ($P < 0.05$) with citric acid addition up to 20 wt %. These results are in accordance with TSM and WCA results, which indicated that the addition of citric acid contents higher than 20 wt % provided citric acid in excess, which remained non-reacted.

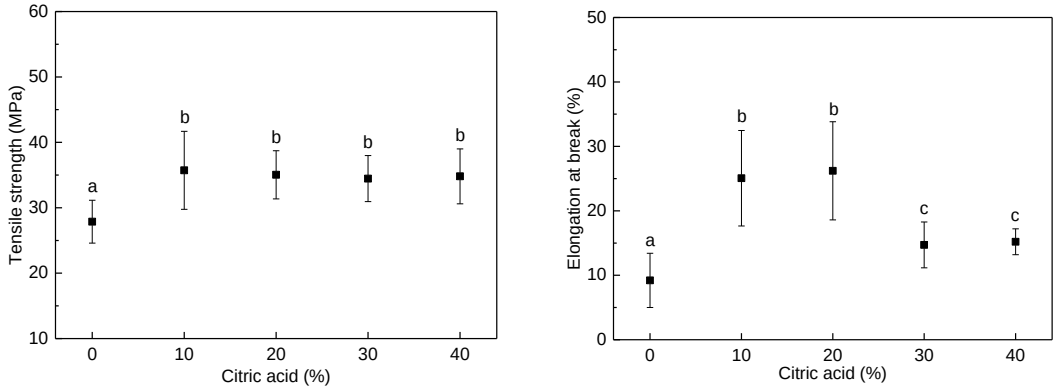

Figure 4.6 Tensile strength (TS) and elongation at break (EB) values of fish gelatin films as a function of citric acid content.

[a-c]Two means followed by the same letter in the same graphic are not significantly ($P > 0.05$) different through the Tukey's multiple range test.

4.2.5 Environmental assessment

Considering the potential application of the films as packaging films, 1 m^2 was the functional unit selected to perform the environmental assessment, in which three stages were taken into account, specifically, raw material extraction, film manufacture, and the end of life.

With regard to the raw material extraction, the environmental charge associated to the extraction of gelatin from fish skins derived from wastes from fish processing industries was considered. Briefly, the extraction method chosen for the environmental

analysis consists of a mild swelling, firstly in sodium hydroxide and afterwards, in acetic acid. Then, gelatin extraction is carried out in distilled water at 70 ºC during 90 min and finally, the sample is dried in an oven for 18 h at 50 ºC.

Concerning film manufacture, fish gelatin films were prepared in our laboratories by solution casting. Film forming solutions were prepared as described in 2.4.2 section. When assessing the environmental impact of this stage, materials employed and energy (heat and electricity) consumed were considered.

In relation to the end of life, composting was considered as the disposal scenario after the film use. This waste treatment, based on the aerobic degradation of the organic waste, was considered self-sufficient from the energetic point of view, so no electric consumption was taken into account.

Data related to those three stages were processed and associated with environmental impacts using IPCC 2007, developed by the International Panel on Climate Change (IPCC). This method lists the climate change factors in three time horizons (20, 100 and 500 years) to perform the carbon footprint, expressed in terms of global warming potential (GWP) for 100 years in this study.

As can be seen in **Figure 4.7**, the raw material extraction was the stage that exhibited the highest GWP. The energetic consumption of gelatin extraction was the main contribution to the carbon footprint in this stage. The energy consumed during the film manufacture was also the factor that mainly contributed to the environmental impact in this stage. As also shown by other authors (Hervy et al., 2015), further improvements are needed to demonstrate the environmental benefits of renewable materials. Nevertheless, in contrast to the aforementioned stages, GWP values were negative in the stage related to the end of life, giving rise to a positive environmental effect, since compost is obtained as a valuable product.

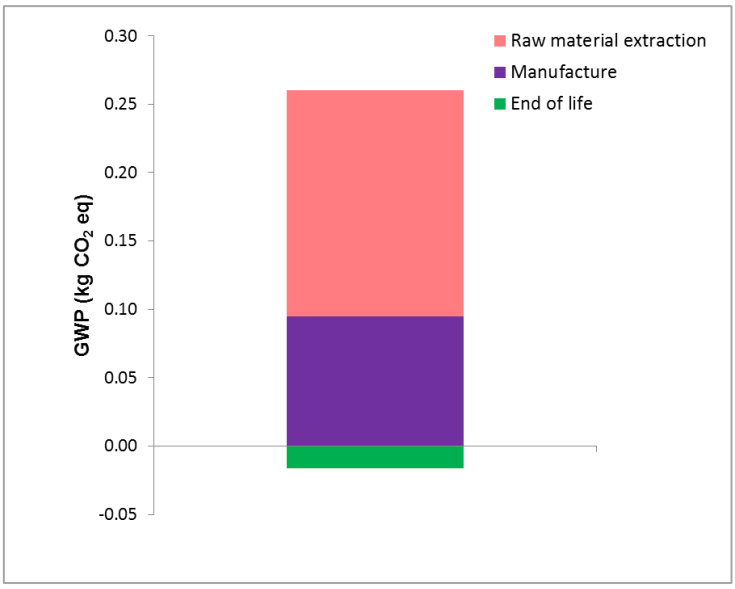

Figure 4.7 Carbon footprint for fish gelatin films.

4.3 Conclusions

Citric acid-modified fish gelatin films were prepared and characterized in this chapter. All films were transparent and homogenous. The changes observed in film properties suggested cross-linking in gelatin systems due to the incorporation of citric acid in film forming solutions. This cross-linking was supported by FTIR analysis, which indicated the reaction between gelatin and citric acid. As a consequence of this reaction, the films modified with citric acid contents up to 20 wt % showed enhanced mechanical properties, since both TS and EB increased. However, higher acid contents provided citric acid in excess that remained non-reacted in the system. In addition to the assessment of functional properties, the sustainability of the films from the raw material extraction to their end of life was considered. The environmental assessment revealed that composting was a beneficial waste treatment after disposal of these renewable films, as shown by the negative GWP values provided by the carbon footprint measurements.

5 Fish gelatin/chitosan composite films

5.1 Summary

Since microbial contamination is considered one of the main causes of spoilage leading to food quality deterioration (Clarke et al., 2017), the development of active films is attracting much attention in the field of food science and technology. Citric acid employed in previous chapters can work as an active compound since its antimicrobial character has been reported in some works (Denghani et al., 2018; Kim & Rhee, 2015; Olaimat et al., 2017). Therefore, in this chapter, citric acid was added as an antimicrobial agent and, specifically, 10 and 20 wt % citric acid concentrations were selected, considering that acid contents higher than 20 wt % provided acid in excess, as shown in chapter 4. In addition to its antimicrobial character, citric acid provides mild acidity conditions and dissolves the chitosan used as an antimicrobial agent, whose antibacterial activity is attributed to the positively charged amino groups that interact with the negatively charged surface of bacteria (Bano et al., 2017; Ganesan, 2017).

The development of fish gelatin/chitosan films (BenBettaïeb et al., 2015; Gómez-Estaca et al., 2011), as well as the effects of the incorporation of active compounds, such as plant extracts (Benbettaïeb et al., 2016; Bonilla & Sobral, 2016) and essential oils (Hosseini et al., 2015; Kakaei & Shahbazi, 2016) into film forming formulations have been documented. However, to the best of our knowledge no manuscript has been focused on the effects of both citric acid and chitosan on the functional properties of fish gelatin-based films. Therefore, the combined effect of citric acid and chitosan on the antibacterial activity of the films and on their physicochemical, thermal, optical, barrier and mechanical properties was analysed in this chapter.

5.2 Results and discussion

5.2.1 Physicochemical properties

The effect of chitosan and citric acid in fish gelatin films was assessed by FTIR analysis. As can be seen in **Figure 5.1**, the most noticeable change occurred in the

relative intensity between the band corresponding to amide I (C=O stretching at ~ 1630 cm^{-1}) and the one associated to amide II (N-H bending coupled with C-N stretching at ~ 1540 cm^{-1}) (Muyonga et al., 2004). In particular, the intensity of the amide I band was higher than that of the amide II for the control film (0CA0CHI); however, the difference in the relative intensity of these two bands became smaller for the films with 10 wt % citric acid (10CA0CHI and 10CA9CHI), similar for the films with 20 wt % citric acid without chitosan (20CA0CHI), and the intensity of the amide II band became larger with respect to that of amide I for the films with 20 wt % citric acid and 9 wt % chitosan (20CA9CHI).

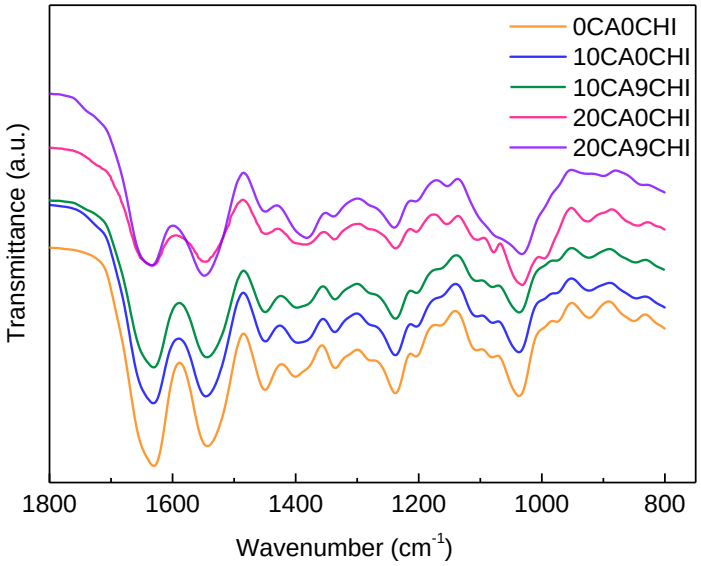

Figure 5.1 FTIR spectra of the control film (0CA0CHI), the films with 10 or 20 wt % citric acid without chitosan (10CA0CHI and 20CA0CHI) and the films with 9 wt % chitosan (10CA9CHI and 20CA9CHI).

According to Lagaron et al. (2007), the band at ~ 1540 cm^{-1} can be related to the biocide activity of chitosan associated to the protonated amino groups and, thus, a relative increase of this band might indicate an increase of the antibacterial capacity of the films, as corroborated below by the antimicrobial assessment. Additionally, the band at ~ 1400 cm^{-1} has been also associated to biocide activity related to carboxyl groups

(Lagaron et al., 2007; Leceta et al., 2013). As can be seen in **Figure 5.1**, the relative intensity of this band with respect to the band at 1450 cm^{-1} was lower for the films without citric acid and chitosan (0CA0CHI), became similar for the films with 10 wt % citric acid (10CA0CHI and 10CA9CHI) and larger for the films with 20 wt % citric acid, especially for the films with 9 wt % chitosan (20CA9CHI), in accordance with the antimicrobial results shown in **Figure 5.7**. Furthermore, the bands in the 1100-1000 cm^{-1} region became a single band for the 20CA9CHI film.

These differences in the relative intensity of FTIR bands suggest different interactions among the polar groups of the formulation components (fish gelatin, citric acid, chitosan and glycerol) depending on chitosan, but mainly on citric acid content. The interactions between gelatin and chitosan are mainly produced by hydrogen bonding between carboxyl, amino and hydroxyl groups of gelatin and amino and hydroxyl groups of chitosan (Gómez-Estaca et al., 2011). These interactions seem to be influenced by the citric acid content incorporated into the film forming solutions; therefore, in order to further analyse the effect of citric acid and chitosan on the protein structure, the curve fitting of the amide I band was carried out.

The amide I profile of gelatin contains three major components: a band associated to the α-helix/random coil conformation at 1650 cm^{-1}, and two bands corresponding to the β-sheet conformation at 1615-1630 cm^{-1} and 1680-1700 cm^{-1} (Etxabide et al., 2016b; Guerrero et al., 2014). As can be seen in **Table 5.1**, no difference was observed in the protein structure with respect to the control film (0CA0CHI) when 10 wt % citric acid was incorporated (10CA0CHI); however a decrease in the content of the β-sheet conformation and an increase of the α-helix/random coil conformation was observed when 20 wt % citric acid was incorporated (20CA0CHI), indicating the great influence of citric acid content in the protein structure. Furthermore, the difference between the contents of β-sheet and α-helix/random coil conformations was bigger for the films prepared with 20 wt % citric acid, which showed higher content of

α-helix/random coil than the films prepared with 10 wt % citric acid. This behaviour could be due to a partial gelatin renaturation (Sow & Yang, 2015), which could be favoured in the presence of higher citric acid contents due to the plasticizing effect of citric acid, as shown below when mechanical properties are analysed.

Table 5.1 Protein conformations in fish gelatin films prepared with different contents of citric acid and chitosan.

Protein conformation	Film	Content (%)	Film	Content (%)
β-sheet (1615-1630 cm^{-1})	0CA0CHI	42	0CA0CHI	42
	10CA0CHI	43	20CA0CHI	29
	10CA3CHI	41	20CA3CHI	22
	10CA6CHI	36	20CA6CHI	23
	10CA9CHI	35	20CA9CHI	25
α-helix/random coil (1650 cm^{-1})	0CA0CHI	54	0CA0CHI	54
	10CA0CHI	53	20CA0CHI	68
	10CA3CHI	55	20CA3CHI	74
	10CA6CHI	60	20CA6CHI	72
	10CA9CHI	61	20CA9CHI	69
β-sheet (1680-1700 cm^{-1})	0CA0CHI	4	0CA0CHI	4
	10CA0CHI	4	20CA0CHI	2
	10CA3CHI	4	20CA3CHI	4
	10CA6CHI	4	20CA6CHI	5
	10CA9CHI	4	20CA9CHI	5

The protein structure was also affected by the addition of chitosan. Specifically, the content of β-sheet decreased and the content of α-helix/random coil increased with the incorporation of chitosan. However, the changes observed when chitosan content increased were different for the films prepared with 10 or 20 wt % citric acid. In particular, β-sheet content decreased and α-helix/random coil content increased when chitosan content increased in the films prepared with 10 wt % citric acid, while the opposite trend, increase of β-sheet content and decrease of α-helix/random coil content, was observed for the films with 20 wt % citric acid. These results indicate the different extension of hydrogen bonding and, as a consequence, the different network formed as a function of the citric acid content in the film forming formulations.

The MC and TSM of the films were also analysed and values are shown in **Table 5.2**. On the one hand, all films showed mean MC values from 11.21 to 13.41%, in agreement with the weight loss associated to the first step of TGA curves (**Figure 5.5**). On the other hand, TSM values were around 40%, probably due to the dissolution of glycerol and citric acid, since the interactions among these components and the biopolymers used in this chapter (fish gelatin and chitosan) occurred by hydrogen bonding, as indicated by FTIR analysis (**Figure 5.1**). It is worth noting that all films maintained their integrity. Although no significant ($P > 0.05$) change was observed for the films with 10 wt % citric acid, in the case of the films with 20 wt % citric acid, the addition of chitosan significantly ($P < 0.05$) decreased film solubility, as also shown by other authors for gelatin-chitosan films (Gómez-Estaca et al., 2011; Hosseini et al., 2013; Matiacevich et al., 2013).

Table 5.2 Moisture content (MC) and total soluble matter (TSM) of fish gelatin films prepared with different contents of citric acid and chitosan.

Film	MC (%)	TSM (%)
0CA0CHI	11.21 ± 0.33^{d}	37.33 ± 1.05^{b}
10CA0CHI	12.33 ± 0.05^{a}	44.96 ± 1.97^{a}
10CA3CHI	12.15 ± 0.06^{b}	38.67 ± 0.87^{a}
10CA6CHI	12.20 ± 0.06^{ab}	45.78 ± 1.76^{a}
10CA9CHI	11.93 ± 0.06^{c}	42.71 ± 4.68^{a}
0CA0CHI	11.21 ± 0.33^{c}	37.33 ± 1.05^{c}
20CA0CHI	13.46 ± 0.09^{a}	44.73 ± 1.86^{a}
20CA3CHI	13.32 ± 0.03^{ab}	42.99 ± 2.01^{ab}
20CA6CHI	13.41 ± 0.10^{a}	41.34 ± 0.82^{ab}
20CA9CHI	12.96 ± 0.24^{b}	40.27 ± 1.30^{b}

$^{a-d}$Two means followed by the same letter in the same section and column are not significantly ($P > 0.05$) different through the Tukey's multiple range test.

Since the swelling behaviour is indicative of cross-linking, the swelling values of the films were measured. First of all, the effect of citric acid was analysed and the swelling curves are shown in **Figure 5.2**. In general, gelatin films swell rapidly at short times but the swelling rate slows down at longer times (Gordon et al., 2010). In the case of 0CA0CHI film, the swelling increased up to values next to 2000%, whereas the

swelling values for the films prepared with citric acid were below 600% after 24 h. The increase of citric acid content from 10 to 20 wt % decreased swelling values. It is worth noting that the citric acid incorporated films maintained their integrity up to the end of the swelling test and the hydrated films obtained were flexible.

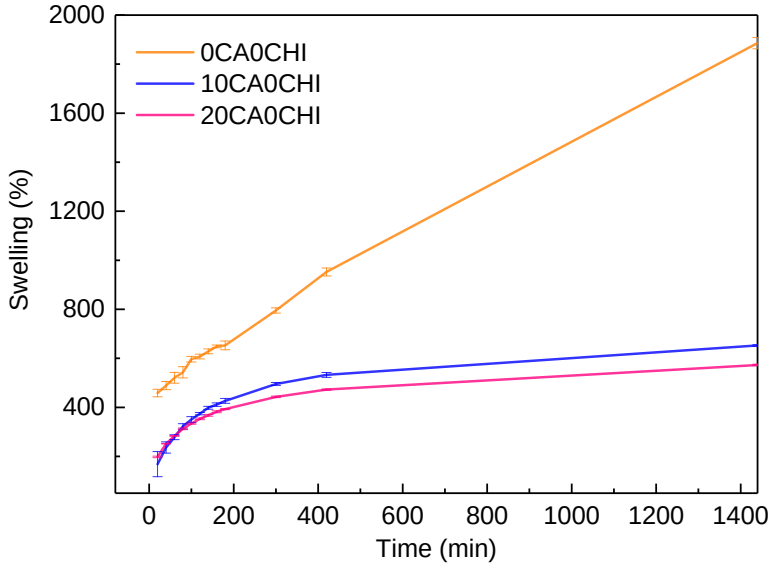

Figure 5.2 Swelling behaviour of the control film (0CA0CHI) and the fish gelatin films prepared with 10 wt % citric acid (10CA0CHI) or 20 wt % citric acid (20CA0CHI) without chitosan.

Regarding the effect of chitosan addition, swelling curves for the films prepared with chitosan are shown in **Figure 5.3**, in which two stages can be distinguished. The first stage until 420 min showed a fast swelling up to 460-620% for the films prepared with 10 wt % citric acid and up to 400-470% for the films prepared with 20 wt % citric acid. In all cases, the highest values were measured for the films without chitosan, suggesting that the incorporation of chitosan promoted the interactions with the polar groups of the formulation components, so less polar groups were accessible to interact with water molecules, leading to a lower swelling degree. This trend was maintained for the films prepared with 10 wt % citric acid until the end of the swelling test, when constant swelling values were reached. These final swelling values decreased from 825 to 750%

when chitosan content increased from 0 to 9 wt %. In contrast, this trend was reversed for the films prepared with 20 wt % citric acid. These results are in agreement with the different protein structures developed in the films with 10 or 20 wt % citric acid, as previously shown by FTIR analysis in **Table 5.1**.

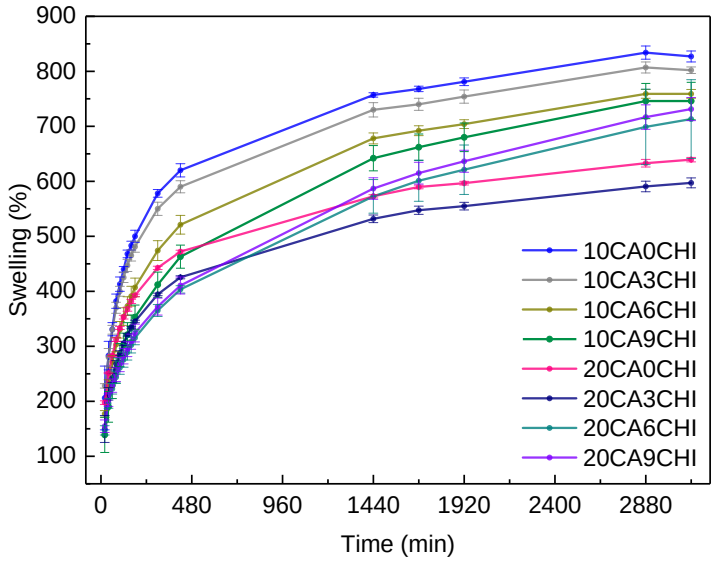

Figure 5.3 Swelling behaviour of the films prepared with different citric acid and chitosan contents.

5.2.2 Thermal properties

In order to relate the physicochemical changes observed as a function of citric acid and chitosan content to thermal properties, DSC measurements were carried out and the curves obtained are shown in **Figure 5.4**. As can be seen, the most noticeable change occurred when citric acid or chitosan was incorporated, regardless of the chitosan content added. In relation to the films with 10 wt % citric acid (**Figure 5.4a**), all films, except the film with the highest chitosan content (10CA9CHI), showed one single band related to water evaporation. As can be seen, the maximum of this band shifted from 83 to 95 ºC when citric acid was incorporated into the formulation, and from 95 to 107 ºC when chitosan content increased from 0 to 9 wt %. These results are indicative of the interactions of citric acid and chitosan with gelatin, which would hinder water

evaporation. Furthermore, the film with 9 wt % chitosan showed a second peak around 220 ºC, associated to chitosan deacetylation (Almeida et al., 2010). In contrast, all the films prepared with 20 wt % citric acid and chitosan (**Figure 5.4b**) showed two peaks. Moreover, the maximum temperature corresponding to this second peak decreased when chitosan content increased, which can be related to the decrease of α-helix/random coil conformation from 3 to 9 wt % chitosan content, as shown in **Table 5.1**.

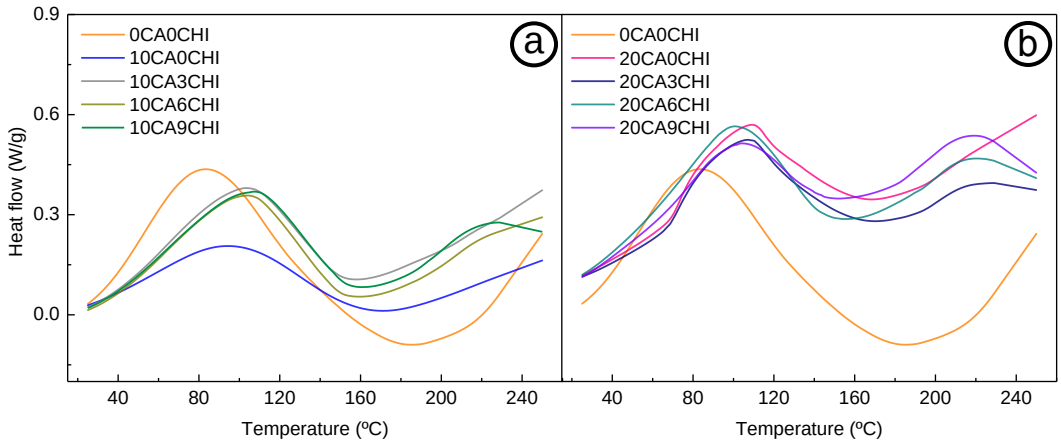

Figure 5.4 DSC thermograms of the films prepared with a) 10 wt % citric acid and b) 20 wt % citric acid and different chitosan contents in comparison to the control film (0CA0CHI).

Regarding TGA, derivative thermo-gravimetric (DTG) curves are shown in **Figure 5.5**, with the weight loss curves in the inset. As can be seen, there are three main weight loss steps. The first one around 100 ºC is related to water evaporation, as also shown by DSC in **Figure 5.4**, and its value was around 10%, in accordance with the MC values shown in **Table 5.2**. The second weight loss step appeared around 250 ºC and it is associated to the evaporation of glycerol (Castelló et al., 2009) and the decomposition of citric acid (Choppali & Gorman, 2008). The maximum temperature corresponding to this second step appeared at lower temperatures for the films prepared with 20 wt % citric acid, which could be related to the different structure of the network formed as a function of citric acid content, as previously shown by FTIR results (**Table 5.1**); in

contrast, the highest value was observed for 0CA0CHI film. Finally, the main weight loss step appeared at 310-320 ºC and it corresponds to fish gelatin (Mohajer et al., 2017) and chitosan degradation (Corazzari et al., 2015). Films showed a residual mass around 30%, except the control film, which showed a residual mass around 20%.

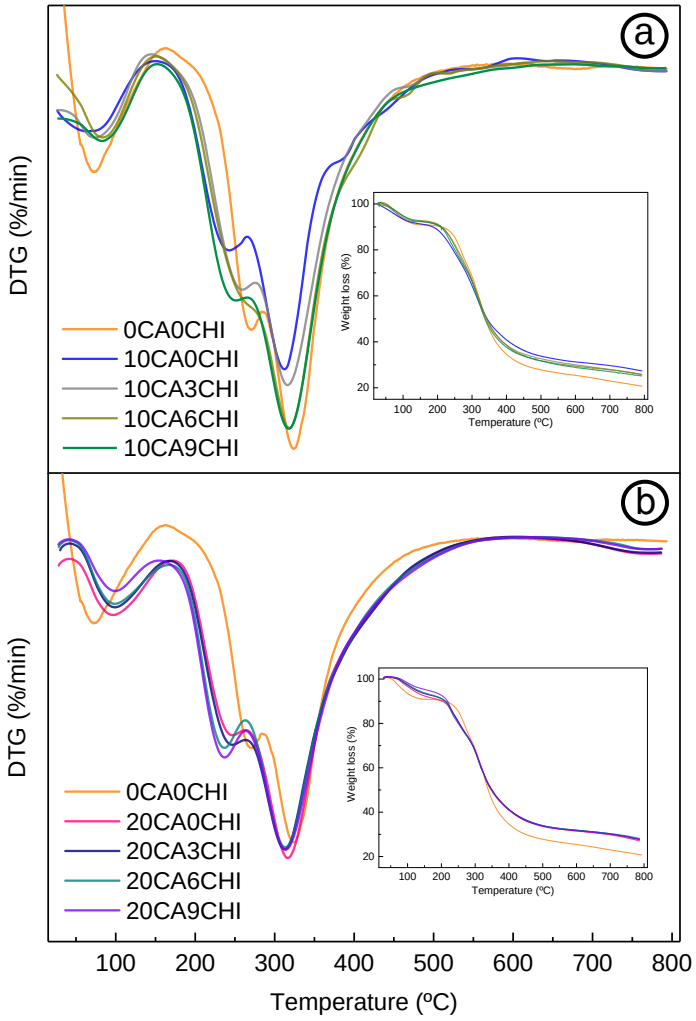

Figure 5.5 Weight loss and DTG curves of the films prepared with a) 10 wt % citric acid and b) 20 wt % citric acid and different chitosan contents in comparison to the control film (0CA0CHI).

5.2.3 Optical properties

In addition to the physicochemical and thermal behaviour, the properties related to the appearance of the films were analysed, in particular, colour, gloss and

transparency. As can be seen in **Table 5.3**, CIELab colour parameters were similar for all films regardless of citric acid and chitosan content. As a consequence, the total colour difference was lower than 1 for all the films, indicating that there was no visual colour difference produced by the incorporation of additives into the formulations.

Table 5.3 CIELab colour parameters (L*, a*, b*) and total colour difference (ΔE*) for fish gelatin films prepared with different contents of citric acid and chitosan.

Film	L*	a*	b*	ΔE*
0CA0CHI	96.81 ± 0.17^{a}	-0.05 ± 0.02^{b}	2.36 ± 0.03^{b}	-
10CA0CHI	96.48 ± 0.07^{b}	0.00 ± 0.02^{a}	2.26 ± 0.04^{a}	0.34 ± 0.07^{a}
10CA3CHI	96.17 ± 0.22^{c}	-0.05 ± 0.01^{b}	2.42 ± 0.11^{b}	0.64 ± 0.12^{b}
10CA6CHI	96.03 ± 0.14^{c}	-0.12 ± 0.02^{c}	2.52 ± 0.06^{b}	0.80 ± 0.09^{c}
10CA9CHI	96.04 ± 0.05^{c}	-0.20 ± 0.02^{d}	2.77 ± 0.08^{c}	0.88 ± 0.06^{c}
0CA0CHI	96.81 ± 0.17^{a}	-0.05 ± 0.02^{b}	2.36 ± 0.03^{b}	-
20CA0CHI	96.69 ± 0.04^{a}	-0.06 ± 0.01^{a}	2.27 ± 0.05^{a}	0.15 ± 0.05^{b}
20CA3CHI	96.51 ± 0.12^{ab}	-0.17 ± 0.01^{b}	2.47 ± 0.05^{c}	0.34 ± 0.11^{a}
20CA6CHI	96.50 ± 0.19^{ab}	-0.19 ± 0.01^{c}	2.58 ± 0.05^{d}	0.41 ± 0.09^{a}
20CA9CHI	96.12 ± 0.36^{b}	-0.28 ± 0.02^{d}	2.79 ± 0.02^{e}	0.84 ± 0.06^{b}

$^{a-e}$Two means followed by the same letter in the same section and column are not significantly (P > 0.05) different through the Tukey's multiple range test.

Regarding gloss values (**Table 5.4**), the most significant difference occurred when chitosan was incorporated into the formulations, which caused a significant (P < 0.05) decrease in gloss values. In spite of the gloss decrease, the films prepared with 10 wt % citric acid maintained a glossy surface with values around 100 GU, regardless of chitosan content, indicative of a smooth surface. In contrast, the surface of the films prepared with 20 wt % citric acid changed from smooth to rough with the incorporation of chitosan, although chitosan content did not significantly (P > 0.05) affect the gloss values. These variations between the films prepared with 10 or 20 wt % citric acid are in accordance with the different physicochemical properties shown in

5.2.1 section. Finally, concerning transparency, fish gelatin films did not absorb light at 600 nm, as can be seen by the low transparency values shown in **Table 5.4**, so it can be said that films were transparent regardless of citric acid and chitosan content.

Table 5.4 Gloss and transparency values of fish gelatin films prepared with different contents of citric acid and chitosan.

Film	Gloss (GU)	Transparency
0CA0CHI	145.5 ± 5.7^{a}	0.66 ± 0.01^{a}
10CA0CHI	155.0 ± 0.7^{a}	1.18 ± 0.05^{b}
10CA3CHI	100.5 ± 2.3^{b}	1.38 ± 0.05^{bc}
10CA6CHI	98.1 ± 3.4^{bc}	0.85 ± 0.06^{a}
10CA9CHI	96.3 ± 0.5^{c}	1.63 ± 0.17^{c}
0CA0CHI	145.5 ± 5.7^{a}	0.66 ± 0.01^{a}
20CA0CHI	127.8 ± 3.2^{b}	0.71 ± 0.03^{a}
20CA3CHI	38.5 ± 0.5^{c}	1.63 ± 0.03^{bc}
20CA6CHI	26.7 ± 3.7^{c}	1.43 ± 0.16^{b}
20CA9CHI	25.9 ± 1.1^{c}	1.74 ± 0.08^{c}

$^{a\text{-}c}$Two means followed by the same letter in the same section and column are not significantly (P > 0.05) different through the Tukey's multiple range test.

5.2.4 Barrier and mechanical properties

Regarding light barrier properties, UV-vis spectra are shown in **Figure 5.6**. As can be seen, films provided UV light barrier from 200 to 250 nm, thanks to tyrosine and phenylalanine amino acid residues in gelatin (Gómez-Guillén et al., 2009; Nagarajan et al., 2015). Moreover, UV light absorbance in the 250-280 nm range increased with the incorporation of citric acid and with the increase of chitosan content due to the carboxyl and hydroxyl auxochrome groups of them (Jadhav & Phugare, 2012).

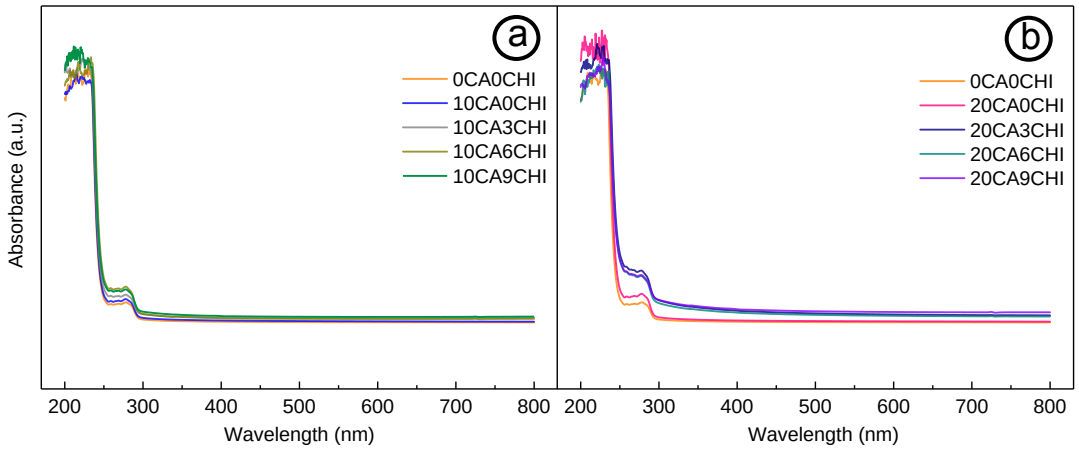

Figure 5.6 UV-vis spectra of the films prepared with a) 10 wt % citric acid and b) 20 wt % citric acid and different chitosan contents in comparison to the control film (0CA0CHI).

Film hydrophobicity was analysed by the measurement of water contact angles (Karbowiak et al., 2006; Kokoszka et al., 2010; Oymaci & Altinkaya, 2016). As shown in **Table 5.5**, WCA values increased by the incorporation of citric acid or chitosan with respect to the control film, leading to hydrophobic surfaces. These values did not significantly ($P > 0.05$) change with chitosan content for the films prepared with 10 wt % citric acid, while WCA values significantly ($P < 0.05$) increased for the films with 20 wt % citric acid when chitosan increased from 0 to 9%, reaching a similar value for the films with 9 wt % chitosan, regardless of citric acid content. This increase in the hydrophobic character of the films can be related to the interactions among polar groups shown by FTIR analysis, which hinder the orientation of polar groups towards the surface. Finally, regarding WVP, similar values were found for all films, indicating that the addition of citric acid and chitosan did not unfavourably affect the film WVP. Water vapour permeability is a two-step process that includes water vapour sorption and water vapour diffusion (Roy et al., 2000). The latter depends on protein structure, which changes as a function of the interactions of protein polar groups, causing the depart from the expected behaviour (Su et al., 2010), as shown by WVP values in this chapter.

Table 5.5 Barrier properties (water contact angle, WCA; water vapour permeability, WVP) and mechanical properties (tensile strength, TS; elongation at break, EB) of fish gelatin films prepared with different contents of citric acid and chitosan.

Film	WCA (º)	WVP·10^{12} (g·cm^{-1}·s^{-1}·Pa^{-1})	TS (MPa)	EB (%)
0CA0CHI	71 ± 4^{a}	1.9 ± 0.1^{a}	68 ± 5^{a}	8 ± 2^{a}
10CA0CHI	112 ± 10^{b}	1.8 ± 0.2^{a}	39 ± 2^{b}	23 ± 3^{b}
10CA3CHI	100 ± 14^{b}	2.5 ± 0.5^{b}	35 ± 1^{b}	18 ± 3^{c}
10CA6CHI	125 ± 13^{b}	2.6 ± 0.2^{b}	30 ± 3^{c}	15 ± 3^{c}
10CA9CHI	118 ± 3^{b}	2.6 ± 0.3^{b}	28 ± 2^{c}	5 ± 1^{a}
0CA0CHI	71 ± 4^{a}	1.9 ± 0.1^{a}	68 ± 5^{a}	8 ± 2^{a}
20CA0CHI	78 ± 5^{b}	2.1 ± 0.3^{a}	29 ± 4^{b}	17 ± 1^{b}
20CA3CHI	64 ± 4^{a}	2.3 ± 0.3^{a}	33 ± 2^{c}	22 ± 3^{c}
20CA6CHI	86 ± 2^{b}	2.5 ± 0.4^{a}	35 ± 3^{c}	18 ± 2^{b}
20CA9CHI	114 ±1^{c}	2.7 ± 0.5^{a}	39 ± 3^{d}	22 ± 2^{c}

$^{a-d}$Two means followed by the same letter in the same section and column are not significantly (P > 0.05) different through the Tukey's multiple range test.

As displayed in **Table 5.5**, mechanical properties were also influenced by the addition of citric acid. Since the residual free citric acid can act as plasticizer (Shi et al., 2008), TS significantly (P < 0.05) decreased, while EB significantly (P < 0.05) increased when citric acid was added. This effect was more pronounced when chitosan was incorporated into the films with 10 wt % citric acid. However, the effect of chitosan on the films prepared with 20 wt % citric acid was different, since both TS and EB values increased when chitosan content was increased. This behaviour is in agreement with the different physicochemical properties shown in 5.2.1 section. The mechanical performance, especially for the films prepared with 20 wt % citric acid, was better than that observed for gelatin/chitosan films with other organic acids, such as gallic acid (Rui et al., 2017) or ferulic acid (Benbettaïeb et al., 2015).

5.2.5 Antibacterial assessment

The antimicrobial activity of films was evaluated against *E. coli* and results are shown in **Figure 5.7**. Although free citric acid has been found to be active against some bacteria (Mahmoud, 2014), including *E.coli* (Firouzabadi et al., 2014), films prepared with

citric acid showed a slight ($P < 0.05$) reduction of bacterial growth, probably due to the fact that citric acid interacted with gelatin, as shown by FTIR results. The incorporation of chitosan significantly ($P < 0.05$) decreased the bacterial growth for the films with 10 wt % citric acid, regardless of chitosan content. In contrast, the increase of chitosan content promoted a further decrease ($P < 0.05$) of bacterial growth for the films prepared with 20 wt % citric acid, in accordance with the FTIR analysis carried out (**Figure 5.1**).

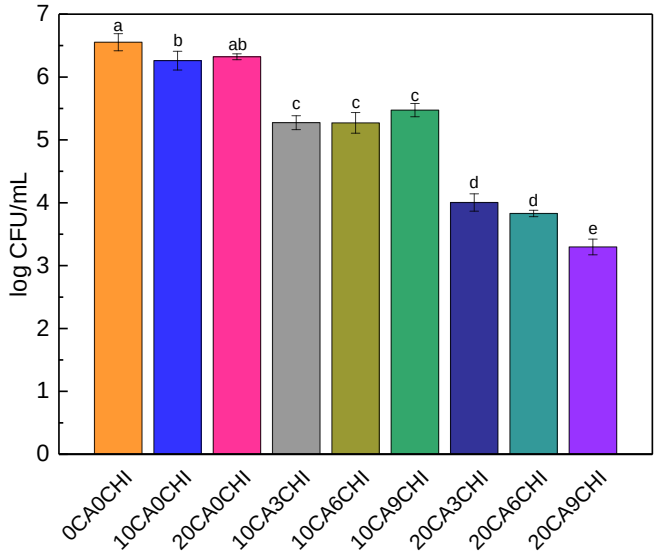

Figure 5.7 Antibacterial activity of the films prepared with a) 10 wt % citric acid and b) 20 wt % citric acid and different chitosan content.

[a-e]Two means followed by the same letter in the same graphic are not significantly ($P > 0.05$) different through the Tukey's multiple range test.

5.3 Conclusions

The incorporation of citric acid into gelatin film forming solutions decreased the swelling of the resulting films, which were flexible and easy to handle. This behaviour could be explained by the new interactions of citric acid with gelatin and glycerol, as shown by FTIR analysis, which suggested the great influence of citric acid content on protein structure and antibacterial activity. In particular, a reduction in the growth of *E. coli* was shown especially for those films prepared with 20 wt % of citric acid and 9 wt % of chitosan, indicating the combined effect of citric acid and chitosan as natural

antimicrobial compounds. The resulting films were transparent, colourless and showed good UV barrier properties and hydrophobic surfaces, essential properties for food packaging applications, highlighting the potential use of these films as active packaging.

6 Anthocyanins containing compression-moulded fish gelatin films

6.1 Summary

Active and intelligent packaging can play a relevant role to reduce food waste. In this regard, apart from antimicrobial agents, a wide series of antioxidant compounds are used in food packaging materials (Yildirim et al., 2018). Even if most of the employed antioxidants are synthetic molecules, natural compounds can also be used, among them, anthocyanins, blue, red or purple pigments found in plants, especially in flowers, fruits and tubers (Gómez-Estaca et al., 2014; Khoo et al., 2017; Stoll et al., 2017). As an example, anthocyanins contained in red cabbage can be mentioned; the annual world production of this vegetable is approximately 68 million tonnes of fresh heads from 3.1 million ha, in more than 130 countries (Demirbas, 2016), and a huge amount of residues with a high antioxidant content are obtained from this large-scale production. It is worth highlighting that besides their antioxidant activity, phenolic antioxidants possess therapeutic benefits, such as anti-cancer, anti-inflammatory and cardioprotective effects, which make them value-added bioactives (Kim et al., 2009; Yates et al., 2017).

The aims of this chapter were to extract and analyse anthocyanins from red cabbage as well as to use them as antioxidants in gelatin film forming formulations. Concerning the manufacturing of antioxidant packaging, in recent years, different production techniques have been employed (Tatara, 2017); however, research on industrial scale production methods, such as extrusion or compression, which are faster and more efficient than traditional casting method, is still needed. In this regard, compression moulding was successfully used in this work with the aim of reducing the production times of gelatin films. Moreover, since antioxidant activity could be affected by the processing conditions used (Lin & Zhou, 2018; Wong & Siow, 2015), manufacture parameters were carefully selected.

Overall, the red cabbage extract identity and pH sensitivity were discussed, and films structural, optical, mechanical and barrier properties were studied. Furthermore, the antioxidant activity of anthocyanin powders and anthocyanin-containing films was

assessed by DPPH radical scavenging, and results were compared with those obtained for α-tocopherol, a widely employed natural antioxidant.

6.2 Results and discussion

6.2.1 Qualitative characterization of anthocyanins

The results of identification of anthocyanins from red cabbage are shown in **Figure 6.1** and **Table S1** (**Supplementary data**). These antioxidants are a sub-group within the flavonoids and they naturally occur as glycosides of flavylium (2-phenylbenzopyrylium) salts (Azeredo et al., 2016). The compounds were identified based on the analysis and comparison of retention times and spectra of the individual peaks of the anthocyanin extract of red cabbage, on the basis of spectral data (UHPLC-Q-TOF-MS/MS).

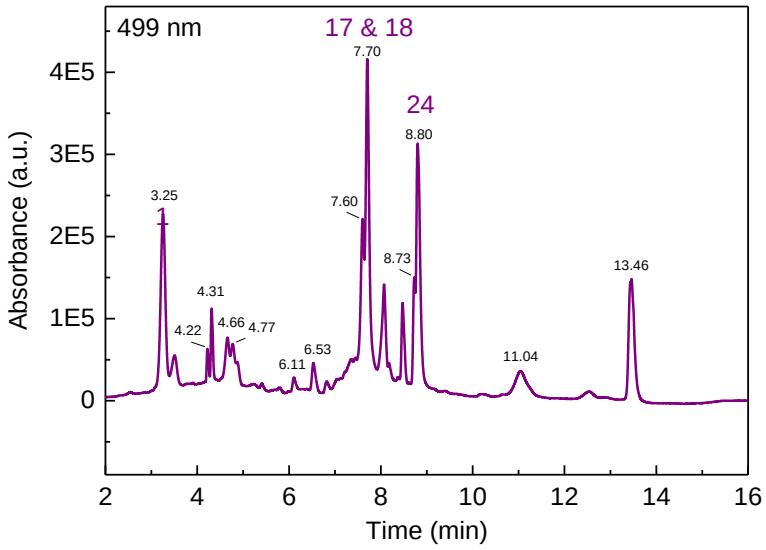

Figure 6.1 Diode-Array Detection (DAD) chromatogram of red cabbage extract at 499 nm.

In the red cabbage extract, 31 peaks related with 11 anthocyanin compounds were identified (**Figures S1-S11**, **Supplementary data**). After the fragmentation of all compounds in the red cabbage extract, results showed that the extract was a rich source

of cyanidin (Cy) based anthocyanins, with various mono- and di-acylating groups. The identified anthocyanins were singly and doubly acylated, mainly with ferulic and sinapic acids. The 31 hydroxycinnamic acid derivatives include mainly residues of p-coumaric, ferulic and sinapic acids or their hydrated forms. Ferulic and sinapic acids were attached to the tetraglucosides, triglucosides, (synapoyl)tetraglucosides and (sinapoyl)triglucosides of cyanidin. Among the major anthocyanin compounds detected, Cy-3-(SinSin)-diGlc-5-Glc was the most abundant one (**Figure 6.1** and **Table S1**, **Supplementary data**). According to Wu & Prior (2005a), red cabbage is a great source of acylated anthocyanins, which may constitute up to 85% of all anthocyanins of this raw material, as confirmed in this study, in which there was only one non-acylated anthocyanin, Cy-3-diGlc-5-Glc.

It is worth noting that around 150 different anthocyanins are known currently in nature (Ortíz et al., 2011). Specifically, in the case of red cabbage extracts, other authors have detected from 9 to 36 anthocyanins (Mizgier et al., 2016). In most red cabbage extracts, the main structures of anthocyanins are cyanidin glycosides, but anthocyanins with other core units like pelargonidin glucoside and peonidin glucosides have also been identified (Wiczkowski et al., 2013). Among the anthocyanins identified in this work, it is worth noting that sinapic acid esterified anthocyanins (peaks 17 and 24) were dominant compared to those esterified by hydroxycinnamic, caffeic, or p-coumaric acids. Similarly, Wu & Prior (2005b) and Ahmadiani et al. (2016) identified sinapic acid-acylated anthocyanins as the major anthocyanins from red cabbage.

Anthocyanins have high sensitivity to degradation reactions, which affect their stability and colour (Qiu et al., 2018). In that way, anthocyanins undergo a reversible structural transformation as a function of pH (Lee et al., 2005; Mazza & Miniati, 2018; Pereira et al., 2015) and the colour variation showed in **Figure 6.2** occurs, suggesting that anthocyanins can be used as pH indicators. Furthermore, this colour change must be considered when anthocyanins are used as pigments (Cortez et al., 2017).

Figure 6.2 Colour change of anthocyanin solutions at different pHs (marked on the lids).

With a view to analyse pH influence, anthocyanin solutions were prepared at three different pHs: basic (2.5), acid (10.0) and non-modified (6.0) pHs. As can be seen in **Table 6.1**, the maximum absorbance ($\lambda_{vis\text{-}max}$) shifted to higher wavelengths when pH values were higher. Moreover, the inhibitory effect of the antioxidant decreased when the pH value increased; in particular, the inhibition effect of the anthocyanin solution at pH 10 was around 15% lower than that of the solution at pH 2.5. Therefore, it could be concluded that the structural transformations occurred in the anthocyanin molecules due to pH changes affected their antioxidant activity.

Table 6.1 $\lambda_{vis\text{-}max}$ and DPPH radical scavenging activity of anthocyanins as a function of solution pH.

Solution pH	$\lambda_{vis\text{-}max}$ (nm)	DPPH scavenging (%)
2.5	526.3	94.5 ± 0.2
6.0	552.4	92.5 ± 0.4
10.0	605.6	79.2 ± 1.5

Considering the high potential of inhibition that anthocyanins exhibited at acid pHs, gelatin film forming solutions were prepared without modifying the gelatin solution pH, since the added citric acid provides an acid pH, at which the antioxidant activity of anthocyanins extracted from red cabbage is high, as shown in **Table 6.1**.

6.2.2 Morphological properties of films

In order to study the influence of anthocyanins addition on the films structure, control and anthocyanin-containing films were compared by SEM analysis. As shown in **Figure 6.3**, no difference could be appreciated between the cross-sections of both films.

Control and anthocyanin-containing films were compact and homogeneous, indicating that anthocyanins were well-distributed in the film.

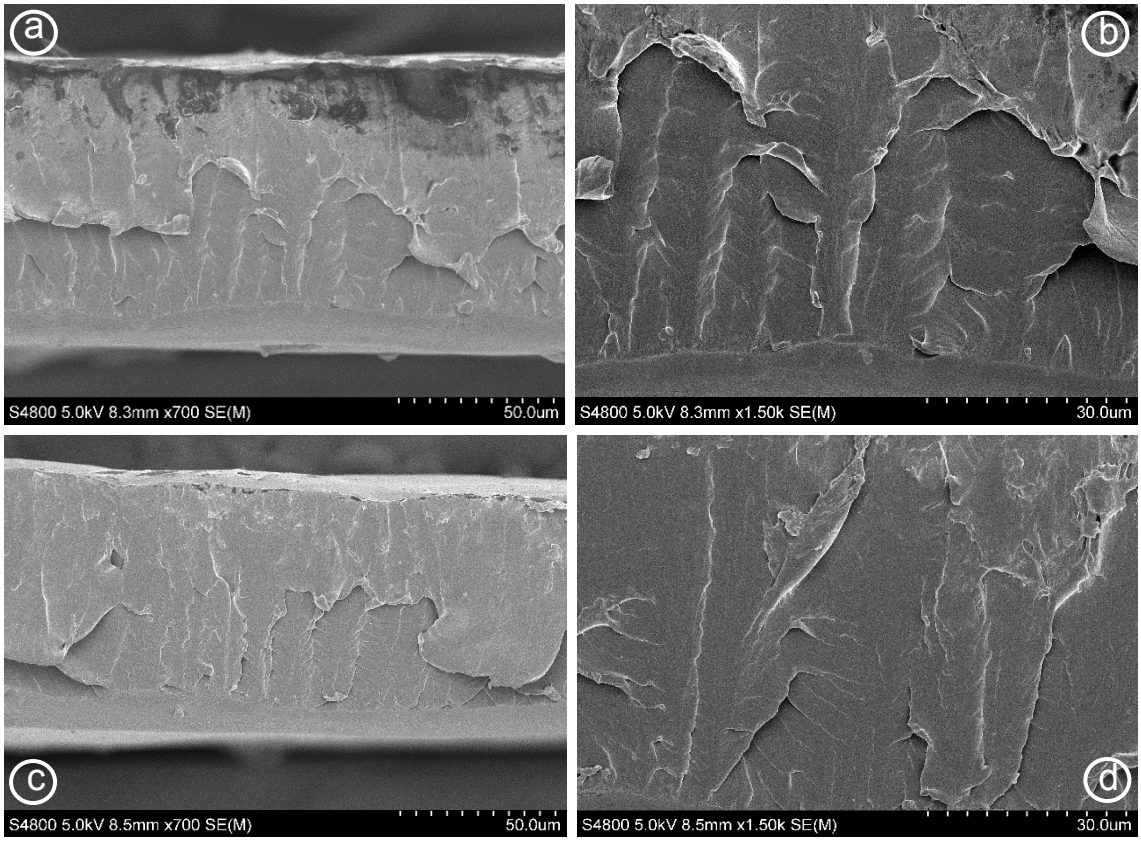

Figure 6.3 Cross-sectional SEM images for control films (a) x700 and (b) x1.50k, and for films prepared with anthocyanins (c) x700 and (d) x1.50k.

6.2.3 Optical properties of films

The appearance of control and anthocyanin-containing films was different due to the pink colour that films acquired when anthocyanins were added, as shown in **Figure 6.4**. Results obtained from colour assessment demonstrated that anthocyanin-containing films were darker, redder and yellower (**Table 6.2**) due to the water-soluble pigments present in anthocyanins (de Moura et al., 2018). Since this is a soft colour and films maintained their transparency, this change is not considered as a drawback for food packaging applications.

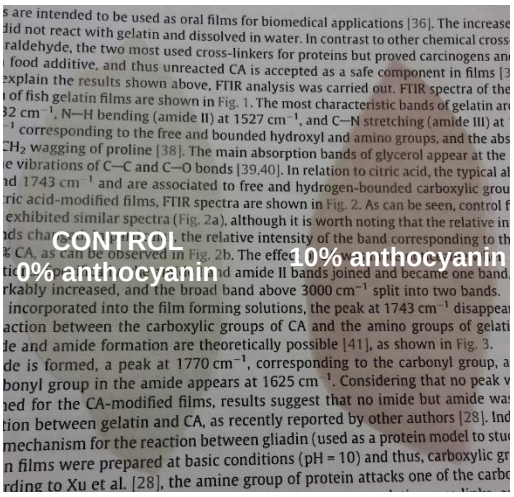

Figure 6.4 The appearance of control and anthocyanin-containing films.

In terms of gloss, there were also differences between control and anthocyanin-containing films. As shown in **Table 6.2**, gloss decreased with the addition of anthocyanins, indicating rougher surfaces that could be more appropriate to be printed (Tišler-Korljan & Gregor-Svetec, 2014). Printability is a required property when films are intended to show information for commercial purposes.

Table 6.2 Colour and gloss values of control and anthocyanin-containing films.

Anthocyanins (%)	L*	a*	b*	ΔE*	Gloss (GU)
0	94.86 ± 0.25	-0.11 ± 0.04	4.98 ± 0.20	-	31.3 ± 1.0
10	89.44 ± 0.81	4.96 ± 0.52	6.41 ± 0.36	7.56 ± 0.98	23.2 ± 0.6

6.2.4 Barrier and mechanical properties

Gelatin films are water sensitive, but the addition of anthocyanins increased WCA, due to the interactions between the hydroxyl groups of anthocyanins and the polar groups of gelatin, which turn polar groups towards the inner film structure, resulting in hydrophobic films (**Table 6.3**). According to the abovementioned statement and considering that permeability depends not only on the surface nature but also on the diffusion of water vapour through the films, it seems that the polar nature of anthocyanins facilitated diffusion since WVP did not change with the addition of anthocyanins. In the

same manner, mechanical properties were not notably affected by the addition of anthocyanins as shown in **Table 6.3**.

Table 6.3 Water contact angle (WCA), water vapour permeability (WVP), tensile strength (TS) and elongation at break (EB) values of control and anthocyanin-containing films.

Anthocyanins (%)	WCA (º)	WVP·10^{12} (g·cm^{-1}·s^{-1}·Pa^{-1})	TS (MPa)	EB (%)
0	76.2 ± 0.2	2.4 ± 0.1	33.4 ± 6.5	3.0 ± 0.8
10	115.9 ± 2.9	2.5 ± 0.1	41.3 ± 2.7	3.9 ± 0.5

6.2.5 Antioxidant release and antioxidant activity of films

The antioxidant release from packaging films can be more effective in inhibiting oxidation than the direct addition of the antioxidant into food, due to the antioxidant protection from degradation. Moreover, the controlled antioxidant release from the packaging film can prevent from effectiveness loss, maintaining the antioxidant activity for longer (Chen et al., 2012). According to the Commission Regulation No 10/2011 (EU, 2011), the antioxidant release from the film was analysed using 50% ethanol as a food simulant, considering that the films prepared in this work could be appropriate to package processed foods (Singh et al., 2009).

Results showed that the antioxidant release proceed rapidly throughout the first day, exhibiting an absorbance of 0.038 at 552 nm and, thus, 1.75 mM anthocyanin was released; then, the release continued and, at the end of the second day, an absorbance of 0.042 at 552 nm was reached, indicating the release of 1.91 mM anthocyanins (**Figure 6.5**). Since the samples prepared had 2 mM anthocyanins, it could be considered that a 95.5% of the antioxidant was released in two days.

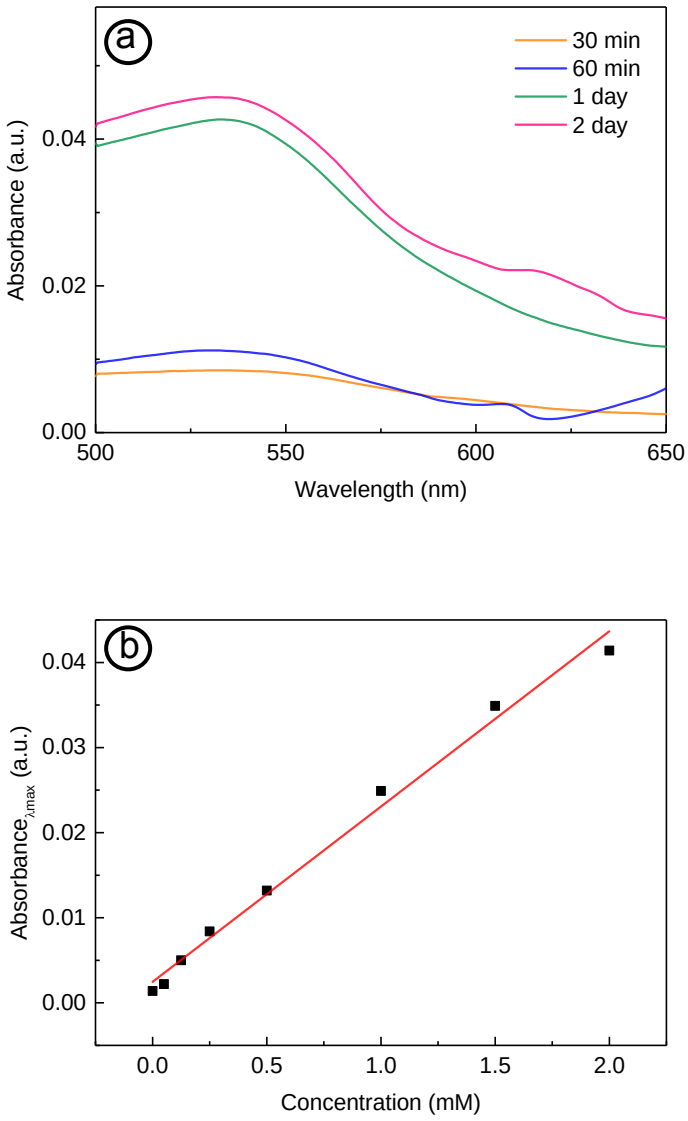

Figure 6.5 Antioxidant release from films over time (a) and calibration curve (b).

Additionally, DPPH radical scavenging capacity was analysed to determine the antioxidant activity of films. In this study, the inhibition value determined was 91.45% (± 1.09); similar to that determined for anthocyanin solution at pH 6.0 (**Table 6.1**). Hence, the anthocyanins incorporated into film forming solutions maintained their activity after film processing, which is of great importance for commercial applications. Finally, this value was compared to that obtained with α-tocopherol, a widely employed natural antioxidant. In the analysis with α-tocopherol, inhibition values increased lineally up to 0.03 mM and α-tocopherol concentrations higher than 0.03 mM did not significantly affect

the antioxidant effect, maintaining the inhibition value around 96%, similar to that found by other authors (Byun et al., 2010; Martins et al., 2012). This value was similar to the one found for the anthocyanins released from gelatin films.

6.3 Conclusions

Anthocyanins were obtained from red cabbage by a simple and environmentally friendly process. These antioxidants were rich in cyanidin and pH-sensitive, showing changes in colour and antioxidant activity as a function of pH. The incorporation of anthocyanins into gelatin film forming solutions resulted in hydrophobic films. These films were successfully prepared by compression moulding, leading to homogeneous films, regardless the addition of anthocyanins, as shown by SEM images. In contrast, optical properties were modified by the anthocyanins addition. Thereby, rougher surfaces were obtained for anthocyanin-incorporated films. Regarding antioxidant properties, films revealed a controlled antioxidant release into food simulant, showing an inhibition value of 92%. Furthermore, anthocyanins showed similar antioxidant activity to α-tocopherol, a widely employed natural antioxidant, highlighting the potential use of anthocyanin-containing fish gelatin films as active films to extend food shelf life.

7 Chitin and THC containing freeze-dried fish gelatin materials

7.1 Summary

Biopolymers extracted from marine waste can be employed to develop active packaging (de la Caba et al., 2019), which can extend food shelf life and decrease food losses, in line with the sustainable development goals, or those biopolymers can be used as bioactive carriers (Centella et al., 2017), in line with the increasing demand of patients for natural and less invasive products. In this way, adding some antioxidant or/and antimicrobial agent into delivery systems, instead of applying them directly, would lengthen the duration of agents' effectiveness and make them more suitable for a sustained release (da Silva et al., 2018; Wang et al., 2019). Furthermore, these systems have been widely analysed for different purposes, such as moisture control (Wang et al., 2017b). Considering that free water is the solvent for chemical or biochemical reactions and microbial growth (Qiu et al., 2019), the control of moisture condensation on these systems could provide benefits for different uses, such as food preservation (Jalali et al., 2019) or wound healing (Etxabide et al., 2017c). In this regard, hydrogels prepared with natural polymers, such as gelatin, can be act as moisture absorbers, since this protein is considered a hygroscopic material with large number of functional groups that can be water molecule adsorption sites (Batista et al., 2019; Esquerdo et al., 2019; Shankar et al., 2016). Regarding absorption characteristics, these depend upon the porous structure, the pore surface and the pore size distribution (Offeddu et al., 2016; Saliba et al., 2016; Varley et al., 2016).

The aim of this study was to valorise marine-derived biowastes, such as fish gelatin obtained from fish skin and chitin extracted from squid pens, in order to prepare porous materials to be employed as bioactive carriers and moisture scavengers. Hence, citric acid cross-linked fish gelatin products were prepared with tetrahydrocurcumin (THC) as a bioactive agent, a hydrogenated colourless metabolite of curcumin (*Curcuma longa* Linn) (Liu et al., 2017), which also exists naturally in *Zingiber officinale* and *Curcuma zedoaria* (Tsai et al., 2017). Moreover, chitin extracted from revalorised squid

pens was employed as a reinforcing agent and this extraction process was environmentally assessed. Additionally, freeze-dried products' characterization was carried out, assessing physicochemical, morphological and mechanical properties as well as moisture scavenging capacity and THC release.

7.2 Results and discussion

7.2.1 Environmental assessment of chitin extraction

Chitin can be extracted from different sources, such as shrimp, crabs, or crayfish shells and cuttlefish or squid pens. It is worth noting that the content of chitin notably changes depending on the marine source used for the extraction. According to the work of Abdou et al. (2008), the content of chitin extracted from crustacean shells is around 20% after a demineralisation process to separate calcium carbonate, whose content can be as high as 50%. However, the content of chitin from squid pens can reach 50%, while the minerals content is lower than 5%. On the one hand, this brings environmental benefits since demineralisation and decolouration processes, with all the chemicals and energy associated to those processes, can be avoided when squid pens are used as raw materials for chitin extraction. Furthermore, the avoidance of those processes brings economic benefits since the extraction procedure implies the use of lower amounts of resources (materials, energy, time), in addition to the higher amounts of chitin that can be extracted from squid pens in comparison to the amounts obtained from crustacean shells.

The environmental charge associated to the extraction of chitin from squid pens was considered. Several stages were taken into account, specifically, squid pens transportation, distilled water production, NaOH preparation, process of chitin extraction, and transportation of wastewater to the residues treatment plant. Regarding distilled water obtaining, it was considered that 3 L of distilled water were employed in the whole process. Moreover, as mentioned in section 2.3, NaOH (1 M) in a ratio of 1:20 (w/v) was

utilized in the extraction process. Thus, the preparation of NaOH solution was taken into account. It is worth mentioning that the employment of squid pens as a source of chitin did not require demineralisation and depigmentation steps because of the low content of inorganic components and the absence of pigments in squid pens (Muxika et al., 2017). Therefore, the processing time, the employment of acid pollutants and the voluminous wastewater discharge can be considerably reduced and so, less chemical solvents were used and less energy was consumed diminishing impact category values (**Table 7.1**).

Table 7.1 Impact category values of the chitin extraction process.

Impact category	Unit	Total
Global warming	kg CO_2 eq	0.9150
Stratospheric ozone depletion	kg CFC11 eq	$4.79 \cdot 10^{-7}$
Ionizing radiation	kBq Co-60 eq	0.4272
Ozone formation, Human health	kg NO_x eq	0.0033
Fine particulate matter formation	kg PM2.5 eq	0.0021
Ozone formation, Terrestrial ecosystems	kg NO_x eq	0.0033
Terrestrial acidification	kg SO_2 eq	0.0052
Freshwater eutrophication	kg P eq	0.0003
Marine eutrophication	kg N eq	$2.73 \cdot 10^{-5}$
Terrestrial ecotoxicity	kg 1,4-DCB	1.1700
Freshwater ecotoxicity	kg 1,4-DCB	0.0104
Marine ecotoxicity	kg 1,4-DCB	0.0149
Human carcinogenic toxicity	kg 1,4-DCB	0.0252
Human non-carcinogenic toxicity	kg 1,4-DCB	0.3039
Land use	m^2a crop eq	0.0180
Mineral resource scarcity	kg Cu eq	0.0008
Fossil resource scarcity	kg oil eq	0.2545
Water consumption	m^3	0.0097

In order to analyse deeply the extraction process, the contribution of each step into the calculated impact categories was assessed (**Figure 7.1**). As expected, the residues transportation and distilled water production were the main contributors to the total impact category values (Lopes et al., 2018), representing around 90% of the total impacts. It is worth noting that the extraction conditions employed in this work are not so sever as those employed in other studies especially in terms of NaOH concentration. Therefore, this led to fewer water utilisation towards pH neutralisation and less wastewater generation, significantly decreasing the weak points of chitin extraction process. Taking all this into consideration, it was concluded that this chitin extraction process provided relevant benefits and lower environmental load comparing to other studies and so, this method was selected to extract the chitin incorporated into gelatin samples.

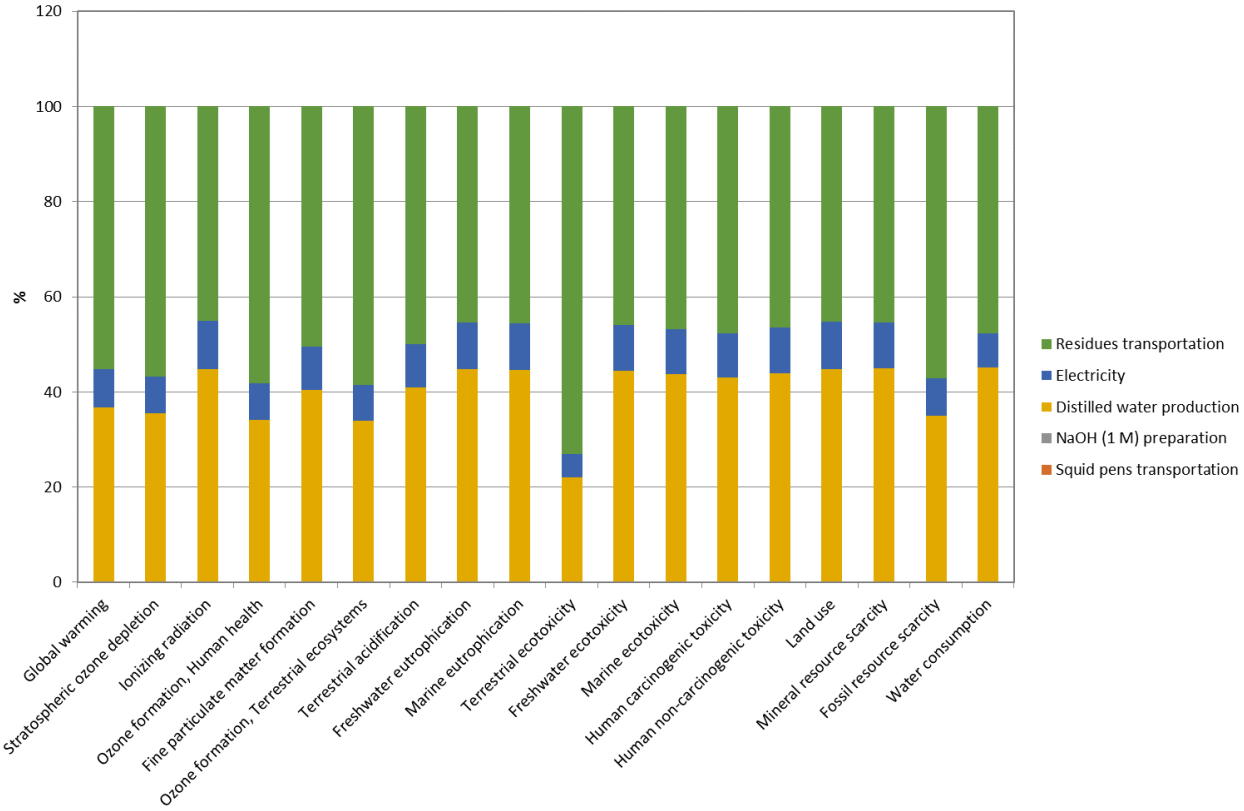

Figure 7.1 Contribution of the different steps (residues transportation, electricity, distilled water production, NaOH (1 M) preparation, and squid pens transportation) to the different impact category values.

7.2.2 Physicochemical properties

In order to assess the interactions occurred in gelatin samples due to the additives incorporation, FTIR analysis was carried out. Regarding pure components (**Table 7.2**), gelatin and chitin showed bands related to -OH and -NH groups (3500-3000 cm^{-1}), amide I (1630 cm^{-1}), amide II (1537 cm^{-1}) and amide III (1238 cm^{-1} for gelatin and 1304 cm^{-1} for chitin) (Jalaja et al., 2016). In the case of citric acid, the two strong bands at 1690 and 1743 cm^{-1} were assigned to C=O stretching modes (Ramirez et al., 2017), specifically associated with free and hydrogen bonded carboxylic groups. Pure glycerol showed five typical absorption bands located from 800 to 1150 cm^{-1}, corresponding to the vibrations of C-C and C-O linkages (Basiak et al., 2018). Finally, the characteristic bands of THC were related to C-C stretching of benzene ring skeleton (1598 cm^{-1}), C-O stretching (1510 cm^{-1}) and C-H in plane bending (1431 cm^{-1}) (Etxabide et al., 2017b; Songtipya et al., 2016).

Table 7.2 Summary of the most relevant FTIR bands of the pure components used in the preparation of gelatin samples.

Pure component	FTIR band (cm^{-1})	Functional group
Gelatin	3500-3000	Free and bounded -OH and -NH
	1632	Amide I (C=O stretching)
	1527	Amide II (N-H bending)
	1238	Amide III (C-N stretching)
Citric acid	1743	Hydrogen bonded -COOH
	1690	Free -COOH
Glycerol	800-1150	Vibrations of C-C and C-O
Chitin	3452	-OH stretching
	3269	-NH stretching
	1629	Amide I (C=O stretching)
	1547	Amide II (in plane N-H bending and C-N stretching)
	1304	Amide III (in-plane mode of the CONH group)
THC	1598	C-C stretching of benzene ring skeleton
	1510	C-O stretching
	1431	C-H in-plane bending

As can be seen in the FTIR spectra of gelatin samples (**Figure 7.2a**), the addition of chitin and THC promoted some changes in the broad band around 3000 cm^{-1}. The

width and intensity of this band changed as a consequence of hydrogen bonding (Chen et al., 2014). Specifically, the lower intensity of the band located around 3500-3000 cm^{-1} might be ascribed to a greater number of intermolecular or intramolecular hydrogen bonds (Deng et al., 2018). In particular, the samples containing a high amount of chitin (30% chitin, CHI30) can be associated with more hydrogen bonding interactions comparing to the samples without chitin or with a lower content of chitin (15% chitin, CHI15). β-chitin has a parallel arrangement with weak intra-sheets hydrogen bonds (Cuong et al., 2016), but the acetyl groups present in chitin can contribute to the formation of hydrogen bonds with gelatin (Yu & Lau, 2017). Furthermore, THC addition increased hydrogen bonding in 15% chitin containing samples due to the hydroxyl groups present in THC (Etxabide et al., 2018), while a similar intensity was observed for CHI30 and CHI30-THC samples, probably due to steric impediments because of high chitin contents (Gutiérrez et al., 2019).

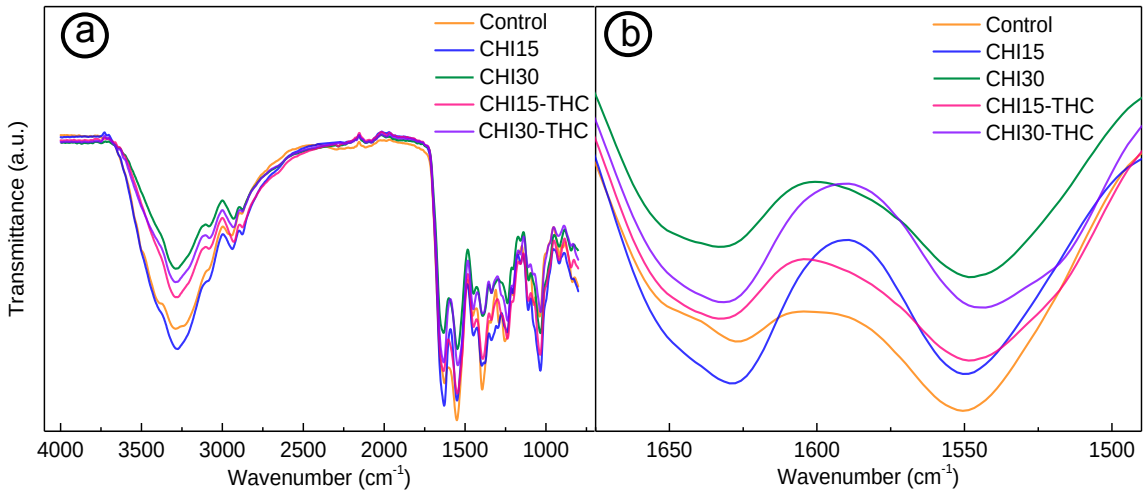

Figure 7.2 FTIR spectra of the gelatin samples as a function of chitin and THC contents.

In addition to hydrogen bonding formation, citric acid provides chemical bonding through the reaction between its carboxylic groups and the amino groups of gelatin (Zhang et al., 2016). This reaction between citric acid and gelatin can be confirmed with the disappearance of the characteristic bands of citric acid at 1743 cm^{-1} and 1690 cm^{-1}

(Zhou et al., 2016). Moreover, as can be seen in **Figure 7.2b**, the change observed in the relative intensity between the bands corresponding to amide I (~1630 cm^{-1}) and amide II (~1550 cm^{-1}) gave some useful information about the reaction. While the relative intensity between these two bands was quite similar for the samples with THC and/or chitin, the intensity of the amide II band was higher related to the intensity of the amide I band for the control samples. As shown in previous chapters, this suggested a more noticeable influence of citric acid on control films and so, the hindering of the reaction due to additives incorporation.

7.2.3 Samples morphology and porosity

Porous materials were prepared in order to promote moisture absorption. As can be seen in SEM images (**Figure 7.3**), all the samples had a porous structure, showing pores with different size and shape, which were distributed randomly. In general, it can be said that chitin containing samples had more defined pores than control ones. Furthermore, a good compatibility between gelatin and chitin was observed, since no chitin aggregation was observed.

The addition of chitin and THC did not influence the average size of pores and these values were maintained around 200 μm. However, high values of deviation revealed the presence of a broad range of pore sizes (**Table 7.3**). Thus, in order to further analyse the inner morphology of gelatin samples, the pore size distribution was studied and results are shown in **Figure 7.4**. In comparison to control samples, the percentage of pores with the size of 100-200 μm was similar in all cases, while the amount of small pores (< 100 μm) decreased with the addition of THC and/or chitin, except for CHI30-THC samples, which presented the highest amount of small pores, probably due to the hindrance of hydrogen bonding as abovementioned in FTIR results. In contrast, the highest percentage of big pores (> 500 μm) was observed for the samples without THC, although this percentage was around or even less than 10% in all cases.

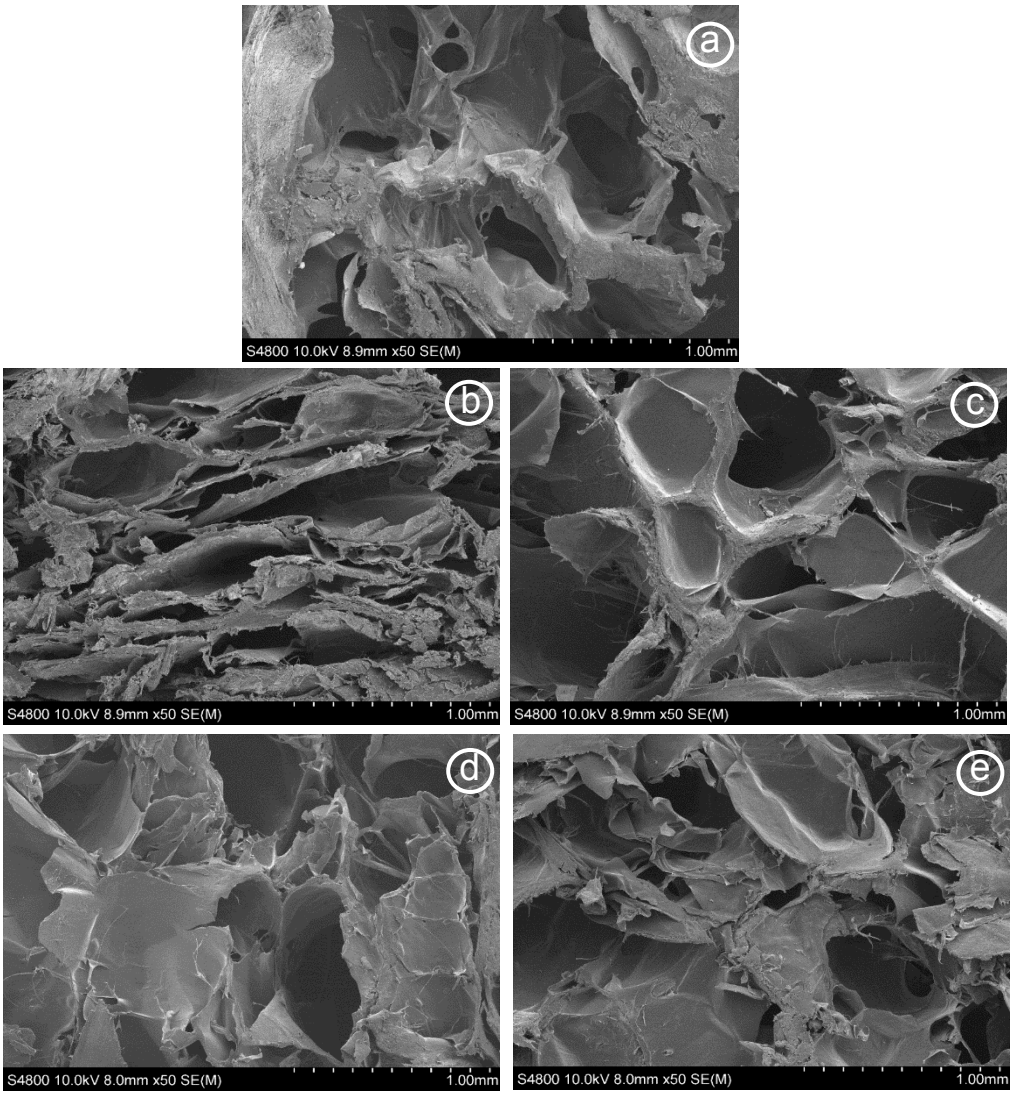

Figure 7.3 SEM micrographs of (a) control, (b) CHI15, (c) CHI30, (d) CHI15-THC and (e) CHI30-THC samples.

Table 7.3 Range of pore sizes of gelatin samples as a function of chitin and THC contents.

Sample	Range of pore sizes (μm)
Control	21-1027
CHI15	29-2129
CHI30	33-1315
CHI15-THC	10-889
CHI30-THC	22-816

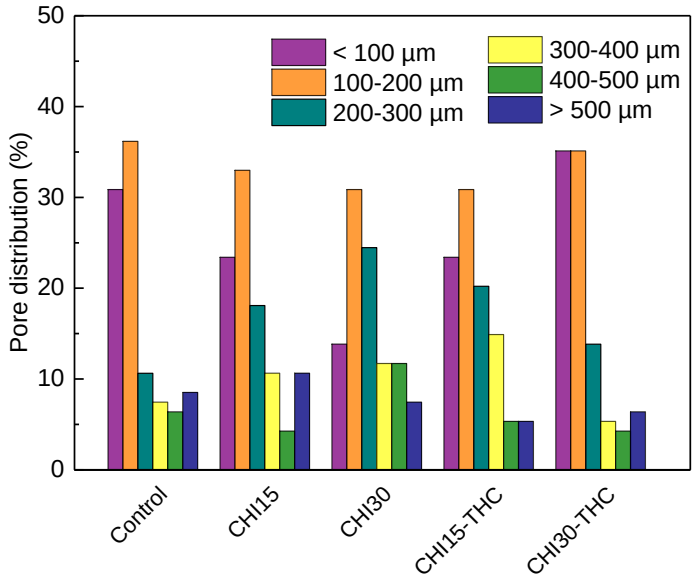

Figure 7.4 Pore size distribution of gelatin samples as a function of chitin and THC contents.

7.2.4 Moisture absorption

The moisture uptake of gelatin samples increased significantly over storage time (**Figure 7.5**); the absorption was rapid in the first days and later, it was substantially slower. Values after 18 days (data not shown) presented high uncertainty due to sample deterioration because of the high moisture content absorbed. Weibull model described the moisture absorption as a function of time adequately, since the coefficient of determination (R^2) was greater than 0.9 (**Table 7.4**). The moisture holding capacity at equilibrium (M_∞) slightly varied among different samples, in accordance with the similar pore average size abovementioned, and the values obtained were around 1.65-1.87 g water/g sample. Similar water absorbance capacity has been found by other authors (Zhang et al., 2019) who isolated two different polysaccharides from *Rosa rugosa* petals that absorbed 0.337 and 0.668 g water/g polysaccharide after 96 h under 81% relative humidity. On the other hand, all gelatin samples needed around 6 days to accomplish approximately 63% of the moisture uptake (β_1).

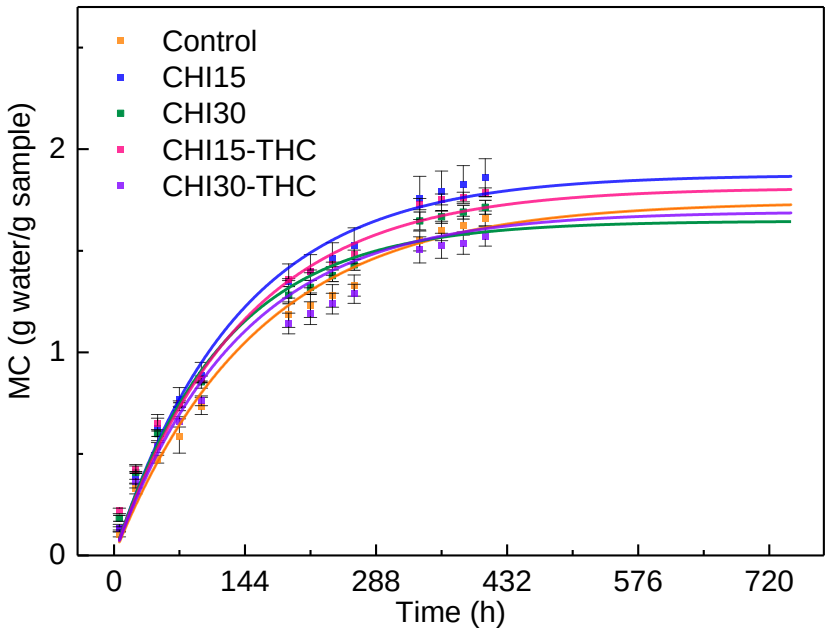

Figure 7.5 Moisture absorption of gelatin samples as a function of chitin and THC contents.

Table 7.4 M_∞, β_1 and R^2 results of gelatin samples as a function of chitin and THC contents.

Sample	M_∞ (g water/g sample)	β_1 (h)	R^2
Control	1.74	156.23	0.99
CHI15	1.87	136.18	0.97
CHI30	1.65	119.27	0.91
CHI15-THC	1.81	139.92	0.98
CHI30-THC	1.69	136.29	0.95

These M_∞ and β_1 values are temperature- and relative humidity-sensitive and they are influenced by the packaging environment (Gaona-Forero et al., 2018): if temperature increased, an increase in both rate and absorption capacity would occur; if relative humidity decreased, lower adsorption capacity would be obtained. It is worth noting that moisture absorbers should be used carefully for high water activity products like fresh fruit and vegetables since excessive moisture loss from those foods should be avoided (Rux et al., 2015). Therefore, even if the gelatin samples prepared in this work showed

the capacity to absorb moisture during several days and, thus, these samples can be considered as good moisture scavengers, the study is still preliminary and a deeper analysis would be needed to assess their suitability for food packaging applications. Furthermore, this kind of materials could find other applications related to sanitary or health-care (Álvarez-Castillo et al., 2018).

7.2.5 Mechanical behaviour

Compression resistance of samples was analysed in order to assess their mechanical behaviour during their lifetime, and the influence of the moisture uptake into mechanical properties. As can be seen in **Figure 7.6** characteristic curves of low density, open-cell foams were obtained, with collapse plateau and densification regimes; indeed, the initial linear elastic region was hard to identify (Grover et al., 2012). Thus, slight stress values were utilized to obtain strain values up to 40%. Thereafter, samples could support higher stress values compressing up to 80% strain. In this densification process porous samples are highly compressed and only low deformations are allowed (Tonda-Turo et al., 2011). Finally, samples recovered their initial shape upon removing the loading force owing to the elasticity that the samples acquired during 6-day storage (**Figure 7.6a**) due to the moisture absorbed (Duconseille et al., 2017). Similar non-linear elastic response was observed by Czerner et al. (2016) for bovine and porcine gels. It is worth highlighting that the addition of chitin and THC increased significantly the stress resistance. In particular, the incorporation of chitin increased the stress resistance from 0.24 MPa (control) to 0.58 MPa (CHI30), and this increase was even more noticeable when both chitin and THC were incorporated into the formulation since CHI30-THC sample supported 1.68 MPa at 80% strain.

The second analysis carried out after other 11 days of samples storage showed similar stress-strain results (**Figure 7.6b**). However, CHI30-THC stress resistance decreased and all samples lost the capacity to recover their initial shape. Therefore, it can be concluded that a deterioration of the chemical structure occurred due to high

moisture contents within samples after 17 days of storage in a chamber with extreme relative humidity conditions (100% relative humidity).

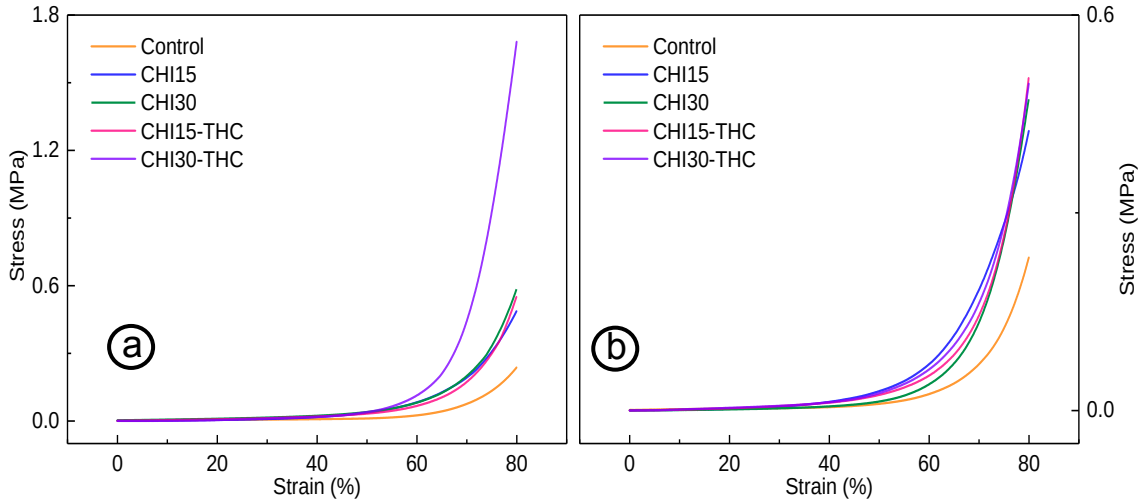

Figure 7.6 Compression test of gelatin samples stored in a controlled chamber (100% relative humidity and room temperature) for a) 6 days and b) 17 days, as a function of chitin and THC contents.

7.2.6 Swelling behaviour

The appearance of dry and swelled samples, specifically the images for CHI30-THC samples are shown in **Figure 7.7a**. As can be seen in **Figure 7.7b**, chitin containing samples, especially CHI15 and CHI30 samples, showed a fast increase of swelling, probably due to the new hydrogen bonds formed between ethanol and water molecules present in the food simulant and the polymers (gelatin and chitin) and additives (THC, citric acid and glycerol) used in the formulations, which could enhance chain mobility and, thus, a fast swelling rate (Madera-Santana et al., 2014).

Comparing the obtained results, significant differences can be appreciated. The lowest values were assigned to control samples, which had a 440% swelling at the second day. Thereby, it can be concluded that control samples had the highest cross-linking extent, as also shown by FTIR analysis. Otherwise, the highest swelling values, 985% and 894%, were reached for CHI15 and CHI30 samples, respectively. The bigger size of pores in these samples could facilitate the entrance of water and ethanol

molecules and, thus, the swelling capacity increased. On the other hand, THC containing samples presented lower maximum values of 524% for CHI15-THC and 622% for CHI30-THC, probably due to the release of THC, as shown below.

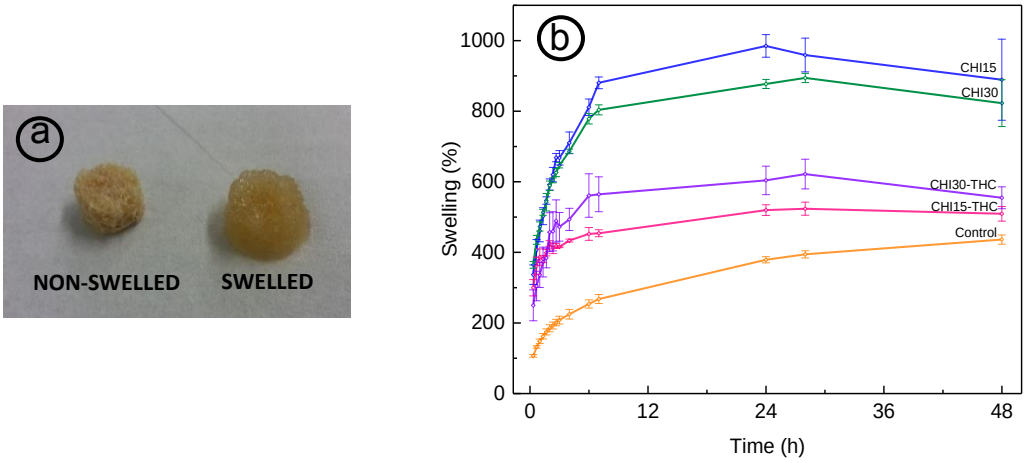

Figure 7.7 The appearance of non-swelled and swelled CHI30-THC samples (a) and the swelling behaviour of gelatin samples as a function of chitin and THC contents (b).

7.2.7 THC release

THC release was analysed and the results are presented in **Figure 7.8**. First, THC was released at fast rates and 44% and 37% of THC was delivered in one day for CHI15-THC and CHI30-THC samples, respectively. The higher stearic hindrance in CHI30-THC samples could cause the lower values of THC release in these samples (Kamalipour et al., 2016). After the first day, the THC release rate was slower, reaching a plateau value, 53% for CHI15-THC and 42% for CHI30-THC at the third day. This behaviour would confirm the interactions of THC with the polar groups of the formulation components, as shown by FTIR analysis. Therefore, all the THC incorporated into the formulations would not be released, but it would contribute to maintain the structure and integrity of gelatin samples.

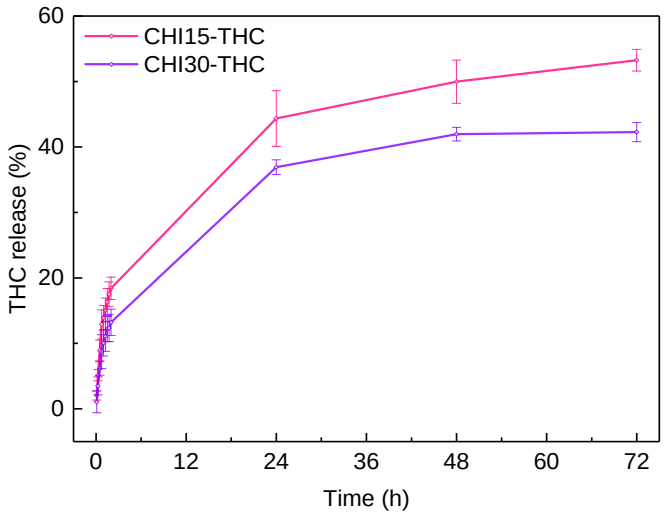

Figure 7.8 THC release from CHI15-THC and CHI30-THC samples over time.

7.3 Conclusions

Porous materials, with a pore average size of 200 µm, were prepared for bioactive release and moisture absorption purposes. Chitin, extracted employing a sustainable method, and THC addition promoted hydrogen bonding interactions among the formulation components, even if steric impediments diminished this type of interactions in the samples with a higher chitin content. Furthermore, additives incorporation hindered the reaction between the carboxylic groups of citric acid and the amino groups of gelatin. This influenced the swelling behaviour of samples with chitin and THC, which showed higher swelling capacity than the control sample. The moisture absorption increased significantly over storage time and the moisture holding capacity values were around 1.65-1.87 g water/g sample. In addition to moisture absorption, chitin-reinforced gelatin samples incorporated with THC showed a sustained release of the bioactive compound.

8 General conclusions

The general conclusions of this doctoral thesis are summarised below:

- Citric acid-incorporated fish gelatin-based solutions were electrospun successfully and the subsequent thermal treatment at 80 ºC of the electrospun mats led to morphological stability improvements.
- The pH of the spinning solutions had a strong influence on the viscoelastic behaviour of the solutions, fibre morphology stability and cross-linking extent.
- The reaction of gelatin and citric acid was favoured at basic pH, leading to films with enhanced mechanical properties.
- The environmental assessment of gelatin films revealed that composting was a beneficial waste treatment after disposal of films, as shown by carbon footprint assessment.
- *E. coli* growth was reduced in fish gelatin/chitosan composite films, indicating the combined effect of citric acid and chitosan as natural antimicrobial compounds.
- Anthocyanins could be extracted from red cabbage by a simple and environmentally friendly process and were pH-sensitive, showing changes in colour as a function of pH, which is suitable for intelligent packaging.
- Anthocyanins added into fish gelatin films prepared by compression maintained their antioxidant activity after film processing.
- Freeze-dried samples showed porous structures, gradual moisture absorption and THC release, and they are considered appropriate as bioactives' carriers and moisture scavengers.

9 References

Abad-García B., Berrueta L.A., Garmón-Lobato S., Gallo B., Vicente F. (2009). A general analytical strategy for the characterization of phenolic compounds in fruit juices by high-performance liquid chromatography with diode array detection coupled to electrospray ionization and triple quadrupole mass spectrometry. Journal of Chromatography A, 1216(28), 5398-5415.

Abdou, E.S., Nagy, K.S.A., Elsabee, M.Z. (2008). Extraction and characterization of chitin and chitosan from local sources. Bioresource Technology, 99(5), 1359-1367.

Aceituno-Medina M., Mendoza S., Lagaron J.M., López-Rubio A. (2015). Photoprotection of folic acid upon encapsulation in food-grade amaranth (*Amaranthus hypochondriacus* L.) protein isolate - Pullulan electrospun fibers. LWT-Food Science and Technology, 62(2), 970-975.

Acosta S., Jiménez A., Cháfer M., González-Martínez C., Chiralt A. (2015). Physical properties and stability of starch-gelatin based films as affected by the addition of esters of fatty acids. Food Hydrocolloids, 49, 135-143.

Adilah A.N., Jamilah B., Noranizan M.A., Hanani Z.A.N. (2018). Utilization of mango peel extracts on the biodegradable films for active packaging. Food Packaging and Shelf Life, 16, 1-7.

Aduba J, Hammer J.A., Yuan Q., Yeudall W.A., Bowlin G.L., Yang H. (2013). Semi-interpenetrating network (sIPN) gelatin nanofiber scaffolds for oral mucosal drug delivery. Acta Biomaterialia, 9(5), 6576-6584.

Ahmadiani N., Robbins R.J., Collins T.M., Giusti M.M. (2016). Molar absorptivity (ε) and spectral characteristics of cyanidin-based anthocyanins from red cabbage. Food Chemistry, 197, 900-906.

Alfaro A.T., Balbinot E., Weber C.I., Tonial I.B., Machado-Lunkes A. (2015). Fish Gelatin: Characteristics, functional properties, applications and future potentials. Food Engineering Reviews, 7(1), 33-44.

Ali A.M.M., Kishimura H., Benjakul S. (2018). Physicochemical and molecular properties of gelatin from skin of Golden carp (*Probarbus Jullieni*) as influenced by acid pretreatment and prior-ultrasonication. Food Hydrocolloids, 82, 164-172.

Almeida E.V.R., Frollini E., Castellan A., Coma, V. (2010). Chitosan, sisal cellulose, and biocomposite chitosan/sisal cellulose films prepared from thiourea/NaOH aqueous solution. Carbohydrate Polymers, 80(3), 655-664.

Altan A., Aytac Z., Uyar T. (2018). Carvacrol loaded electrospun fibrous films from zein and poly (lactic acid) for active food packaging. Food Hydrocolloids, 81, 48-59.

Álvarez-Castillo E., Del Toro A., Aguilar J.M., Guerrero A., Bengoechea, C. (2018). Optimization of a thermal process for the production of superabsorbent materials based on a soy protein isolate. Industrial Crops and Products, 125, 573-581.

Angarano M, Schulz S., Fabritius M., Vogt R., Steinberg T., Tomakidi P., Friedrich C., Mülhaupt R. (2013). Layered gradient nonwovens of in situ crosslinked electrospun collagenous nanofibers used as modular scaffold systems for soft tissue regeneration. Advanced Functional Materials, 23(26), 3277-3285.

Arrieta M.P., Peltzer M.A., Garrigós M.C., Jiménez A. (2013). Structure and mechanical properties of sodium and calcium caseinate edible active films with carvacrol. Journal of Food Engineering, 114(4), 486-494.

Arya S.K., Manohar M., Singh G., Siddiqui W.A. (2017). Chitin and chitosan-complexes and their applications. In: Ahmed S., & Ikram S. (eds.). Chitosan: Derivatives, composites and applications. Wiley, USA, pp. 151-165.

ASTM D523-14. (2014). Standard test method for specular gloss. In: Annual Book of ASTM Standards, American Society for testing and materials, Philadelphia.

ASTM D638-03. (2003). Standard test method for tensile properties of plastics. In: Annual Book of ASTM Standards, American Society for testing and materials, Philadelphia.

ASTM E96-00. (2000). Standard test methods for water vapour transmission of material. In: Annual Book of ASTM Standards, American Society for testing and materials, Philadelphia.

Aytac Z., Ipek S., Durgun E., Tekinay T., Uyar T. (2017). Antibacterial electrospun zein nanofibrous web encapsulating thymol/cyclodextrin-inclusion complex for food packaging. Food Chemistry, 233, 117-124.

Azeredo H.M.C., & Waldron K.W. (2016). Crosslinking in polysaccharide and protein films and coatings for food contact - A review. Trends in Food Science & Technology, 52, 109-122.

Azeredo H.M.C., Morrugares-Carmona R., Wellner N., Cross K., Bajka B., Waldron K.W. (2016). Development of pectin films with pomegranate juice and citric acid. Food Chemistry, 198, 101-106.

Azevedo V.M., Dias M.V., Borges S.V., Costa A.L.R., Silva E.K., Medeiros E.A.A., Soares N.F.F. (2015b). Development of whey protein isolate bio-nanocomposites: Effect of montmorillonite and citric acid on structural, thermal, morphological and mechanical properties. Food Hydrocolloids, 48, 179-188.

Azevedo V.M., Silva E.K., Pereira C.F.G., da Costa J.M.G., Borges S.V. (2015a). Whey protein isolate biodegradable films: Influence of the citric acid and montmorillonite clay nanoparticles on the physical properties. Food Hydrocolloids, 43, 252-258.

Balakrishnan P., Geethamma V.G., Sreekala M.S., Thomas S. (2018). Polymeric biomaterials: State-of-the-art and new challenges. In: Thomas S., Balakrishnan P., Sreekala M.S. (eds.). Fundamental biomaterials: Polymers. Woodhead Publishing, UK, pp. 1-20.

Balcão V.M., & Vila M.M.D.C. (2015). Structural and functional stabilization of protein entities: *State-of-the-art*. Advanced Drug Delivery Reviews, 93, 25-41.

Baniasadi H., Ramazani S.A.A., Mashayekhan S. (2015). Fabrication and characterization of conductive chitosan/gelatin-based scaffolds for nerve tissue engineering. International Journal of Biological Macromolecules, 74, 360-366.

Bano I., Arshad M., Yasin T., Ghauri M.A., Younus M. (2017). Chitosan: A potential biopolymer for wound management. International Journal of Biological Macromolecules, 102, 380-383.

Barbosa M., & Martins M.C.L. (2018). Peptides and proteins as biomaterials for tissue regeneration and repair. Woodhead Publishing, UK.

Basiak E., Lenart A., Debeaufort F. (2018). How glycerol and water contents affect the structural and functional properties of starch-based edible films. Polymers, 10(4), 412-429.

Batista R.A., Espitia P.J.P., Quintans J.S.S., Freitas M.M., Cerqueira M.Â., Teixeira J.A., Cardoso J.C. (2019). Hydrogel as an alternative structure for food packaging systems. Carbohydrate Polymers, 205, 106-116.

Benbettaïeb N., Chambin O., Assifaoui A., Al-Assaf S., Karbowiak T., Debeaufort F. (2016). Release of coumarin incorporated into chitosan-gelatin irradiated films. Food Hydrocolloids, 56, 266-276.

BenBettaïeb N., Karbowiak T., Bornaz S., Debeaufort F. (2015). Spectroscopic analyses of the influence of electron beam irradiation doses on mechanical, transport properties and microstructure of chitosan-fish gelatin blend films. Food Hydrocolloids, 46, 37-51.

Benbettaïeb N., Karbowiak T., Brachais C.H., Debeaufort F. (2015). Coupling tyrosol, quercetin or ferulic acid and electron beam irradiation to cross-link chitosan-gelatin films: A structure-function approach. European Polymer Journal, 67, 113-127.

Benbettaïeb N., Tanner C., Cayot P., Karbowiak T., Debeaufort F. (2018). Impact of functional properties and release kinetics on antioxidant activity of biopolymer active films and coatings. Food Chemistry, 242, 369-377.

Berkowitz S.A., & Houde D.J. (2015). The complexity of protein structure and the challenges it poses in developing biopharmaceuticals. In: Houde D.J., & Berkowitz S.A. (eds.). Biophysical characterisation of proteins in developing biopharmaceuticals (1st edition). Elsevier, Netherlands, pp. 1-21.

Bermúdez-Oria A., Rodríguez-Gutiérrez G., Vioque B., Rubio-Senent F., Fernández-Bolaños J. (2017). Physical and functional properties of pectin-fish gelatin films containing the olive phenols hydroxytyrosol and 3,4-dihydroxyphenylglycol. Carbohydrate Polymers, 178, 368-377.

Bharathidasan T., Narayanan T.N., Sathyanaryanan S., Sreejakumari S.S. (2015). Above 170º water contact angle and oleophobicity of fluorinated graphene oxide based transparent polymeric films. Carbon, 84, 207-213.

Bhattacharyya I., Molaro M.C., Braatz R.D., Rutledge G.C. (2016). Free surface electrospinning of aqueous polymer solutions from a wire electrode. Chemical Engineering Journal, 289, 203-211.

Bhushani J.A., & Anandharamakrishnan C. (2014). Electrospinning and electrospraying techniques: Potential food based applications. Trends in Food Science & Technology, 38(1), 21-33.

Bitencourt C.M., Fávaro-Trindade C.S., Sobral P.J.A., Cavalho R.A. (2014). Gelatin-based films additivated with curcuma ethanol extract: Antioxidant activity and physical properties of films. Food Hydrocolloids, 40, 145-152.

Bonilla J., & Sobral P.J.A. (2016). Investigation of the physicochemical, antimicrobial and antioxidant properties of gelatin-chitosan edible film mixed with plant ethanolic extracts. Food Bioscience, 16, 17-25.

Bovi G.G., Caleb O.J., Klaus E., Tintchev F., Rauh C., Mahajan, P.V. (2018). Moisture absorption kinetics of FruitPad for packaging of fresh strawberry. Journal of Food Engineering, 223, 248-254.

Bracaglia L.G., Smith B.T., Watson E., Arumugasaamy N., Mikos A.G., Fisher J.P. (2017). 3D printing for the design and fabrication of polymer-based gradient scaffolds. Acta Biomaterialia, 56, 3-13.

Byler D.M., & Susi H. (1986). Examination of the secondary structure 457 of proteins by deconvolved FTIR spectra. Biopolymers, 25(3), 469-487.

Byun Y., Kim Y.T., Whiteside S. (2010). Characterization of an antioxidant polylactic acid (PLA) film prepared with α-tocopherol, BHT and polyethylene glycol using film cast extruder. Journal of Food Engineering, 100(2), 239-244.

Castelló M.L., Dweck J., Aranda D.A.G. (2009). Thermal stability and water content determination of glycerol by thermogravimetry. Journal of Thermal Analysis and Calorimetry, 97, 627-630.

Castillo L.A., Farenzena S., Pintos E., Rodríguez M.S., Villar M.A., García M.A., López O.V. (2017). Active films based on thermoplastic corn starch and chitosan oligomer for food packaging applications. Food Packaging and Shelf Life, 14, 128-136.

Centella M.H., Arévalo-Gallegos A., Parra-Saldivar R., Iqbal H.M.N. (2017). Marine-derived bioactive compounds for value-added applications in bio- and non-bio sectors. Journal of Cleaner Production, 168, 1559-1565.

Cerqueira M.A.P.R., Pereira R.N.C., Ramos O.L.S., Teixeira J.A.C., Vicente A.A. (2016). Edible food packaging: Materials and processing technologies. CRC Press, USA.

Chen J., Li L., Yi R., Xu N., Gao R., Hong B. (2016). Extraction and characterization of acid-soluble collagen from scales and skin of tilapia (*Oreachromis niloticus*). LWT-Food Science and Technology, 66, 453-459.

Chen M., Liu F., Chiou B.S., Sharif H.R., Xu J., Zhong F. (2017). Characterization of film-forming solutions and films incorporating free and nanoencapsulated tea polyphenol prepared by gelatins with different Bloom values. Food Hydrocolloids, 72, 381-388.

Chen X., Chew S.L., Kerton F.M., Yan N. (2014). Direct conversion of chitin into a N-containing furan derivative. Green Chemistry, 16(4), 2204-2212.

Chen X., Lee D.S., Zhu X., Yam K.L. (2012). Release kinetics of tocopherol and quercetin from binary antioxidant controlled-release packaging films. Journal of Agricultural and Food Chemistry, 60(13), 3492-3497.

Chin S.S., Lyn F.H., Hanani Z.A.N. (2017). Effect of *Aloe vera* (*Aloe barbadensis Miller*) gel on the physical and functional properties of fish gelatin films as active packaging. Food Packaging and Shelf Life, 12, 128-134.

Chiralt A., González-Martínez C., Vargas M., Atarés L. (2018). Edible films and coatings from proteins. In: Yada R.Y. (ed.). Proteins in food processing (2nd edition). Woodhead Publishing, UK, pp. 477-500.

Choppali U, & Gorman B.P. (2008). Structural and optical properties of nanocrystalline ZnO thin films synthesized by the citrate precursor route. Journal of Luminescence, 128(10), 1641-1648.

Ciannamea E.M., Stefani P.M., Ruseckaite R.A. (2016). Properties and antioxidant activity of soy protein concentrate films incorporated with red grape extract processed by casting and compression molding. LWT-Food Science and Technology, 74, 353-362.

Clarke D., Tyuftin A.A., Cruz-Romero M.C., Bolton D., Fanning S., Pankaj S.K., Bueno-Ferrer C., Cullen P.J., Kerry J.P. (2017). Surface attachment of active antimicrobial coatings onto conventional plastic-based laminates and performance assessment of these materials on the storage life of vacuum packaged beef sub-primals. Food Microbiology, 62, 196-201.

Corazzari I., Nisticò R., Turci F., Faga M.G., Franzoso F., Tabasso S., Magnacca G. (2015). Advanced physico-chemical characterization of chitosan by means of TGA coupled on-line with FTIR and GCMS: Thermal degradation and water adsorption capacity. Polymer Degradation and Stability, 112, 1-9.

Córdoba L.J.P., & Sobral P.J.A. (2017). Physical and antioxidant properties of films based on gelatin, gelatin-chitosan or gelatin-sodium caseinate blends loaded with nanoemulsified active compounds. Journal of Food Engineering, 213, 47-53.

Cortez R., Luna-Vital D.A., Margulis D., de Mejia E.G. (2017). Natural pigments: Stabilization methods of anthocyanins for food applications. Comprehensive Reviews in Food Science and Food Safety, 16(1), 180-198.

Costa F., Silva R., Boccaccini A. (2018). Fibrous protein-based biomaterials (silk, keratin, elastin, and resilin proteins) for tissue regeneration and repair. In: Barbosa M.A., & Martins M.C.L. (eds.). Peptides and proteins as biomaterials for tissue regeneration and repair. Woodhead publishing, UK, pp. 175-204.

Cui Z., Beach E.S., Anastas P.T. (2011). Modification of chitosan films with environmentally benign reagents for increased water resistance. Green Chemistry Letters and Reviews, 4(1), 35-40.

Cumming M.H., Leonard A.R., Le Corre-Bordes D.S., Hofman K. (2018). Intra-fibrillar citric acid crosslinking of marine collagen electrospun nanofibres. International Journal of Biological Macromolecules, 114, 874-881.

Cuong H.N., Minh N.C., Hoa N.V., Trung T.S. (2016). Preparation and characterization of high purity β-chitin from squid pens (*Loligo chenisis*). International Journal of Biological Macromolecules, 93, 442-447.

Czerner M., Fasce L.A., Martucci J.F., Ruseckaite R., Frontini P.M. (2016). Deformation and fracture behavior of physical gelatin gel systems. Food Hydrocolloids, 60, 299-307.

da Silva F.T., da Cunha K.F., Fonseca L.M., Antunes M.D., El Halal S.L.M., Fiorentin Â.M., Zavareze E.R., Dias A.R.G. (2018). Action of ginger essential oil (*Zingiber officinale*) encapsulated in proteins ultrafine fibers on the antimicrobial control *in situ*. International Journal of Biological Macromolecules, 118, 107-115.

de la Caba K., Guerrero P., Trung T.S., Cruz-Romero M., Kerry J.P., Fluhr J., Maurer M., Kruijssen F., Albalat A., Bunting S., Burt S., Little D., Newton R. (2019). From seafood waste to active seafood packaging: An emerging opportunity of the circular economy. Journal of Cleaner Production, 208, 86-98.

de Moraes J.O., Scheibe A.S., Augusto B., Carciofi M., Laurindo J.B. (2015). Conductive drying of starch-fiber films prepared by tape casting: Drying rates and film properties. LWT-Food Science and Technology, 64(1), 356-366.

de Moura S.C.S.R., Berling C.L., Germer S.P.M., Alvim I.D., Hubinger M.D. (2018). Encapsulating anthocyanins from *Hibiscus sabdariffa* L. calyces by ionic gelation: Pigment stability during storage of microparticles. Food Chemistry, 241, 317-327.

Demirbas A. (2016). Red cabbage extract as a natural antioxidant with application to packaged fresh tilapia and enhancement of silver and iron nanoparticles. Doctoral dissertation, University of Florida.

Deng L., Kang X., Liu Y., Feng F., Zhang H. (2017). Effects of surfactants on the formation of gelatin nanofibres for controlled release of curcumin. Food Chemistry, 231, 70-77.

Deng L., Zhang X., Li Y., Que F., Kang X., Liu Y., Feng F., Zhang H. (2018). Characterization of gelatin/zein nanofibers by hybrid electrospinning. Food Hydrocolloids, 75, 72-80.

Deng Y., & Kuiper J. (2017). Functional 3D tissue engineering scaffolds: Materials, technologies, and applications. Woodhead Publishing, UK.

Denghani S., Hosseini S.V., Regenstein J.M. (2018). Edible films and coatings in seafood preservation: A review. Food Chemistry, 240, 505-513.

Djabourov M., Leblond J., Papon P. (1988). Gelation of aqueous gelatin solutions. I. Structural investigation. Journal de Physique, 49, 319-332.

Dolci L.S., Liguori A., Panzavolta S., Miserocchi A., Passerini N., Gherardi M., Colombo V., Bigi A., Albertini B. (2018). Non-equilibrium atmospheric pressure plasma as innovative method to crosslink and enhance mucoadhesion of econazole-loaded gelatin films for buccal drug delivery. Colloids and Surfaces B: Biointerfaces, 163, 73-82.

Domon B., & Costello C.E. (1988). A systematic nomenclature for carbohydrate fragmentations in FAB-MS/MS spectra of glycoconjugates. Glycoconjugate Journal, 5(4), 397-409.

Drosou C., Krokida M., Biliaderis C.G. (2018). Composite pullulan-whey protein nanofibers made by electrospinning: Impact of process parameters on fiber morphology and physical properties. Food Hydrocolloids, 77, 726-735.

Duan B., Hockaday L.A., Kang K.H., Butcher J.T. (2013). 3D bioprinting of heterogeneous aortic valve conduits with alginate/gelatin hydrogels. Journal of Biomedical Materials Research, Part A, 101(5), 1255-1264.

Duconseille A., Wien F., Audonnet F., Traore A., Refregiers M., Astruc T., Santé-Lhoutellier V. (2017). The effect of origin of the gelatine and ageing on the secondary structure and water dissolution. Food Hydrocolloids, 66, 378-388.

Ebnesajjad S. (2012). Handbook of biopolymers and biodegradable plastics: Properties, processing and applications. William Andrew, USA.

Erencia M., Cano F., Tornero J.A., Fernandes M.M., Tzanov T., Macanás J., Carrillo F. (2015). Electrospinning of gelatin fibers using solutions with low acetic acid concentration: Effect of solvent composition on both diameter of electrospun fibers and cytotoxicity. Journal of Applied Polymer Science, 132(25), 42115-42125.

Esquerdo V.M., Monte M.L., Pinto L.A.A. (2019). Microstructures containing nanocapsules of unsaturated fatty acids with biopolymers: Characterization and thermodynamic properties. Journal of Food Engineering, 248, 28-35.

Etxabide A., Coma V., Guerrero P., Gardrat C., de la Caba K. (2017b). Effect of cross-linking in surface properties and antioxidant activity of gelatin films incorporated with a curcumin derivative. Food Hydrocolloids, 66, 168-175.

Etxabide A., Leceta I., Cabezudo S., Guerrero P., de la Caba K. (2016b). Sustainable fish gelatin films: From food processing waste to compost. ACS Sustainable Chemistry & Engineering, 4(9), 4626-4634.

Etxabide A., Ribeiro R.D.C., Guerrero P., Ferreira A.M., Stafford G.P., Dalgarno K., de la Caba K., Gentile P. (2018). Lactose-crosslinked fish gelatin-based porous scaffolds embedded with tetrahydrocurcumin for cartilage regeneration. International Journal of Biological Macromolecules, 117, 199-208.

Etxabide A., Uranga J., Guerrero P., de la Caba K. (2015). Improvement of barrier properties of fish gelatins promoted by gelatin glycation with lactose at high temperatures. LWT-Food Science and Technology, 63(1), 315-321.

Etxabide A., Uranga J., Guerrero P., de la Caba K. (2017a). Development of active gelatin films by means of valorisation of food processing waste: A review. Food Hydrocolloids, 68, 192-198.

Etxabide A., Urdanpilleta M., de la Caba K., Guerrero P. (2016a). Control of cross-linking reaction to tailor the properties of thin films based on gelatin. Materials Letters, 185, 366-369.

Etxabide A., Vairo C., Santos-Vizcaino E., Guerrero P., Pedraz J.L., Igartua M., de la Caba K., Hernandez R.M. (2017c). Ultra thin hydro-films based on lactose-crosslinked fish gelatin for wound healing applications. International Journal of Pharmaceutics, 530(1-2), 455-467.

European Commission. (2011). Commission Regulation (EU) No 10/2011 of 14 January 2011 on plastic materials and articles intended to come into contact with food. Official Journal of the European Union, 12, 1-89.

Fabra M.J., López-Rubio A., Lagaron J.M. (2016). Use of the electrohydrodynamic process to develop active/bioactive bilayer films for food packaging applications. Food Hydrocolloids, 55, 11-18.

Farjami T., Madadlou A., Labbafi M. (2015). Characteristics of the bulk hydrogels made of the citric acid cross-linked whey protein microgels. Food Hydrocolloids, 50, 159-165.

Feng X., Bansal N., Yang H. (2016). Fish gelatin combined with chitosan coating inhibits myofibril degradation of golden pomfret (*Trachinotus blochii*) fillet during cold storage. Food Chemistry, 200, 283-292.

Feng X., Ng V.K., Mikš-Krajnik M., Yang H. (2017). Effects of fish gelatin and tea polyphenol coating on the spoilage and degradation of myofibril in fish fillet during cold storage. Food and Bioprocess Technology, 10(1), 89-102.

Ferraro V., Gaillard-Martinie B., Sayd T., Chambon C., Anton M., Santé-Lhoutellier V. (2017). Collagen type I from bovine bone. Effect of animal age, bone anatomy and drying methodology on extraction yield, self-assembly, thermal behaviour and electrokinetic potential. International Journal of Biological Macromolecules, 97, 55-66.

Firouzabadi F.B., Noori M., Edalatpanah Y., Mirhosseini M. (2014). ZnO nanoparticle suspensions containing citric acid as antimicrobial to control *Listeria monocytogenes*, *Escherichia coli*, *Staphylococcus aureus* and *Bacillus cereus* in mango juice. Food Control, 42, 310-314.

Food and Agriculture Organization of the United Nations (FAO). (2018). The state of world fisheries and aquaculture 2018. Meeting the sustainable development goals. Rome.

Francisco C.R.L., Heleno S.A., Fernandes I.P.M., Barreira J.C.M., Calhelha R.C., Barros L., Gonçalves O.H., Ferreira I.C.F.R., Barreiro M.F. (2018). Functionalization of yogurts with *Agaricus bisporus* extracts encapsulated in spray-dried maltodextrin crosslinked with citric acid. Food Chemistry, 245, 845-853.

Ganesan P. (2017). Natural and bio polymer curative films for wound dressing medical applications. Wound Medicine, 18, 33-40.

Gaona-Forero A., Agudelo-Rodríguez G., Herrera A.O., Castellanos D.A. (2018). Modeling and simulation of an active packaging system with moisture adsorption for fresh produce. Application in 'Hass' avocado. Food Packaging and Shelf Life, 17, 187-195.

García-Moreno P.J., Stephansen K., van der Kruijs J., Guadix A., Guadix E.M., Chronakis I.S., Jacobsen C. (2016). Encapsulation of fish oil in nanofibers by emulsion electrospinning: Physical characterization and oxidative stability. Journal of Food Engineering, 183, 39-49.

Garrido T., Etxabide A., de la Caba K., Guerrero P. (2017). Versatile soy protein films and hydrogels by the incorporation of β-chitin from squid pens (*Loligo* sp.). Green Chemistry, 19(24), 5923-5931.

Garrido T., Etxabide A., Guerrero P., de la Caba K. (2016b). Characterization of agar/soy protein biocomposite films: Effect of agar on the extruded pellets and compression moulded films. Carbohydrate Polymers, 151, 408-416.

Garrido T., Leceta I., Cabezudo S., Guerrero P., de la Caba K. (2016a). Tailoring soy protein film properties by selecting casting or compression as processing methods. European Polymer Journal, 85, 499-507.

Gioffrè M., Torricelli P., Panzavolta S., Rubini K., Bigi A. (2012). Role of pH on stability and mechanical properties of gelatin films. Journal of Bioactive and Compatible Polymers, 27(1), 67-77.

Gómez-Estaca J., Gavara R., Hernández-Muñoz P. (2015). Encapsulation of curcumin in electrosprayed gelatin microspheres enhances its bioaccessibility and widens its uses in food applications. Innovative Food Science & Emerging Technologies, 29, 302-307.

Gómez-Estaca J., Gómez-Guillén M.C., Fernández-Martín F., Montero P. (2011). Effects of gelatin origin, bovine-hide and tuna skin, on the properties of compound gelatin-chitosan films. Food Hydrocolloids, 25(6), 1461-1469.

Gómez-Estaca J., López-de-Dicastillo C., Hernández-Muñoz P., Catalá R., Gavara R. (2014). Advances in antioxidant active food packaging. Trends in Food Science & Technology, 35(1), 42-51.

Gómez-Guillén M.C., Giménez B., Lopez-Caballero M.E., Montero M.P. (2011). Functional and bioactive properties of collagen and gelatin from alternative sources: A review. Food Hydrocolloids, 25(8), 1813-1827.

Gómez-Guillén M.C., Pérez-Mateos M., Gómez-Estaca J., López-Caballero E., Giménez B., Montero P. (2009). Fish gelatin: A renewable material for developing active biodegradable films. Trends in Food Science & Technology, 20(1), 3-16.

Gómez-Siurana A., Marcilla A., Beltrán M., Berenguer D., Martínez-Castellanos I., Menargues S. (2013). TGA/FTIR study of tobacco and glycerol-tobacco mixtures. Thermochimica Acta, 573, 146-157.

Gordon P.W., Brooker A.D.M., Chew Y.M.J., Wilson D.I., York D.W. (2010). Studies into the swelling of gelatine films using a scanning fluid dynamic gauge. Food and Bioproducts Processing, 88(4), 357-364.

Grover C.N., Cameron R.E., Best S.M. (2012). Investigating the morphological, mechanical and degradation properties of scaffolds comprising collagen, gelatin and elastin for use in soft tissue engineering. Journal of the Mechanical Behavior of Biomedical Materials, 10, 62-74.

Grumezescu A.M., & Holban A.M. (2017). Food packaging and preservation. Academic Press, UK.

Gualandi C., Torricelli P., Panzavolta S., Pagani S., Focarete M.L., Bigi A. (2016). An innovative co-axial system to electrospin *in situ* crosslinked gelatin nanofibers. Biomedical Materials, 11(2), 025007-025018.

Gudipati V. (2013). Fish gelatin: A versatile ingredient for the food and pharmaceutical industries. In: Kim S.K. (ed.). Marine proteins and peptides: Biological activities and applications. John Wiley & Sons, UK, pp. 271-295.

Guerrero P., & de la Caba K. (2010). Thermal and mechanical properties of soy protein films processed at different pH by compression. Journal of Food Engineering, 100(2), 261-269.

Guerrero P., Arana P., O'Grady M.N., Kerry J.P., de la Caba K. (2015). Valorization of industrial by-products: Development of active coatings to reduce food losses. Journal of Cleaner Production, 100, 179-184.

Guerrero P., Beatty E., Kerry J.P., de la Caba K. (2012). Extrusion of soy protein with gelatin and sugars at low moisture content. Journal of Food Engineering, 110(1), 53-59.

Guerrero P., Kerry J.P., de la Caba K. (2014). FTIR characterization of protein-polysaccharide interactions in extruded blends. Carbohydrate Polymers, 111, 598-605.

Guerrero P., Stefani P.M., Ruseckaite R.A., de la Caba K. (2011). Functional properties of films based on soy protein isolate and gelatin processed by compression molding. Journal of Food Engineering, 105(1), 65-72.

Gutiérrez T.J., Toro-Márquez L.A., Merino D., Mendieta J.R. (2019). Hydrogen-bonding interactions and compostability of bionanocomposite films prepared from corn starch and nano-fillers with and without added Jamaica flower extract. Food Hydrocolloids, 89, 283-293.

Hamed I., Özogul F., Regenstein J.M. (2016). Industrial applications of crustacean by-products (chitin, chitosan, and chitooligosaccharides): A review. Trends in Food Science & Technology, 48, 40-50.

Hammann F., & Schmid M. (2014). Determination and quantification of molecular interactions in protein films: A review. Materials, 7(12), 7975-7996.

Han Y., Yu M., Wang L. (2018). Preparation and characterization of antioxidant soy protein isolate films incorporating licorice residue extract. Food Hydrocolloids, 75, 13-21.

Hashim P., Ridzwan M.S.M., Bakar J., Hashim D.M. (2015). Collagen in food and beverage industries. International Food Research Journal, 22(1), 1-8.

Hassan B., Chatha S.A.S., Hussain A.I., Zia K.M., Akhtar N. (2018). Recent advances on polysaccharides, lipids and protein based edible films and coatings: A review. International Journal of Biological Macromolecules, 109, 1095-1107.

Hattrem M.N., Molnes S., Haug I.J., Draget K.I. (2015). Interfacial and rheological properties of gelatin based solid emulsions prepared with acid or alkali pretreated gelatins. Food Hydrocolloids, 43, 700-707.

Hazarika D., & Karak N. (2015). Waterborne sustainable tough hyperbranched aliphatic polyester thermosets. ACS Sustainable Chemistry & Engineering, 3(10), 2458-2468.

Hervy M., Evangelisti S., Lettieri P., Lee K.Y. (2015). Life cycle assessment of nanocellulose-reinforced advanced fibre composites. Composites Science and Technology, 118, 154-162.

Higuchi T., Miki T., Shah A.C., Herd A.K (1963). Facilitated reversible formation of amides from carboxylic acids in aqueous solutions. Intermediate production of acid anhydride. Journal of the American Chemical Society, 85(22), 3655-3660.

Horn J., Schanda J., Friess W. (2018). Impact of fast and conservative freeze-drying on product quality of protein-mannitol-sucrose-glycerol lyophilizates. European Journal of Pharmaceutics and Biopharmaceutics, 127, 342-354.

Hosseini S.F., Rezaei M., Zandi M., Farahmandghavi F. (2015). Bio-based composite edible films containing *Origanum vulgare* L. essential oil. Industrial Crops and Products, 67, 403-413.

Hosseini S.F., Rezaei M., Zandi M., Farahmandghavi F. (2016). Development of bioactive fish gelatin/chitosan nanoparticles composite films with antimicrobial properties. Food Chemistry, 194, 1266-1274.

Hosseini S.F., Rezaei M., Zandi M., Ghavi F.F. (2013). Preparation and functional properties of fish gelatin-chitosan blend edible films. Food Chemistry, 136(3-4), 1490-1495.

Hou Y., Shavandi A., Carne A., Bekhit A.A., Ng T.B., Cheung R.C.F., Bekhit A.E.A. (2016). Marine shells: Potential opportunities for extraction of functional and health-promoting materials. Critical Reviews in Environmental Science and Technology, 46(11-12), 1047-1116.

Huang T., Tu Z., Wang H., Shangguan X., Zhang L., Zhang N., Bansal N. (2017). Pectin and enzyme complex modified fish scales gelatin: Rheological behavior, gel properties and nanostructure. Carbohydrate Polymers, 156, 294-302.

Iahnke A.O.S., Costa T.M.H., Rios A.O., Flôres S.H. (2015). Residues of minimally processed carrot and gelatin capsules: Potential materials for packaging films. Industrial Crops and Products, 76, 1071-1078.

Isik B.S., Altay F., Capanoglu E. (2018). The uniaxial and coaxial encapsulations of sour cherry (*Prunus cerasus* L.) concentrate by electrospinning and their *in vitro* bioaccessibility. Food Chemistry, 265, 260-273.

ISO 14040 (2006). Environmental Management - Life Cycle Assessment - Principals and Framework.

Jadhav J.P., & Phugare S.S. (2012). Textile dyes: General information and environmental aspects. In: El Nemr A. (ed.). Non-conventional textile waste water treatment. Nova Science Publisher, Inc., New York, USA, pp. 1-29.

Jalaja K., Naskar D., Kundu S.C., James N.R. (2016). Potential of electrospun core-shell structured gelatin-chitosan nanofibers for biomedical applications. Carbohydrate Polymers, 136, 1098-1107.

Jalali A., Rux G., Linke M., Geyer M., Pant A., Saengerlaub S., Mahajan P. (2019). Application of humidity absorbing trays to fresh produce packaging: Mathematical modeling and experimental validation. Journal of Food Engineering, 244, 115-125.

Jiang Q, Reddy N., Yang Y. (2010). Cytocompatible cross-linking of electrospun zein fibers for the development of water-stable tissue engineering scaffolds. Acta Biomaterialia, 6(10), 4042-4051.

Jiang Q., Reddy N., Zhang S., Roscioli N., Yang Y. (2013). Water-stable electrospun collagen fibers from a non-toxic solvent and crosslinking system. Journal of Biomedical Materials Research, 101(5), 1237-1247.

Jiang Q., Xu H., Cai S., Yang Y. (2014). Ultrafine fibrous gelatin scaffolds with deep cell infiltration mimicking 3D ECMs for soft tissue repair. Journal of Materials Science: Materials in Medicine, 25(7), 1789-1800.

Jiang T., Carbone E.J., Lo K.W.H., Laurencin C.T. (2015). Electrospinning of polymer nanofibers for tissue regeneration. Progress in Polymer Science, 46, 1-24.

Jridi M., Mora L., Souissi N., Aristoy M.C., Nasri M., Toldrá F. (2018). Effects of active gelatin coated with henna (*L. inermis*) extract on beef meat quality during chilled storage. Food Control, 84, 238-245.

Kadam S.U., Pankaj S.K., Tiwari B.K., Cullen P.J., O'Donnell C.P. (2015). Development of biopolymer-based gelatin and casein films incorporating brown seaweed *Ascophyllum nodosum* extract. Food Packaging and Shelf Life, 6, 68-74.

Kaewprachu P., Osako K., Benjakul S., Suthiluk P., Rawdkuen S. (2017). Shelf life extension for Bluefin tuna slices (*Thunnus thynnus*) wrapped with myofibrillar protein film incorporated with catechin-Kradon extract. Food Control, 79, 333-343.

Kaewprachu P., Osako K., Rungraeng N., Rawdkuen S. (2018). Characterization of fish myofibrillar protein film incorporated with catechin-Kradon extract. International Journal of Biological Macromolecules, 107, 1463-1473.

Kafle G.K., Kim S.H., Sung, K.I. (2013). Ensiling of fish industry waste for biogas production: A lab scale evaluation of biochemical methane potential (BMP) and kinetics. Bioresource Technology, 127, 326-336.

Kakaei S., & Shahbazi Y. (2016). Effect of chitosan-gelatin film incorporated with ethanolic red grape seed extract and *Ziziphora clinopodioides* essential oil on survival of *Listeria monocytogenes* and chemical, microbial and sensory properties of minced trout fillet. LWT-Food Science and Technology, 72, 432-438.

Kamalipour J., Masoomi M., Khonakdar H.A., Razavi S.M.R. (2016). Preparation and release study of Triclosan in polyethylene/Triclosan anti-bacterial blend. Colloids and Surfaces B: Biointerfaces, 145, 891-898.

Karbowiak T., Debeaufort F., Voilley A. (2006). Importance of surface tension characterization for food, pharmaceutical and packaging products: A review. Critical Reviews in Food Science and Nutrition, 46(5), 391-407.

Kchaou H., Jridi M., Abdelhedi O., Nasreddine B., Karbowiak T., Nasri M., Debeaufort, F. (2017). Development and characterization of cuttlefish (*Sepia officinalis*) skin gelatin-protein isolate blend films. International Journal of Biological Macromolecules, 105, 1491-1500.

Khoo H.E., Azlan A., Tang S.T., Lim S.M. (2017). Anthocyanidins and anthocyanins: Colored pigments as food, pharmaceutical ingredients, and the potential health benefits. Food & Nutrition Research, 61(1), 1361779-1361799.

Khor E. (1997). Methods for the treatment of collagenous tissues for bioprostheses. Biomaterials, 18(2), 95-105.

Kim H., Beak S.E., Song K.B. (2018). Development of a hagfish skin gelatin film containing cinnamon bark essential oil. LWT-Food Science and Technology, 96, 583-588.

Kim S.A., & Rhee M.S. (2015). Synergistic antimicrobial activity of caprylic acid in combination with citric acid against both *Escherichia coli* O157:H7 and indigenous microflora in carrot juice. Food Microbiology, 49, 166-172.

Kim S.H., Joo M.H., Yoo S.H. (2009). Structural identification and antioxidant properties of major anthocyanin extracted from Omija (*Schizandra chinensis*) fruit. Journal of Food Science, 74(2), 134-140.

Kokoszka S., Debeaufort F., Lenart A., Voilley A. (2010). Water vapour permeability, thermal and wetting properties of whey protein isolate based edible films. International Dairy Journal, 20(1), 53-60.

Kowalczyk D. (2016). Biopolymer/candelilla wax emulsion films as carriers of ascorbic acid - A comparative study. Food Hydrocolloids, 52, 543-553.

Kowalczyk D., & Biendl M. (2016). Physicochemical and antioxidant properties of biopolymer/candelilla wax emulsion films containing hop extract - A comparative study. Food Hydrocolloids, 60, 384-392.

Lacroix M., & Vu K.D. (2014). Edible coating and film materials: Proteins. In: Han J.H. (ed.). Innovations in food packaging (2nd edition). Academic Press, UK, pp. 277-304.

Lagaron J.M., Fernandez-Saiz P., Ocio M.J. (2007). Using ATR-FTIR spectroscopy to design active antimicrobial food packaging structures based on high molecular weight chitosan polysaccharide. Journal of Agricultural and Food Chemistry, 55(7), 2554-2562.

Lau H.H., Murney R., Yakovlev N.L., Novoselova M.V., Lim S.H., Roy N., Singh H., Sukhorukov G.B., Haigh B., Kiryukhin M.V. (2017). Protein-tannic acid multilayer films:

A multifunctional material for microencapsulation of food-derived bioactives. Journal of Colloid and Interface Science, 505, 332-340.

Leceta I., Guerrero P., Ibarburu I., Dueñas M.T., de la Caba K. (2013). Characterization and antimicrobial analysis of chitosan-based films. Journal of Food Engineering, 116(4), 889-899.

Lee J., Durst R.W., Wrolstad R.E. (2005). Determination of total monomeric anthocyanin pigment content of fruit juices, beverages, natural colorants, and wines by the pH differential method: Collaborative study. Journal of AOAC International, 88(5), 1269-1278.

Lee K.Y., Lee J.H., Yang H.J., Song K.B. (2016). Production and characterisation of skate skin gelatin films incorporated with thyme essential oil and their application in chicken tenderloin packaging. International Journal of Food Science and Technology, 51(6), 1465-1472.

Li M., Mondrinos M.J., Gandhi M.R., Ko F.K., Weiss A.S., Lelkes P.I. (2005). Electrospun protein fibers as matrices for tissue engineering. Biomaterials, 26(30), 5999-6008.

Li M., Ngadi M.O., Ma Y. (2014). Optimisation of pulsed ultrasonic and microwave-assisted extraction for curcuminoids by response surface methodology and kinetic study. Food Chemistry, 165, 29-34.

Liang C., Jia M., Tian D., Tang Y., Ju W., Ding S., Tian L., Ren X., Wang X. (2017). Edible sturgeon skin gelatine films: Tensile strength and UV light-barrier as enhanced by blending with esculine. Journal of Functional Foods, 37, 219-228.

Liguori A., Bigi A., Colombo V., Focarete M.L., Gherardi M., Gualandi C., Oleari M.C., Panzavolta S. (2016). Atmospheric pressure non-equilibrium plasma as a green tool to crosslink gelatin nanofibers. Scientific Reports, 6, 38542.

Lille M., Nurmela A., Nordlund E., Metsä-Kortelainen S., Sozer N. (2018). Applicability of protein and fiber-rich food materials in extrusion-based 3D printing. Journal of Food Engineering, 220, 20-27.

Lin J., & Zhou W. (2018). Role of quercetin in the physicochemical properties, antioxidant and antiglycation activities of bread. Journal of Functional Foods, 40, 299-306.

Lin L., Regenstein J.M., Lv S., Lu J., Jiang S. (2017). An overview of gelatin derived from aquatic animals: Properties and modification. Trends in Food Science & Technology, 68, 102-112.

Lin Y.M., Nierop K.G.J., Girbal-Neuhauser E., Adriaanse M., van Loosdrecht M.C.M. (2015). Sustainable polysaccharide-based biomaterial recovered from waste aerobic granular sludge as a surface coating material. Sustainable Materials and Technologies, 4, 24-29.

Liu W., Zhang Z., Lin G., Luo D., Chen H., Yang H., Liang J., Liu Y., Xie J., Su Z., Cao H. (2017). Tetrahydrocurcumin is more effective than curcumin in inducing the apoptosis of H22 cells *via* regulation of a mitochondrial apoptosis pathway in ascites tumor-bearing mice. Food & Function, 8(9), 3120-3129.

Lopes C., Antelo L.T., Franco-Uría A., Alonso A.A., Pérez-Martín R. (2018). Chitin production from crustacean biomass: Sustainability assessment of chemical and enzymatic processes. Journal of Cleaner Production, 172, 4140-4151.

López D., Márquez A., Gutiérrez-Cutiño M., Venegas-Yazigi D., Bustos R., Matiacevich S. (2017). Edible film with antioxidant capacity based on salmon gelatin and boldine. LWT-Food Science and Technology, 77, 160-169.

Luo X., Guo Z., He P., Chen T., Li L., Ding S., Li H. (2018a). Study on structure, mechanical property and cell cytocompatibility of electrospun collagen nanofibers

crosslinked by common agents. International Journal of Biological Macromolecules, 113, 476-486.

Luo Y., Li Y., Qin X., Wa Q. (2018b). 3D printing of concentrated alginate/gelatin scaffolds with homogeneous nano apatite coating for bone tissue engineering. Materials & Design, 146, 12-19.

Madera-Santana T.J., Freile-Pelegrín Y., Azamar-Barrios J.A. (2014). Physicochemical and morphological properties of plasticized poly (vinyl alcohol)-agar biodegradable films. International Journal of Biological Macromolecules, 69, 176-184.

Mahmood K., Kamilah H., Sudesh K., Karim A.A., Ariffin F. (2019). Study of electrospun fish gelatin nanofilms from benign organic acids as solvents. Food Packaging and Shelf Life, 19 66-75.

Mahmoud B.S.M. (2014). The efficacy of grape seed extract, citric acid and lactic acid on the inactivation of *Vibrio parahaemolyticus* in shucked oysters. Food Control, 41, 13-16.

Mandrycky C., Wang Z., Kim K., Kim D.H. (2016). 3D bioprinting for engineering complex tissues. Biotechnology Advances, 34(4), 422-434.

Mano J.F., & Reis R.L. (2007). Osteochondral defects: present situation and tissue engineering approaches. Journal of Tissue Engineering and Regenerative Medicine, 1(4), 261-273.

Martins J.T., Cerqueira M.A., Vicente A.A. (2012). Influence of α-tocopherol on physicochemical properties of chitosan-based films. Food Hydrocolloids, 27(1), 220-227.

Martucci J.F., Gende L.B., Neira L.M., Ruseckaite R.A. (2015). Oregano and lavender essential oils as antioxidant and antimicrobial additives of biogenic gelatin films. Industrial Crops and Products, 71, 205-213.

Matiacevich S., Cofré D.C., Schebor C., Enrione J. (2013). Physicochemical and antimicrobial properties of bovine and salmon gelatin-chitosan films. CyTA-Journal of Food, 11(4), 366-378.

Mazza G., & Miniati E. (2018). Anthocyanins in fruits, vegetables, and grains. CRC press, USA.

Mendes A.C., Stephansen K., Chronakis I.S. (2017). Electrospinning of food proteins and polysaccharides. Food Hydrocolloids, 68, 53-68.

Mirabella N., Castellani V., Sala S. (2014). Current options for the valorization of food manufacturing waste: A review. Journal of Cleaner Production, 65, 28-41.

Mizgier P., Kucharska A.Z., Sokół-Łętowska A., Kolniak-Ostek J., Kidoń M., Fecka I. (2016). Characterization of phenolic compounds and antioxidant and anti-inflammatory properties of red cabbage and purple carrot extracts. Journal of Functional Foods, 21, 133-146.

Moaddab M., Nourmohammadi J., Rezayan A.H. (2018). Bioactive composite scaffolds of carboxymethyl chitosan-silk fibroin containing chitosan nanoparticles for sustained release of ascorbic acid. European Polymer Journal, 103, 40-50.

Mohajer S., Rezaei M., Hosseini S.F. (2017). Physico-chemical and microstructural properties of fish gelatin/agar bio-based blend films. Carbohydrate Polymers, 157, 784-793.

Moheman A., Alam M.S., Mohammad A. (2016). Recent trends in electrospinning of polymer nanofibers and their applications in ultra thin layer chromatography. Advances in Colloid and Interface Science, 229, 1-24.

Moomand K., & Lim L.T. (2015). Properties of encapsulated fish oil in electrospun zein fibres under simulated in vitro conditions. Food and Bioprocess Technology, 8(2), 431-444.

Moreira J.B., Lim L.T., Zavareze E.R., Dias A.R.G., Costa J.A.V., de Morais M.G. (2018). Microalgae protein heating in acid/basic solution for nanofibers production by free surface electrospinning. Journal of Food Engineering, 230, 49-54.

Moreno O., Atarés L., Chiralt A., Cruz-Romero M.C., Kerry J. (2018). Starch-gelatin antimicrobial packaging materials to extend the shelf life of chicken breast fillets. LWT-Food Science and Technology, 97, 483-490.

Muxika A., Etxabide A., Uranga J., Guerrero P., de la Caba K. (2017). Chitosan as a bioactive polymer: Processing, properties and applications. International Journal of Biological Macromolecules, 105, 1358-1368.

Muyonga J.H., Cole C.G.B., Duodu K.G. (2004). Fourier transform infrared (FTIR) spectroscopic study of acid soluble collagen and gelatin from skins and bones of young and adult Nile perch (*Lates niloticus*). Food Chemistry, 86(3), 325-332.

Na K., Shin S., Lee H., Shin D., Baek J., Kwak H., Park M., Shin J., Hyun J. (2018). Effect of solution viscosity on retardation of cell sedimentation in DLP 3D printing of gelatin methacrylate/silk fibroin bioink. Journal of Industrial and Engineering Chemistry, 61, 340-347.

Nagarajan M., Benjakul S., Prodpran T., Songtipya P. (2015). Properties and characteristics of nanocomposite films from tilapia skin gelatin incorporated with ethanolic extract from coconut husk. Journal of Food Science and Technology, 52(12), 7669-7682.

Nilsuwan K., Benjakul S., Prodpran T. (2018). Properties and antioxidative activity of fish gelatin-based film incorporated with epigallocatechin gallate. Food Hydrocolloids, 80, 212-221.

Offeddu G.S., Ashworth J.C., Cameron R.E., Oyen M.L. (2016). Structural determinants of hydration, mechanics and fluid flow in freeze-dried collagen scaffolds. Acta Biomaterialia, 41, 193-203.

Olaimat A.N., Al-Nabulsi A.A., Osaili T.M., Al-Holy M., Ayyash M.M., Mehyar G.F., Jaradat Z.W., Ghoush M.A. (2017). Survival and inhibition of *Staphylococcus aureus* in commercial and hydrated tahini using acetic and citric acids. Food Control, 77, 179-186.

Ortiz C.M., de Moraes J.O., Vicente A.R., Laurindo J.B., Mauri A.N. (2017). Scale-up of the production of soy (*Glycine max* L.) protein films using tape casting: Formulation of film-forming suspension and drying conditions. Food Hydrocolloids, 66, 110-117.

Ortíz M.A., Vargas M.C.R., Madinaveitia R.G.C., Velázquez J.A.M. (2011). Functional properties of anthocyanins. BIOtecnia, 13(2), 16-22.

Oymaci P., & Altinkaya S.A. (2016). Improvement of barrier and mechanical properties of whey protein isolate based food packaging films by incorporation of zein nanoparticles as a novel bionanocomposite. Food Hydrocolloids, 54, 1-9.

Pallottino F., Hakola L., Costa C., Antonucci F., Figorilli S., Seisto A., Menesatti P. (2016). Printing on food or food printing: A review. Food and Bioprocess Technology, 9(5), 725-733.

Panzavolta S., Gioffrè M., Focarete M.L., Gualandi C., Foroni L., Bigi A. (2011). Electrospun gelatin nanofibers: Optimization of genipin cross-linking to preserve fiber morphology after exposure to water. Acta Biomaterialia, 7(4), 1702-1709.

Patel S., Srivastava S., Singh M.R., Singh D. (2018). Preparation and optimization of chitosan-gelatin films for sustained delivery of lupeol for wound healing. International Journal of Biological Macromolecules, 107, 1888-1897.

Pereira V.A., de Arruda I.N.Q., Stefani R. (2015). Active chitosan/PVA films with anthocyanins from *Brassica oleraceae* (red cabbage) as time-temperature indicators for application in intelligent food packaging. Food Hydrocolloids, 43, 180-188.

Perumal R.K., Perumal S., Thangam R., Gopinath A., Ramadass S.K., Madhan B., Sivasubramanian S. (2018). Collagen-fucoidan blend film with the potential to induce fibroblast proliferation for regenerative applications. International Journal of Biological Macromolecules, 106, 1032-1040.

Pezeshki-Modaress M., Rajabi-Zeleti S., Zandi M., Mirzadeh H., Sodeifi N., Nekookar A., Aghdami N. (2014). Cell-loaded gelatin/chitosan scaffolds fabricated by salt-leaching/lyophilization for skin tissue engineering: In vitro and in vivo study. Journal of Biomedical Materials Research, Part A, 102(11), 3908-3917.

Posati T., Giuri D., Nocchetti M., Sagnella A., Gariboldi M., Ferroni C., Sotgiu G., Varchi G., Zamboni R., Aluigi A. (2018). Keratin-hydrotalcites hybrid films for drug delivery applications. European Polymer Journal, 105, 177-185.

Pourchet L.J., Thepot A., Albouy M., Courtial E.J., Boher A., Blum L.J., Marquette C.A. (2017). Human skin 3D bioprinting using scaffold-free approach. Advanced Healthcare Materials, 6(4), 1601101-1601108.

Qiu G., Wang D., Song X., Deng Y., Zhao Y. (2018). Degradation kinetics and antioxidant capacity of anthocyanins in air-impingement jet dried purple potato slices. Food Research International, 105, 121-128.

Qiu L., Zhang M., Tang J., Adhikari B., Cao P. (2019). Innovative technologies for producing and preserving intermediate moisture foods: A review. Food Research International, 116, 90-102.

Raja I.S., & Fathima N.N. (2015). A gelatin based antioxidant enriched biomaterial by grafting and saturation: Towards sustained drug delivery from antioxidant matrix. Colloids and Surfaces B: Biointerfaces, 128, 537-543.

Ramirez D.O.S., Carletto R.A., Tonetti C., Giachet F.T., Varesano A., Vineis C. (2017). Wool keratin film plasticized by citric acid for food packaging. Food Packaging and Shelf Life, 12, 100-106.

Ratanavaraporn J., Rangkupan R., Jeeratawatchai K., Kanokpanont S., Damrongsakkul S. (2010). Influences of physical and chemical crosslinking techniques on electrospun type A and B gelatin fiber mats. International Journal of Biological Macromolecules, 47(4), 431-438.

Reddy N., Reddy R., Jiang Q. (2015). Crosslinking biopolymers for biomedical applications. Trends in Biotechnology, 33(6), 362-369.

Reddy N., Warner K., Yang Y. (2011). Low-temperature wet-cross-linking of silk with citric acid. Industrial & Engineering Chemistry Research, 50(8), 4458-4463.

Ribeiro V.P., Morais A.S., Maia F.R., Canadas R.F., Costa J.B., Oliveira A.L., Oliveira J.M., Reis R.L. (2018). Combinatory approach for developing silk fibroin scaffolds for cartilage regeneration. Acta Biomaterialia, 72, 167-181.

Rocha M.A.M., Coimbra M.A., Nunes C. (2017). Applications of chitosan and their derivatives in beverages: A critical review. Current Opinion in Food Science, 15, 61-69.

Rocha-García D., Guerra-Contreras A., Reyes-Hernández J., Palestino G. (2017). Thermal and kinetic evaluation of biodegradable thermo-sensitive gelatin/poly(ethylene glycol) diamine crosslinked citric acid hydrogels for controlled release of tramadol. European Polymer Journal, 89, 42-56.

Rodriguez M.J., Brown J., Giordano J., Lin S.J., Omenetto F.G., Kaplan D.L. (2017). Silk based bioinks for soft tissue reconstruction using 3-dimensional (3D) printing with *in vitro* and *in vivo* assessments. Biomaterials,117, 105-115.

Roy B.C., Das C., Hong H., Betti M., Bruce H.L. (2017). Extraction and characterization of gelatin from bovine heart. Food Bioscience, 20, 116-124.

Roy S., Gennadios A., Weller C.L., Testin R.F. (2000). Water vapor transport parameters of a cast wheat gluten film. Industrial Crops and Products, 11(1), 43-50.

Rui L., Xie M., Hu B., Zhou L. Yin D., Zeng X. (2017). A comparative study on chitosan/gelatin composite films with conjugated or incorporated gallic acid. Carbohydrate Polymers, 173, 473-481.

Ruiz-Ruiz F., Mancera-Andrade E.I., Iqbal H.M.N. (2017). Marine-derived bioactive peptides for biomedical sectors: A review. Protein & Peptide Letters, 24(2), 109-117.

Rux G., Mahajan P.V., Geyer M., Linke M., Pant A., Saengerlaub S., Caleb, O.J. (2015). Application of humidity-regulating tray for packaging of mushrooms. Postharvest Biology and Technology, 108, 102-110.

Shafagh N., Sabzi M., Afshari M.J. (2018). Development of pH-sensitive and antibacterial gelatin/citric acid/Ag nanocomposite hydrogels with potential for biomedical applications. Journal of Polymer Research, 25, 259-266.

Saito H., Taguchi T., Kobayashi H., Kataoka K., Tanaka J., Murabayashi S., Mitamura Y. (2004). Physicochemical properties of gelatin gels prepared using citric acid derivative. Materials Science and Engineering: C, 24(6-8), 781-785.

Saliba S., Ruch P., Volksen W., Magbitang T.P., Dubois G., Michel B. (2016). Combined influence of pore size distribution and surface hydrophilicity on the water adsorption characteristics of micro-and mesoporous silica. Microporous and Mesoporous Materials, 226, 221-228.

Sambrook J., Fritsch E.F., Maniatis T. (1989). Molecular cloning: a laboratory manual. (2nd ed.). Cold Spring Harbor Laboratory Press, USA.

Santoro M., Tatara A.M., Mikos A.G. (2014). Gelatin carriers for drug and cell delivery in tissue engineering. Journal of Controlled Release, 190, 210-218.

Santos J.P.F., Arjmand M., Melo G.H.F., Chizari K., Bretas R.E.S., Sundararaj U. (2018). Electrical conductivity of electrospun nanofiber mats of polyamide 6/polyaniline coated with nitrogen-doped carbon nanotubes. Materials & Design, 141, 333-341.

Sayari N., Sila A., Abdelmalek B.E., Abdallah R.B., Ellouz-Chaabouni S., Bougatef A., Balti R. (2016). Chitin and chitosan from the Norway lobster by-products: Antimicrobial and anti-proliferative activities. International Journal of Biological Macromolecules, 87, 163-171.

Sha X.M., Tu Z.C., Liu W., Wang H., Shi Y., Huang T., Man Z.Z. (2014). Effect of ammonium sulfate fractional precipitation on gel strength and characteristics of gelatin from bighead carp (*Hypophthalmichthys nobilis*) scale. Food Hydrocolloids, 36, 173-180.

Shahbazarab Z., Teimouri A., Chermahini A.N., Azadi M. (2017). Fabrication and characterization of nanobiocomposite scaffold of zein/chitosan/nanohydroxyapatite prepared by freeze-drying method for bone tissue engineering. International Journal of Biological Macromolecules, 108, 1017-1027.

Shankar S., Jaiswal L., Rhim J.W. (2016). Gelatin-based nanocomposite films: Potential use in antimicrobial active packaging. In: Barros-Velázquez J. (ed.). Antimicrobial food packaging. Academic press, UK, pp. 339-348.

Shi R., Bi J., Zhang Z., Zhu A., Chen D., Zhou X., Zhang L., Tian W. (2008). The effect of citric acid on the structural properties and cytotoxicity of the polyvinyl alcohol/starch films when molding at high temperature. Carbohydrate Polymers, 74(4), 763-770.

Singh H., Ye A., Horne D. (2009). Structuring food emulsions in the gastrointestinal tract to modify lipid digestion. Progress in Lipid Research, 48(2), 92-100.

Sinthusamran S., Benjakul S., Kishimura H. (2014). Characteristics and gel properties of gelatin from skin of seabass (*Lates calcarifer*) as influenced by extraction conditions. Food Chemistry, 152, 276-284.

Siqueira N.M., Paiva B., Camassola M., Rosenthal-Kim E.Q., Garcia K.C., dos Santos F.P., Soares R.M.D. (2015). Gelatin and galactomannan-based scaffolds: Characterization and potential for tissue engineering applications. Carbohydrate Polymers, 133, 8-18.

Soares N.M., Fernandes T.A., Vicente A.A. (2016). Effect of variables on the thickness of an edible coating applied on frozen fish - Establishment of the concept of safe dipping time. Journal of Food Engineering, 171, 111-118.

Songtipya L., Thies M.C., Sane A. (2016). Effect of rapid expansion of subcritical solutions processing conditions on loading capacity of tetrahydrocurcumin encapsulated in poly(L-lactide) particles. The Journal of Supercritical Fluids, 113, 119-127.

Sow L.C., & Yang H. (2015). Effects of salt and sugar addition on the physicochemical properties and nanostructure of fish gelatin. Food Hydrocolloids, 45, 72-82.

Stoll L., da Silva A.M., Iahnke A.O.S., Costa T.M.H., Flôres S.H., Rios A.O. (2017). Active biodegradable film with encapsulated anthocyanins: Effect on the quality attributes of extra-virgin olive oil during storage. Journal of Food Processing and Preservation, 41(6), 13218-13225.

Su J.F., Huang Z., Zhao Y.H, Yuan X.Y., Wang X.Y, Li M. (2010). Moisture sorption and water vapor permeability of soy protein isolate/poly(vinyl alcohol)/glycerol blend films. Industrial Crops and Products, 31(2), 266-276.

Su K., & Wang C. (2015). Recent advances in the use of gelatin in biomedical research. Biotechnology Letters, 37(11), 2139-4215.

Sun J., Zhou W., Huang D., Fuh J.Y.H., Hong G.S. (2015). An overview of 3D printing technologies for food fabrication. Food and Bioprocess Technology, 8(8), 1605-1615.

Sun X., Guo X., Ji M., Wu J., Zhu W., Wang J., Cheng C., Chen L., Zhang Q. (2019). Preservative effects of fish gelatin coating enriched with CUR/βCD emulsion on grass carp (*Ctenopharyngodon idellus*) fillets during storage at 4 ºC. Food Chemistry, 272, 643-652.

Taghizadeh M., Mohammadifar M.A., Sadeghi E., Rouhi M., Mohammadi R., Askari F., Mortazavian A.M., Kariminejad M. (2018). Photosensitizer-induced cross-linking: A novel approach for improvement of physicochemical and structural properties of gelatin edible films. Food Research International, 112, 90-97.

Tatara R.A. (2017). Compression molding. In: Kutz M. (ed.). Applied plastics engineering handbook: Processing, materials, and applications (2nd edition). William Andrew, USA, pp. 291-320.

Teimouri A., Azadi M., Emadi R., Lari J., Chermahini A.N. (2015). Preparation, characterization, degradation and biocompatibility of different silk fibroin based composite scaffolds prepared by freeze-drying method for tissue engineering application. Polymer Degradation and Stability, 121, 18-29.

Tišler-Korljan B., & Gregor-Svetec D. (2014). Properties and printability of compression moulded recycled polyethylene. Materials & Design, 55, 583-590.

Tonda-Turo C., Gentile P., Saracino S., Chiono V., Nandagiri V.K., Muzio G., Canuto R.A., Ciardelli G. (2011). Comparative analysis of gelatin scaffolds crosslinked by genipin and silane coupling agent. International Journal of Biological Macromolecules, 49(4), 700-706.

Tsai M.L., Tsai S.P., Ho C.T. (2017). Tetrahydrocurcumin attenuates carbon tetrachloride-induced hepatic fibrogenesis by inhibiting the activation and autophagy of hepatic stellate cells. Journal of Functional Foods, 36, 418-428.

Uranga J., Etxabide A., Guerrero P., de la Caba K. (2018). Development of active fish gelatin films with anthocyanins by compression molding. Food Hydrocolloids, 84, 313-320.

Uranga J., Leceta I., Etxabide A., Guerrero P., de la Caba K. (2016). Cross-linking of fish gelatins to develop sustainable films with enhanced properties. European Polymer Journal, 78, 82-90.

Varley M.C., Neelakantan S., Clyne T.W., Dean J., Brooks R.A., Markaki A.E. (2016). Cell structure, stiffness and permeability of freeze-dried collagen scaffolds in dry and hydrated states. Acta Biomaterialia, 33, 166-175.

Venkatesan J., Anil S., Kim S.K., Shim M.S. (2017). Marine fish proteins and peptides for cosmeceuticals: A review. Marine Drugs, 15(5), 143-160.

Wang H., Gong X., Guo X., Liu C., Fan Y.Y., Zhang J., Niu B., Li W. (2019). Characterization, release, and antioxidant activity of curcumin-loaded sodium alginate/ZnO hydrogel beads. International Journal of Biological Macromolecules, 121, 1118-1125.

Wang H., Hao L., Niu B., Jiang S., Cheng J., Jiang S. (2016). Kinetics and antioxidant capacity of proanthocyanidins encapsulated in zein electrospun fibers by cyclic voltammetry. Journal of Agricultural and Food Chemistry, 64(15), 3083-3090.

Wang H., Hao L., Wang P., Chen M., Jiang S., Jiang S. (2017a). Release kinetics and antibacterial activity of curcumin loaded zein fibers. Food Hydrocolloids, 63, 437-446.

Wang H.J., An D.S., Rhim J.W., Lee D.S. (2017b). Shiitake mushroom packages tuned in active CO_2 and moisture absorption requirements. Food Packaging and Shelf Life, 11, 10-15.

Wang L., Zhang M., Bhandari B., Yang C. (2018). Investigation on fish surimi gel as promising food material for 3D printing. Journal of Food Engineering, 220, 101-108.

Wang S., Ren J., Li W., Sun R., Liu S. (2014). Properties of polyvinyl alcohol/xylan composite films with citric acid. Carbohydrate Polymers, 103, 94-99.

Wiczkowski W., Szawara-Nowak D., Topolska J. (2013). Red cabbage anthocyanins: Profile, isolation, identification, and antioxidant activity. Food Research International, 51(1), 303-309.

Włodarczyk-Biegun M.K., & del Campo A. (2017). 3D bioprinting of structural proteins. Biomaterials, 134, 180-201.

Wong Y.M., & Siow L.F. (2015). Effects of heat, pH, antioxidant, agitation and light on betacyanin stability using red-fleshed dragon fruit (*Hylocereus polyrhizus*) juice and concentrate as models. Journal of Food Science and Technology, 52(5), 3086-3092.

Wu J., Sun X., Guo X., Ji M., Wang J., Cheng C., Chen L., Wen C., Zhang Q. (2018). Physicochemical, antioxidant, in vitro release, and heat sealing properties of fish gelatin films incorporated with β-cyclodextrin/curcumin complexes for apple juice preservation. Food and Bioprocess Technology, 11(2), 447-461.

Wu X., & Prior R.L. (2005a). Systematic identification and characterization of anthocyanins by HPLC-ESI-MS/MS in common foods in the United States: Fruits and berries. Journal of Agricultural and Food Chemistry, 53, 2589-2599.

Wu X., & Prior R.L. (2005b). Identification and characterization of anthocyanins by high-performance liquid chromatography- electrospray ionization- tandem mass spectrometry

in common foods in the United States: Vegetables, nuts, and grains. Journal of Agricultural and Food Chemistry, 53(8), 3101-3113.

Xiao J., Shi C., Zheng H., Shi Z., Jiang D., Li Y., Huang Q. (2016). Kafirin protein based electrospun fibers with tunable mechanical property, wettability, and release profile. Journal of Agricultural and Food Chemistry, 64(16), 3226-3233.

Xu H., Shen L., Xu L., Yang Y. (2015). Low-temperature crosslinking of proteins using non-toxic citric acid in neutral aqueous medium: Mechanism and kinetic study. Industrial Crops and Products, 74, 234-240.

Yanwong S., & Threepopnatkul P. (2015). Effect of peppermint and citronella essential oils on properties of fish skin gelatin edible films. IOP Conference Series: Materials Science and Engineering, 87(1), 012064-012072.

Yao Z.C., Chang M.W., Ahmad Z., Li J.S. (2016). Encapsulation of rose hip seed oil into fibrous zein films for ambient and on demand food preservation via coaxial electrospinning. Journal of Food Engineering, 191, 115-123.

Yates M., Gomez M.R., Martin-Luengo M.A., Ibañez V.Z., Serrano A.M.M. (2017). Multivalorization of apple pomace towards materials and chemical. Waste to wealth. Journal of Cleaner Production, 143, 847-853.

Yildirim S., Röcker B., Pettersen M.K., Nilsen-Nygaard J., Ayhan Z., Rutkaite R., Radusin T., Suminska P., Marcos B., Coma V. (2018). Active packaging applications for food. Comprehensive Reviews in Food Science and Food Safety, 17(1), 165-199.

Yoon S.D., Chough S.H., Park H.R. (2006). Properties of starch-based blend films using citric acid as additive. Journal of Applied Polymer Science, 100(3), 2554-2560.

Yoon S.D., Chough S.H., Park H.R. (2007). Preparation of resistant starch/poly(vinyl alcohol) blend films with added plasticizer and crosslinking agents. Journal of Applied Polymer Science, 106(4), 2485-2493.

Yu Z., & Lau D. (2017). Flexibility of backbone fibrils in α-chitin crystals with different degree of acetylation. Carbohydrate Polymers, 174, 941-947.

Yu Z., Sun L., Wang W., Zeng W., Mustapha A., Lin M. (2018). Soy protein-based films incorporated with cellulose nanocrystals and pine needle extract for active packaging. Industrial Crops and Products, 112, 412-419.

Zhang C., Zhao F., Li R., Wu Y., Liu S., Liang Q. (2019). Purification, characterization, antioxidant and moisture-preserving activities of polysaccharides from *Rosa rugosa* petals. International Journal of Biological Macromolecules, 124, 938-945.

Zhang L.L., Li H.H., Shi Y.H., Fan C.Y., Wu X.L., Wang H.F., Sun H.Z., Zhang J.P. (2016). A novel layered sedimentary rocks structure of the oxygen-enriched carbon for ultrahigh-rate-performance supercapacitors. ACS Applied Materials & Interfaces, 8(6), 4233-4241.

Zhang Y.Z, Venugopal J., Huang Z.M., Lim C.T., Ramakrishna S. (2006). Crosslinking of the electrospun gelatin nanofibers. Polymer, 47(8), 2911-2917.

Zhou J., Tong J., Su X., Ren L. (2016). Hydrophobic starch nanocrystals preparations through crosslinking modification using citric acid. International Journal of Biological Macromolecules, 91, 1186-1193.

Zhuang C., Tao F., Cui Y. (2015). Anti-degradation gelatin films crosslinked by active ester based on cellulose. RSC Advances, 5(64), 52183-52193.

Supplementary data

Table S1 Characterization of anthocyanins from red cabbage extract determined by UHPLC-Q-TOF-MS/MS analysis.

Peak	t_r (min)	Exp. Acc. Mass $[M]^+$ Error (mDa)	Teor. Acc. Mass $[M]^+$	Formula	Fragment of $[M]^+$	Tentative identification
1	3.27	773.2144 0.9	773.2135	$C_{33}H_{41}O_{21}^+$	611.1660 $[Y^3_1]^+$ or $[Y^5_0]^+$ 449.1139 $[Y^3_1Y^5_0]^+$ or $[Y^3_0]^+$ 287.0564 $[Y^3_0Y^5_0]^+$	Cy-3-diGlc-5-Glc
2	3.77	1111.3091 -4.6	1111.3137	$C_{49}H_{59}O_{29}^+$	949.2684 $[Y^5_0]^+$ 449.1093 $[Y^3_0]^+$ 287.0562 $[Y^3_0Y^5_0]^+$	Cy-3-(Glcfer)-diGlc-5-Glc
3	3.91	1141.3226 -1.6	1141.3242	$C_{50}H_{61}O_{30}^+$	979.2687 $[Y^5_0]^+$ 449.1119 $[Y^3_0]^+$ 287.0546 $[Y^3_0Y^5_0]^+$	Cy-3-(Glcsin)-diGlc-5-Glc
4	4.03	935.2411 -4.1	935.2452	$C_{42}H_{47}O_{24}^+$	773.1953 $[Y^3_1]^+$ or $[Y^5_0]^+$ 449.1084 $[Y^3_0]^+$ 287.0571 $[Y^3_0Y^5_0]^+$	Cy-3-(Caff)-diGlc-5-Glc
5	4.28	1141.3235 -0.7	1141.3242	$C_{50}H_{61}O_{30}^+$	979.2664 $[Y^5_0]^+$ 449.1124 $[Y^3_0]^+$ 287.0561 $[Y^3_0Y^5_0]^+$	Cy-3-(Glcsin)-diGlc-5-Glc
6	4.36	979.2722 0.8	979.2714	$C_{44}H_{51}O_{25}^+$	817.2207 $[Y^3_1]^+$ or $[Y^5_0]^+$ 449.1093 $[Y^3_0]^+$ 287.0556 $[Y^3_0Y^5_0]^+$	Cy-3-(Sin)-diGlc-5-Glc
7	4.83	1111.3118 -1.9	1111.3137	$C_{49}H_{59}O_{29}^+$	949.2596 $[Y^5_0]^+$ 449.1093 $[Y^3_0]^+$ 287.0562 $[Y^3_0Y^5_0]^+$	Cy-3-(Glcfer)-diGlc-5-Glc
8	4.91	1141.3185 -5.7	1141.3242	$C_{50}H_{61}O_{30}^+$	979.2748 $[Y^5_0]^+$ 449.1042 $[Y^3_0]^+$ 287.0569 $[Y^3_0Y^5_0]^+$	Cy-3-(Glcsin)-diGlc-5-Glc
9	5.06	919.2469 -3.4	919.2503	$C_{42}H_{47}O_{23}^+$	757.1963 $[Y^3_1]^+$ or $[Y^5_0]^+$ 449.1077 $[Y^3_0]^+$ 287.0551 $[Y^3_0Y^5_0]^+$	Cy-3-(pC)-diGlc-5-Glc
10	5.50	949.2593 -1.5	949.2608	$C_{43}H_{49}O_{24}^+$	787.2090 $[Y^3_1]^+$ or $[Y^5_0]^+$ 449.1101 $[Y^3_0]^+$ 287.0569 $[Y^3_0Y^5_0]^+$	Cy-3-(Fer)-diGlc-5-Glc
11	5.54	979.2709 -0.5	979.2714	$C_{44}H_{51}O_{25}^+$	817.2166 $[Y^3_1]^+$ or $[Y^5_0]^+$ 449.1089 $[Y^3_0]^+$ 287.0568 $[Y^3_0Y^5_0]^+$	Cy-3-(Sin)-diGlc-5-Glc
12	6.13	1287.3589 -2.1	1287.3610	$C_{59}H_{67}O_{32}^+$	1125.3154 $[Y^3_2]^+$ or $[Y^5_0]^+$ 449.1075 $[Y^3_0]^+$ 287.0556 $[Y^3_0Y^5_0]^+$	Cy-3-(FerFer)-triGlc-5-Glc
13	6.56	1317.3705 -1.1	1317.3716	$C_{60}H_{69}O_{33}^+$	1155.3214 $[Y^3_2]^+$ or $[Y^5_0]^+$ 449.1079 $[Y^3_0]^+$ 287.0552 $[Y^3_0Y^5_0]^+$	Cy-3-(SinFer)-triGlc-5-Glc
14	6.86	1347.3826 0.5	1347.3821	$C_{61}H_{71}O_{34}^+$	1317.3705 $[Y^3_2]^+$ or $[Y^5_0]^+$ 449.1052 $[Y^3_0]^+$ 287.0561 $[Y^3_0Y^5_0]^+$	Cy-3-(SinSin)-triGlc-5-Glc
15	7.08	935.2413 -3.9	935.2452	$C_{42}H_{47}O_{24}^+$	773.1977 $[Y^3_1]^+$ or $[Y^5_0]^+$ 449.1087 $[Y^3_0]^+$ 287.0561 $[Y^3_0Y^5_0]^+$	Cy-3-(Caff)-diGlc-5-Glc
16	7.65	919.2508 0.5	919.2503	$C_{42}H_{47}O_{23}^+$	757.1967 $[Y^3_1]^+$ or $[Y^5_0]^+$ 449.1098 $[Y^3_0]^+$ 287.0565 $[Y^3_0Y^5_0]^+$	Cy-3-(pC)-diGlc-5-Glc

17	7.75	979.2704 -1	979.2714	$C_{44}H_{51}O_{25}^+$	817.2170 $[Y^3_1]^+$ or $[Y^5_0]^+$ 449.1088 $[Y^3_0]^+$ 287.0565 $[Y^3_0Y^5_0]^+$	Cy-3-(Sin)-diGlc-5-Glc
18	7.76	949.2604 -0.4	949.2608	$C_{43}H_{49}O_{24}^+$	787.2070 $[Y^3_1]^+$ or $[Y^5_0]^+$ 449.1084 $[Y^3_0]^+$ 287.0565 $[Y^3_0Y^5_0]^+$	Cy-3-(Fer)-diGlc-5-Glc
19	7.84	1125.3065 -1.7	1125.3082	$C_{53}H_{57}O_{27}^+$	963.2619 $[Y^5_0]^+$ 449.1095 $[Y^3_0]^+$ 287.0571 $[Y^3_0Y^5_0]^+$	Cy-3-(FerFer)-diGlc-5-Glc
20	8.13	1185.3282 -1.1	1185.3293	$C_{55}H_{61}O_{29}^+$	1023.2699 $[Y^5_0]^+$ 449.1090 $[Y^3_0]^+$ 287.0565 $[Y^3_0Y^5_0]^+$	Cy-3-(SinSin)-diGlc-5-Glc
21	8.22	1155.3162 -2.5	1155.3187	$C_{54}H_{59}O_{28}^+$	993.2650$[Y^5_0]^+$ 449.1105 $[Y^3_0]^+$ 287.0567 $[Y^3_0Y^5_0]^+$	Cy-3-(FerSin)-diGlc-5-Glc
22	8.52	1125.3066 -1.6	1125.3082	$C_{53}H_{57}O_{27}^+$	963.2545 $[Y^5_0]^+$ 449.1105 $[Y^3_0]^+$ 287.0567 $[Y^3_0Y^5_0]^+$	Cy-3-(FerFer)-diGlc-5-Glc
23	8.76	1155.3179 -0.8	1155.3187	$C_{54}H_{59}O_{28}^+$	993.2670 $[Y^5_0]^+$ 449.1086 $[Y^3_0]^+$ 287.0567 $[Y^3_0Y^5_0]^+$	Cy-3-(FerSin)-diGlc-5-Glc
24	8.86	1185.3279 -1.4	1185.3293	$C_{55}H_{61}O_{29}^+$	1023.2749 $[Y^5_0]^+$ 449.1093 $[Y^3_0]^+$ 287.0565 $[Y^3_0Y^5_0]^+$	Cy-3-(SinSin)-diGlc-5-Glc
25	8.99	1125.3037 -4.5	1125.3082	$C_{53}H_{57}O_{27}^+$	963.2572$[Y^5_0]^+$ 449.1090 $[Y^3_0]^+$ 287.0563 $[Y^3_0Y^5_0]^+$	Cy-3-(FerFer)-diGlc-5-Glc
26	9.30	1185.3282 -1.1	1185.3293	$C_{55}H_{61}O_{29}^+$	1023.2786 $[Y^5_0]^+$ 449.1053 $[Y^3_0]^+$ 287.0575 $[Y^3_0Y^5_0]^+$	Cy-3-(SinSin)-diGlc-5-Glc
27	9.50	1155.3173 -1.4	1155.3187	$C_{54}H_{59}O_{28}^+$	993.2668 $[Y^5_0]^+$ 449.1137 $[Y^3_0]^+$ 287.0568 $[Y^3_0Y^5_0]^+$	Cy-3-(FerSin)-diGlc-5-Glc
28	10.98	1125.3081 -0.1	1125.3082	$C_{53}H_{57}O_{27}^+$	963.2639 $[Y^5_0]^+$ 449.1097 $[Y^3_0]^+$ 287.0656$[Y^3_0Y^5_0]^+$	Cy-3-(FerFer)-diGlc-5-Glc
29	11.08	1185.3282 -1.1	1185.3293	$C_{55}H_{61}O_{29}^+$	1023.2736 $[Y^5_0]^+$ 449.1088 $[Y^3_0]^+$ 287.0569 $[Y^3_0Y^5_0]^+$	Cy-3-(SinSin)-diGlc-5-Glc
30	11.27	1155.3171 -1.6	1155.3187	$C_{54}H_{59}O_{28}^+$	993.2573 $[Y^5_0]^+$ 449.1090 $[Y^3_0]^+$ 287.0565 $[Y^3_0Y^5_0]^+$	Cy-3-(FerSin)-diGlc-5-Glc
31	12.55	1185.3282 -1.1	1185.3293	$C_{55}H_{61}O_{29}^+$	1023.2736 $[Y^5_0]^+$ 449.1088 $[Y^3_0]^+$ 287.0569 $[Y^3_0Y^5_0]^+$	Cy-3-(SinSin)-diGlc-5-Glc

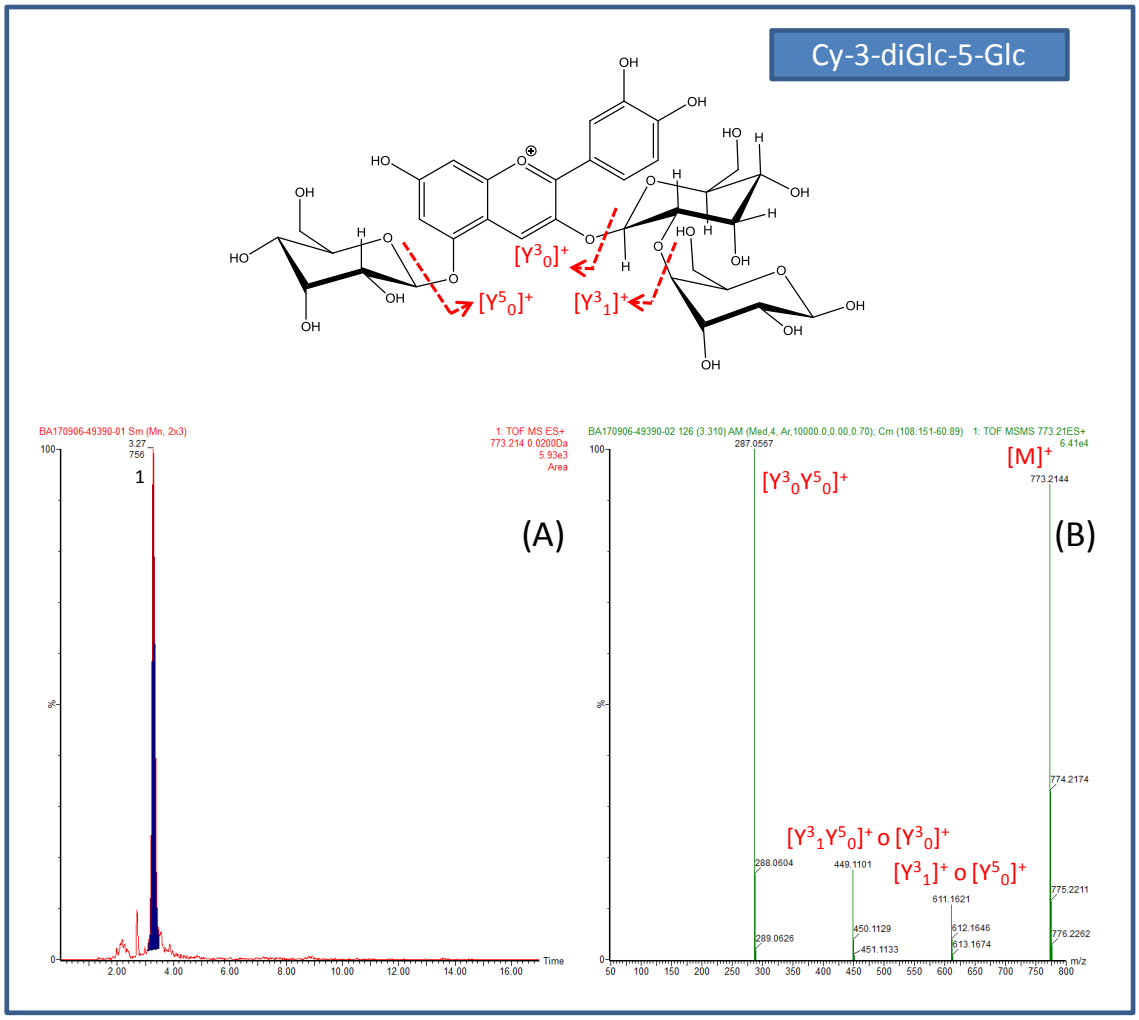

Figure S1 Chromatogram of extracted ion at 773.2135 m/z $[M]^+$ (A) and ESI-MS/MS spectra of Cy-3-diGlc-5-Glc at t_r 3.27 min (1) (B).

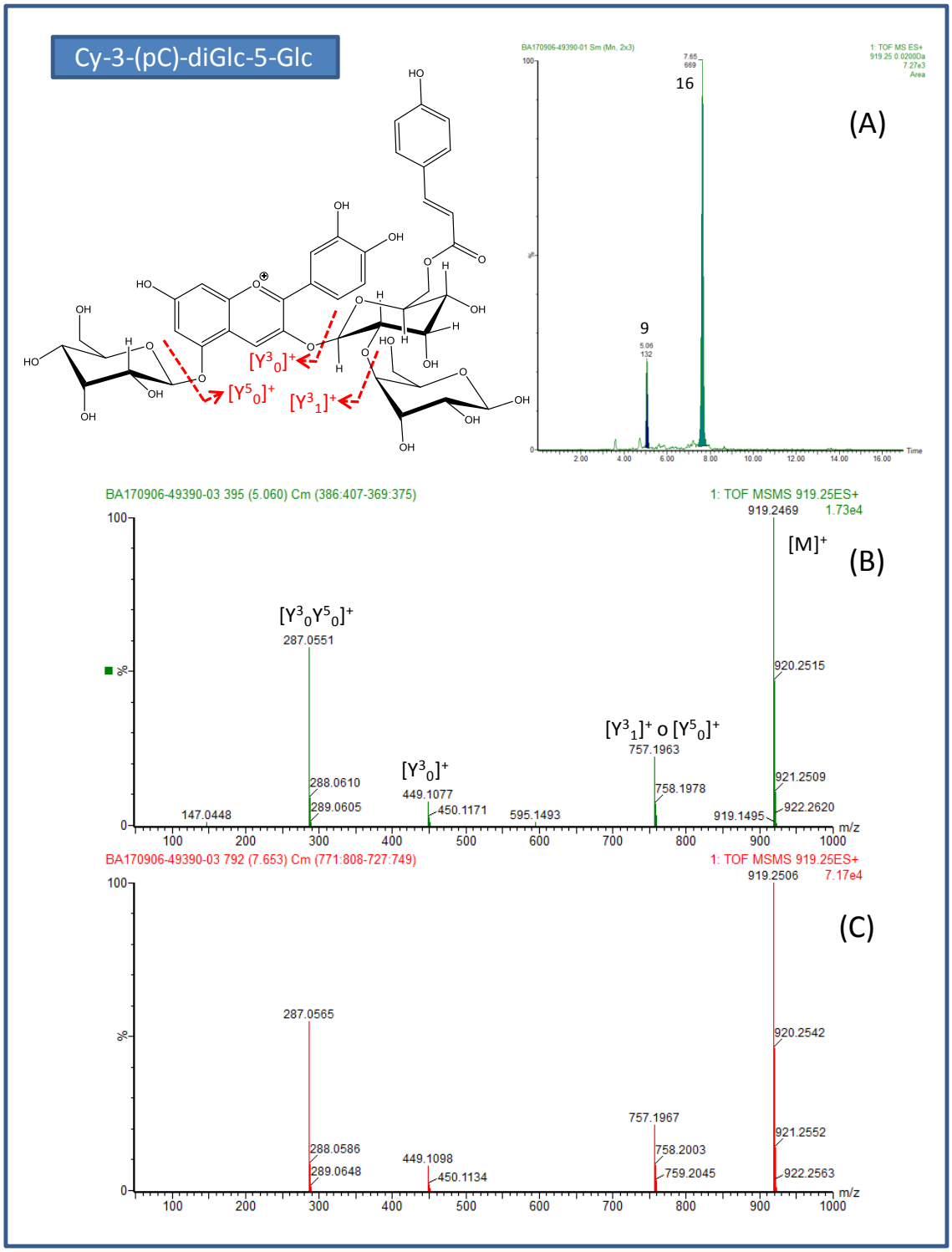

Figure S2 Chromatogram of extracted ion at 919.2503 m/z $[M]^+$ (A) and ESI-MS/MS spectra of Cy-3-(pC)-diGlc-5-Glc isomers at t_r 5.06 min (9) (B) and at t_r 7.65 min (16) (C).

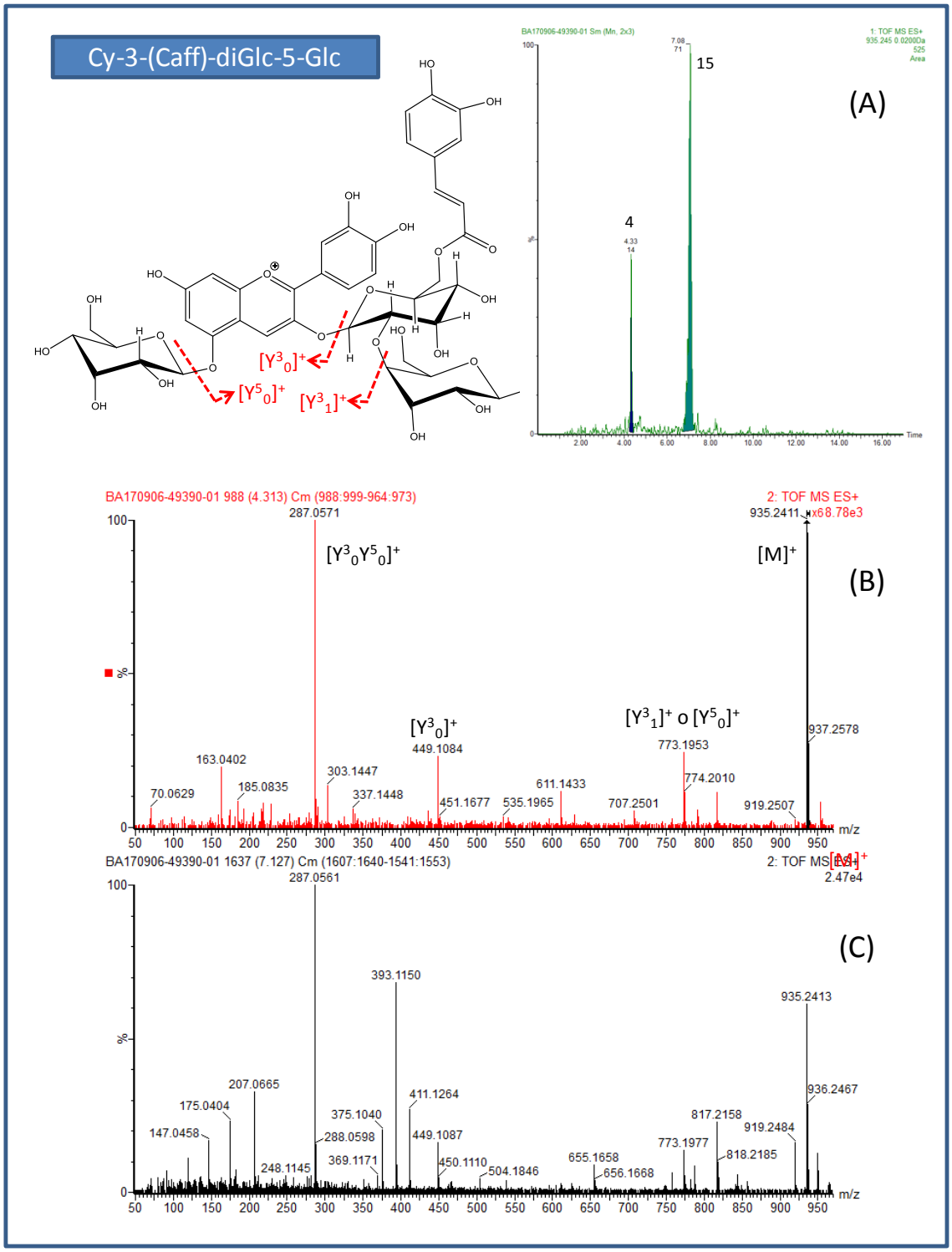

Figure S3 Chromatogram of extracted ion at 935.2452 m/z $[M]^+$ (A) and ESI-MS/MS spectra of Cy-3-(Caff)-diGlc-5-Glc isomers at t_r 4.03 min (4) (B) and at t_r 7.08 min (15) (C).

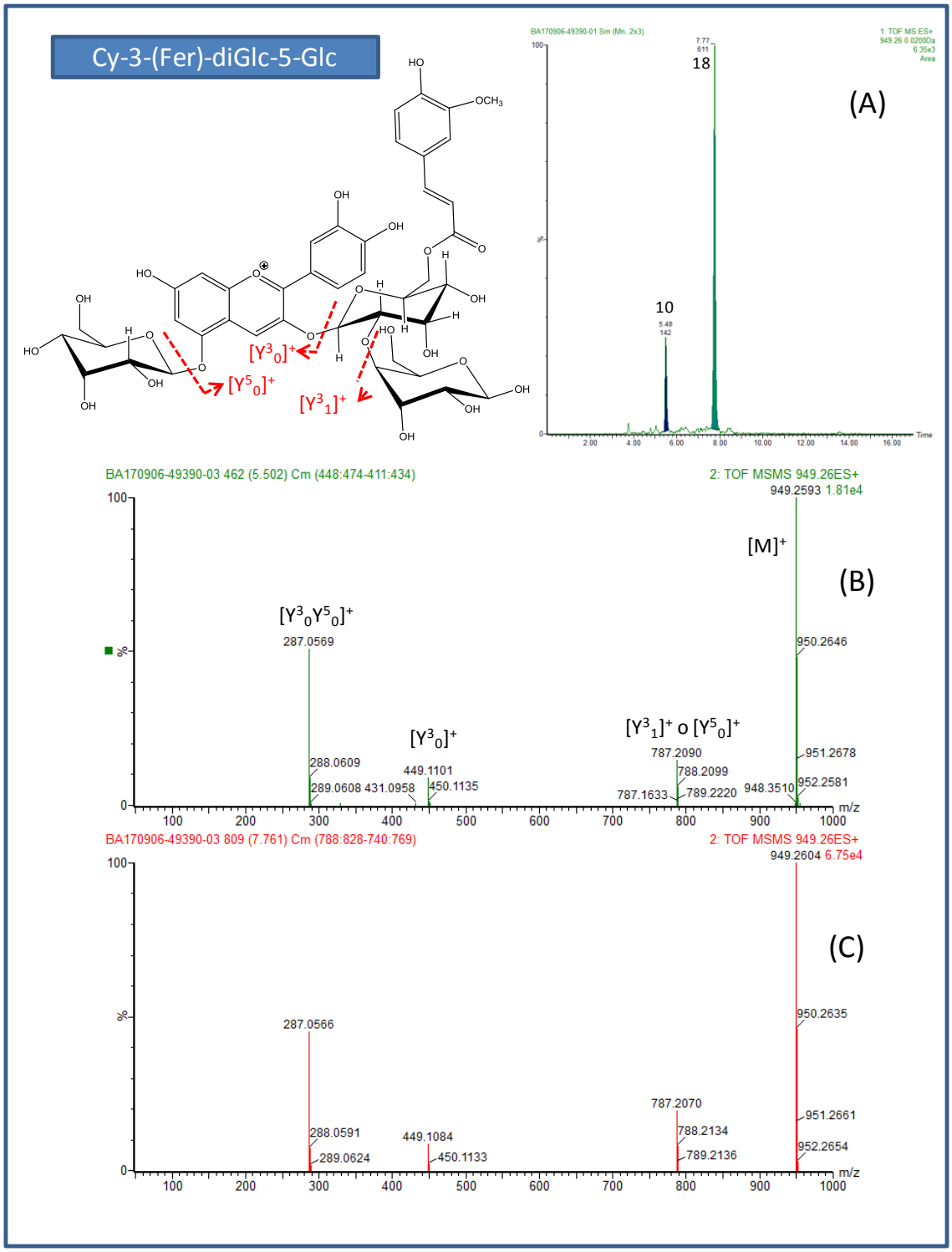

Figure S4 Chromatogram of extracted ion at 949.2608 m/z $[M]^+$ (A) and ESI-MS/MS spectra of Cy-3-(Fer)-diGlc-5-Glc isomers at t_r 5.50 min (10) (B) and at t_r 7.76 min (18) (C).

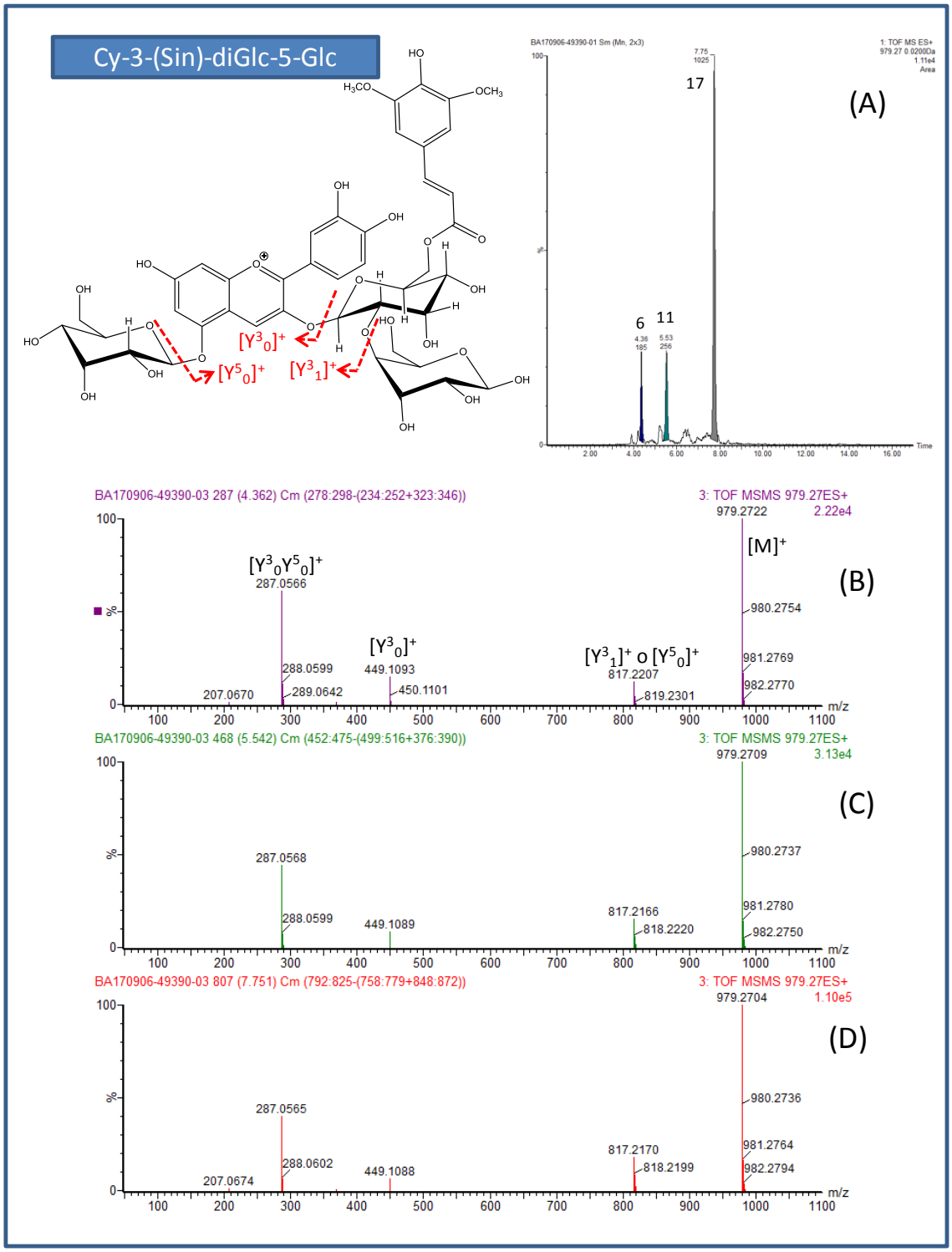

Figure S5 Chromatogram of extracted ion at 979.2714 m/z $[M]^+$ (A) and ESI-MS/MS spectra of Cy-3-(Sin)-diGlc-5-Glc isomers at t_r 4.36 min (6) (B), at t_r 5.54 min (11) (C) and at t_r 7.75 min (17) (D).

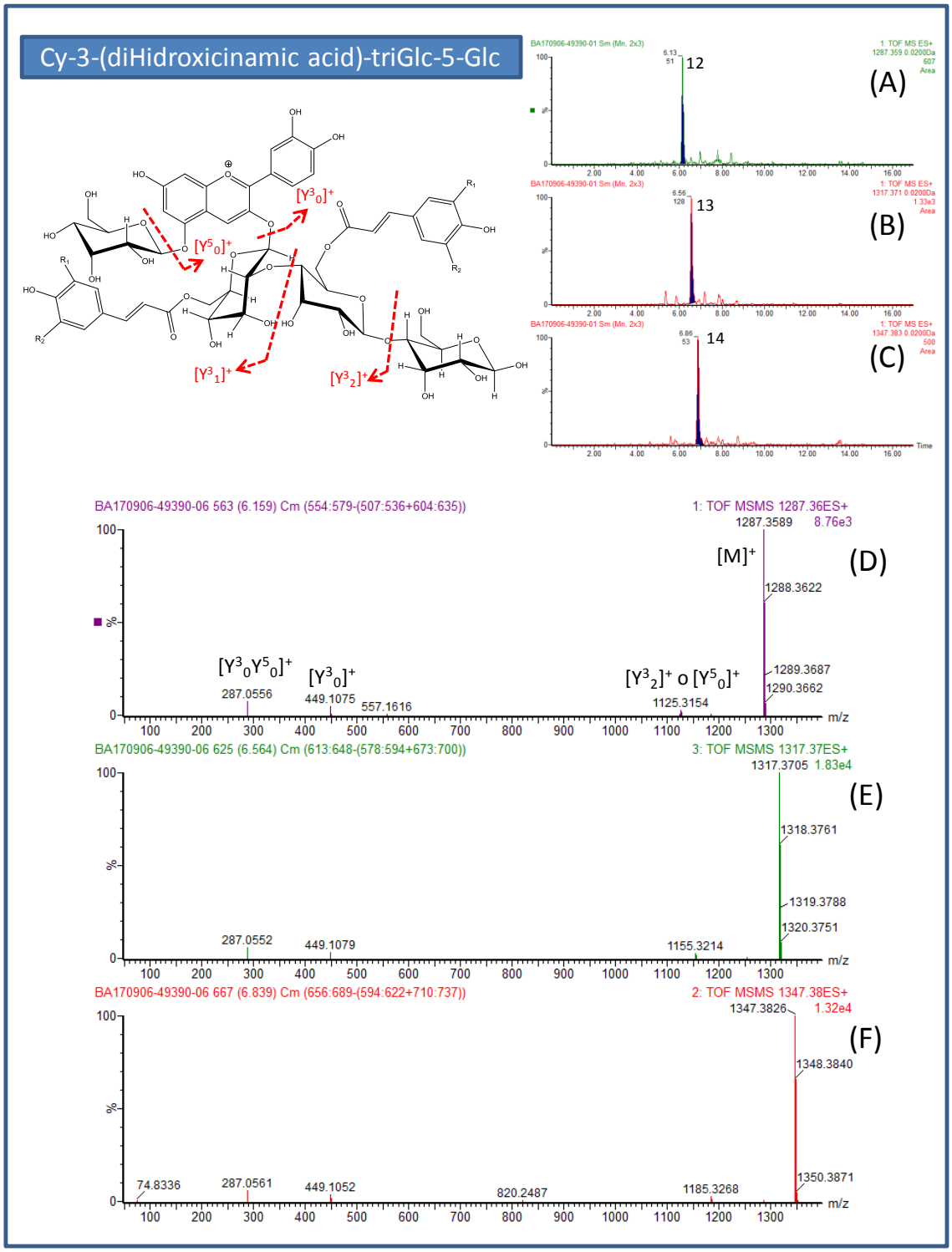

Figure S6 Chromatogram of extracted ion at 1287.3610 m/z $[M]^+$ (A), at 1317.3716 m/z $[M]^+$ (B), and at 1347.3821 m/z $[M]^+$ (C) as well as ESI-MS/MS spectra of Cy-3-(FerFer)-triGlc-5-Glc at t_r 6.13 min (12) (D), Cy-3-(SinFer)-triGlc-5-Glc at t_r 6.56 min (13) (E) and Cy-3-(SinSin)-triGlc-5-Glc at t_r 6.86 min (14) (F).

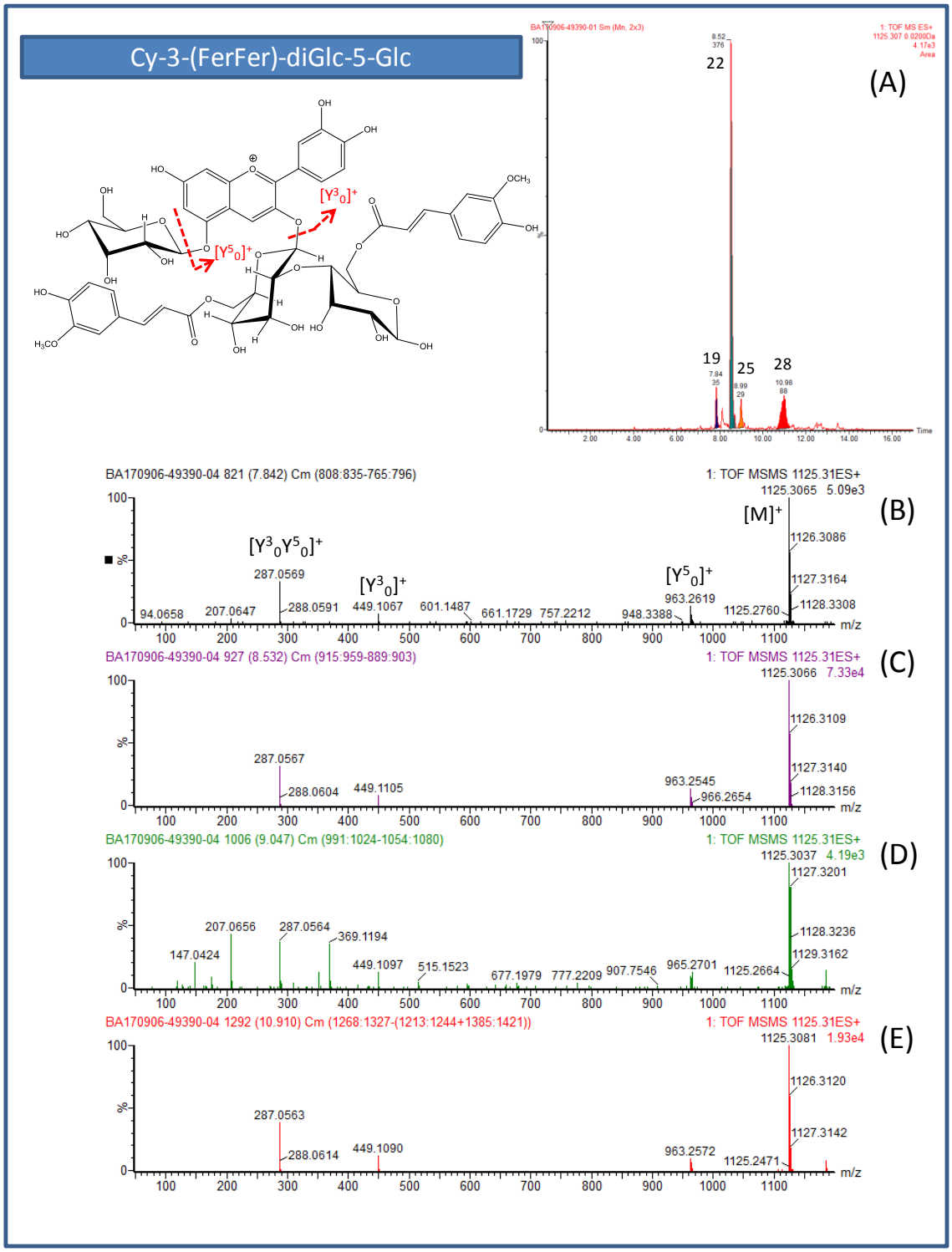

Figure S7 Chromatogram of extracted ion at 1125.3065 m/z $[M]^+$ (A) and ESI-MS/MS spectra of Cy-3-(FerFer)-diGlc-5-Glc isomers at t_r 7.84 min (19) (B), at t_r 8.52 min (22) (C), at t_r 8.99 min (25) (D) and at t_r 10.98 min (28) (E).

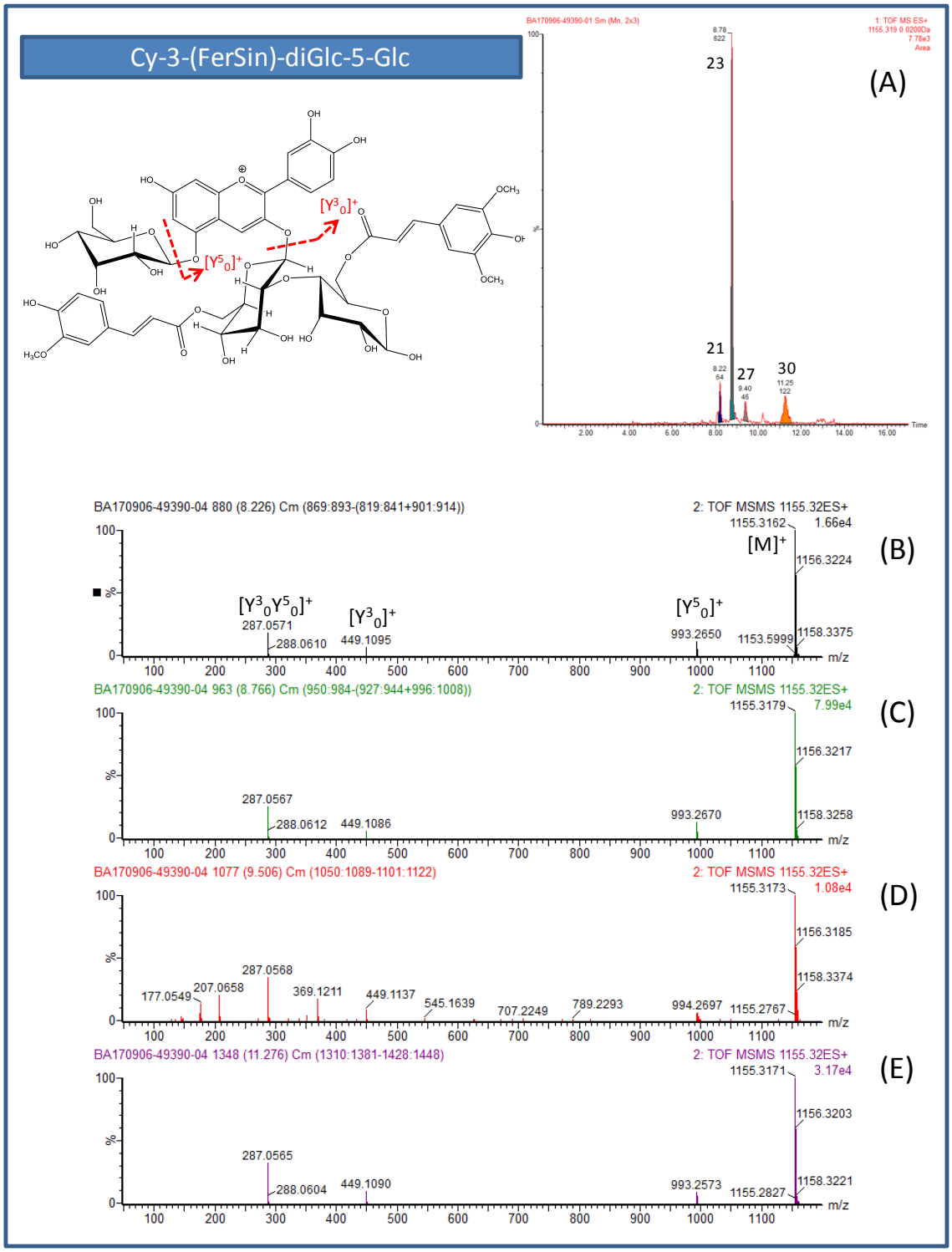

Figure S8 Chromatogram of extracted ion at 1155.3173 m/z $[M]^+$ (A) and ESI-MS/MS spectra of Cy-3-(FerSin)-diGlc-5-Glc isomers at t_r 8.22 min (21) (B), at t_r 8.76 min (23) (C), at t_r 9.50 min (27) (D) and at t_r 11.27 min (30) (E).

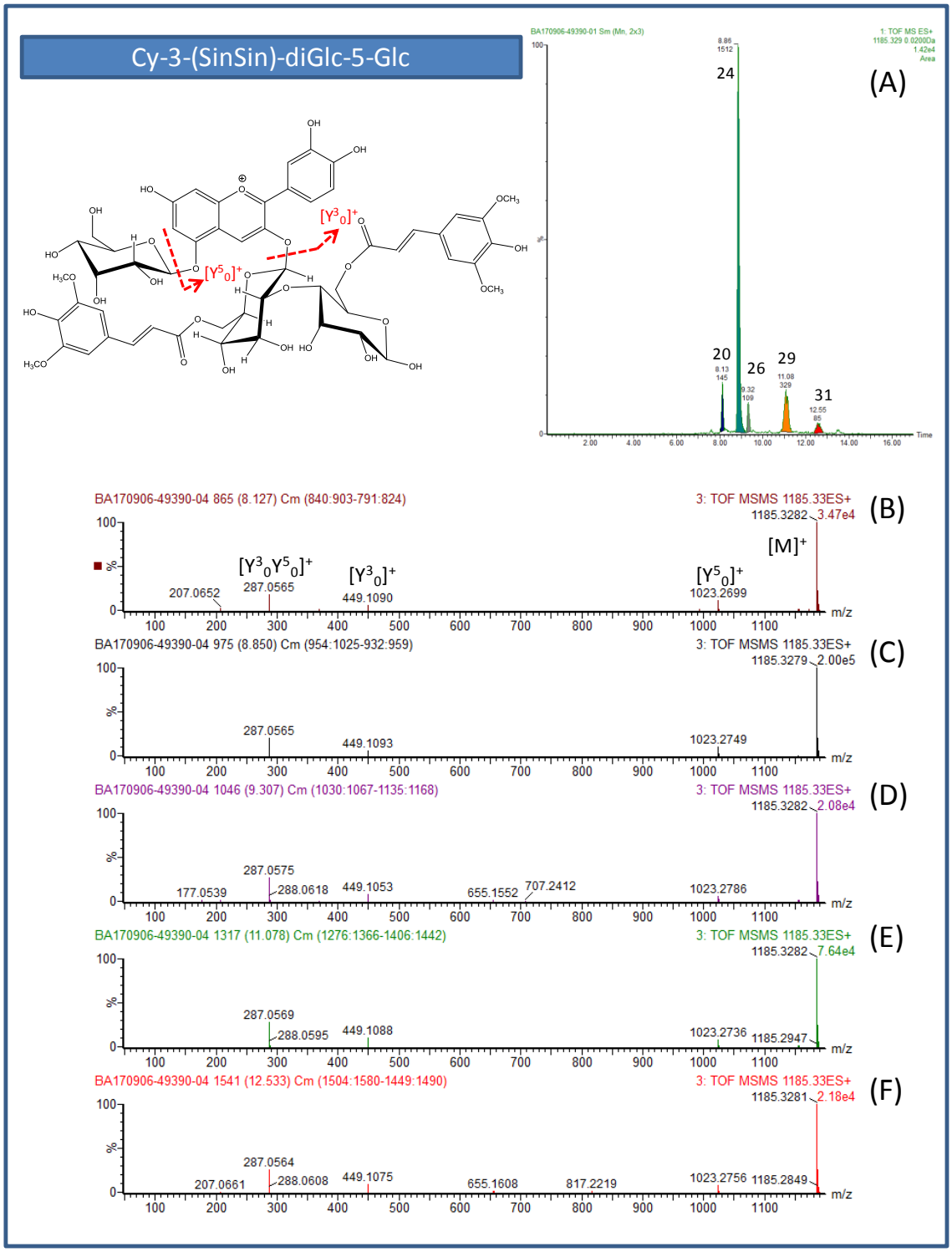

Figure S9 Chromatogram of extracted ion at 1185.3293 m/z $[M]^+$ (A) and ESI-MS/MS spectra of Cy-3-(SinSin)-diGlc-5-Glc isomers at t_r 8.13 min (20) (B), at t_r 8.86 min (24) (C), at t_r 9.30 min (26) (D), at t_r 11.08 min (29) (E) and at t_r 12.55 min (31) (F).

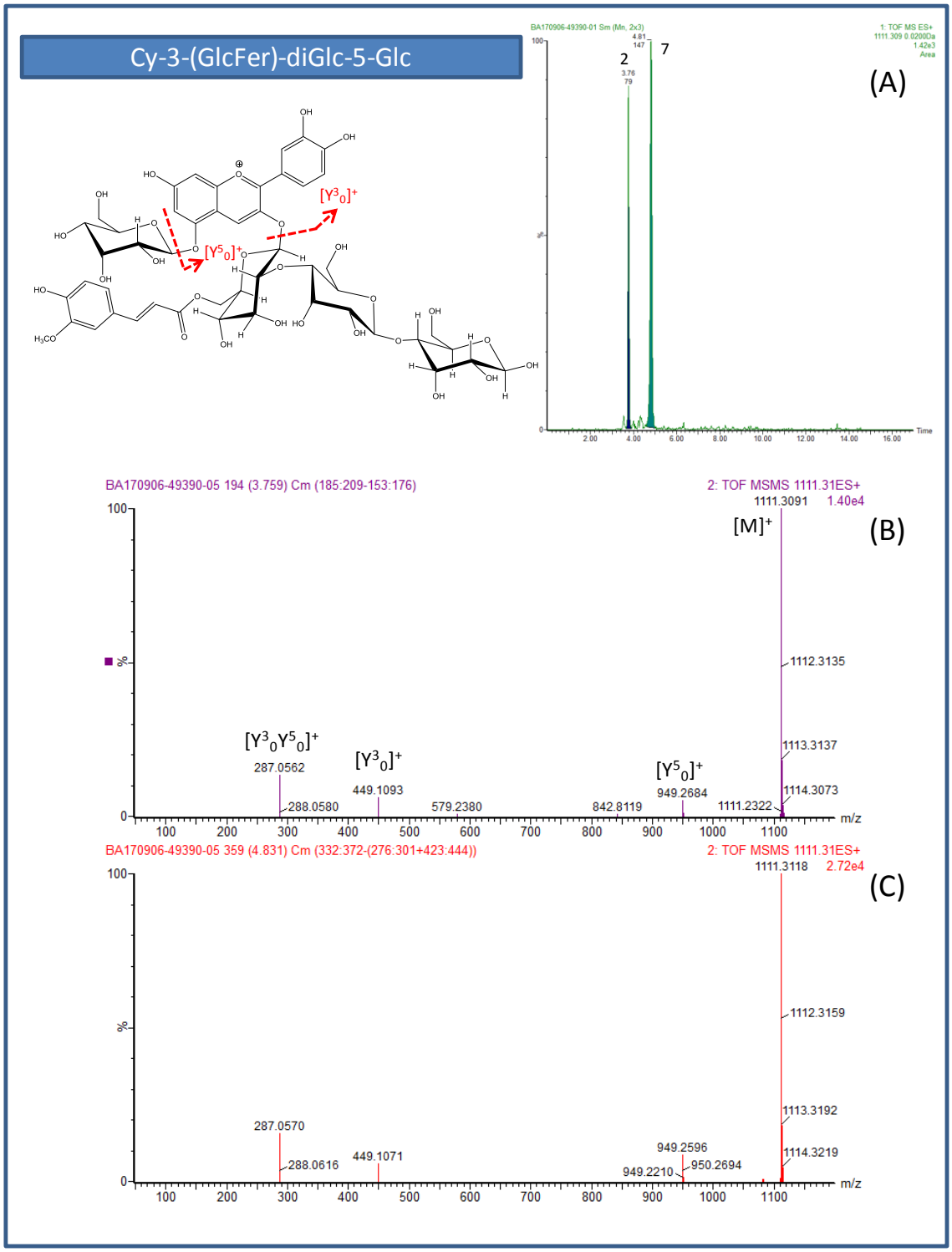

Figure S10 Chromatogram of extracted ion at 1111.3137 m/z $[M]^+$ (A) and ESI-MS/MS spectra of Cy-3-(GlcFer)-diGlc-5-Glc isomers at t_r 3.77 min (2) (B) and at t_r 4.83 min (7) (C).

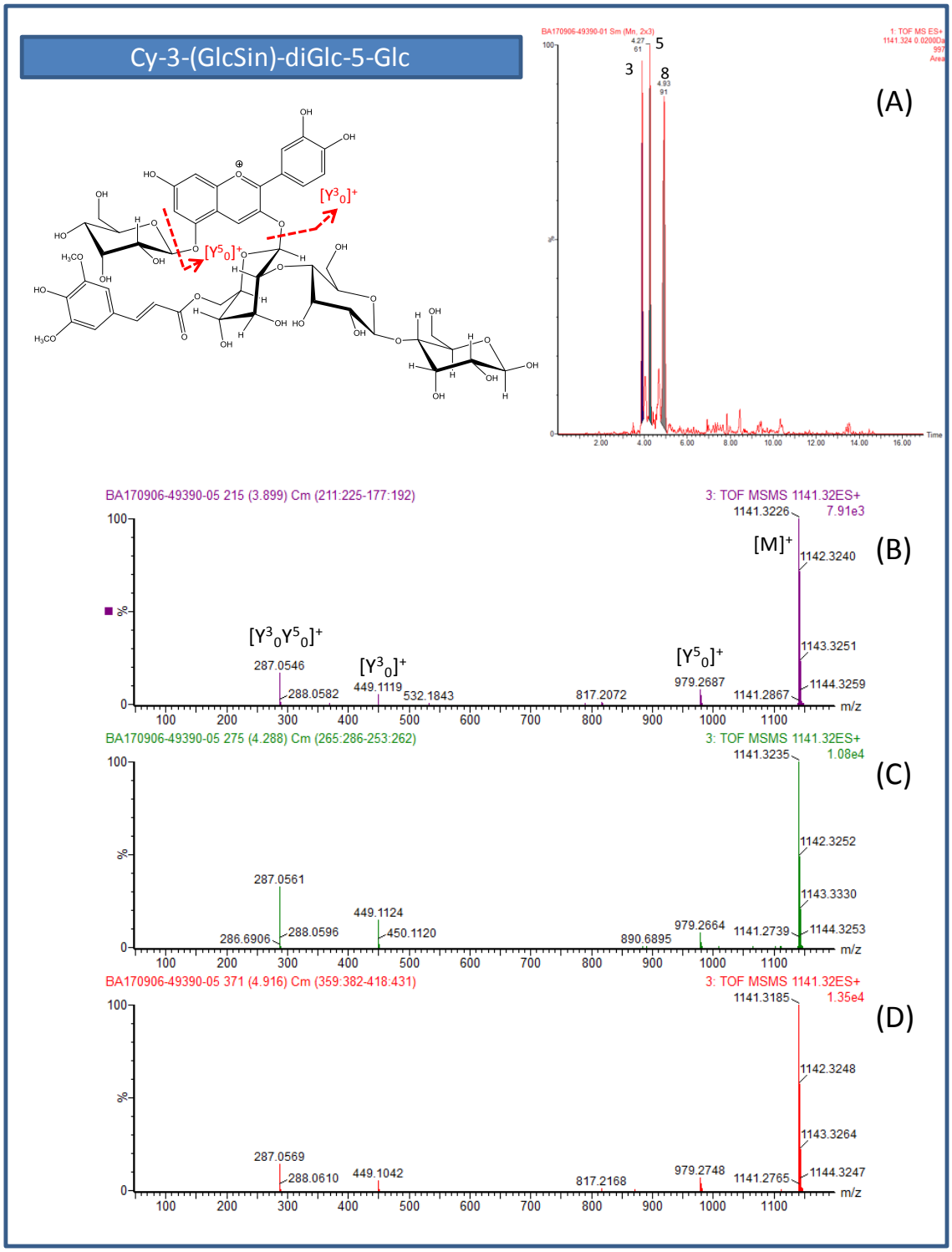

Figure S11 Chromatogram of extracted ion at 1141.3242 m/z $[M]^+$ (A) and ESI-MS/MS spectra of Cy-3-(GlcSin)-diGlc-5-Glc isomers at t_r 3.91 min (3) (B), at t_r 4.28 min (5) (C) and at t_r 4.91 min (8) (D).


BioMat